USGS
science for a changing world

Prepared in cooperation with the Idaho Water Resource Board and the Idaho Department of Water Resources

Groundwater-Flow Model of the Treasure Valley, Southwestern Idaho, 1986–2015

Scientific Investigations Report 2023–5096

U.S. Department of the Interior
U.S. Geological Survey

Cover. View west across New York Canal and Boise River from clifftop just south of Diversion Dam in Boise, Idaho. Photograph by Gerhard Hundt, April 30, 2021 (used with permission).

Groundwater-Flow Model of the Treasure Valley, Southwestern Idaho, 1986–2015

By Stephen A. Hundt and James R. Bartolino

Prepared in cooperation with the Idaho Water Resource Board and the Idaho Department of Water Resources

Scientific Investigations Report 2023–5096

U.S. Department of the Interior
U.S. Geological Survey

U.S. Geological Survey, Reston, Virginia: 2023

For more information on the USGS—the Federal source for science about the Earth, its natural and living resources, natural hazards, and the environment—visit https://www.usgs.gov or call 1–888–392–8545.

For an overview of USGS information products, including maps, imagery, and publications, visit https://store.usgs.gov/ or contact the store at 1–888–275–8747.

Suggested citation:
Hundt, S.A., and Bartolino, J.R., 2023, Groundwater-flow model of the Treasure Valley, southwestern Idaho, 1986–2015: U.S. Geological Survey Scientific Investigations Report 2023–5096, 107 p., https://doi.org/10.3133/sir20235096.

Associated data for this publication:
Hundt, S.A., 2023, Data and archive for a groundwater flow model of the Treasure Valley aquifer system, southwestern Idaho: U.S. Geological Survey data release, https://doi.org/10.5066/P9U6OOPH.

ISSN 2328-0328 (online)

Acknowledgments

The authors thank the people and organizations that supplied data or provided technical guidance used in this study. It could not have been completed without their contributions. Many thanks to the Idaho Department of Water Resources, Boise Project Board of Control, Suez Water Company, City of Boise, City of Nampa, City of Meridian, City of Garden City, Micron, Bureau of Reclamation, Idaho Power Company, and Idaho Department of Environmental Quality. Thank you to the Idaho Water Resource Board for financial support of this study. Finally, we owe a debt of gratitude to all members of the technical advisory committee for their feedback and patience. Particular thanks go to Alex Moody, Allan Wylie, Bob Carter, Christian Petrich, Clarence Robison, Darcy Sharp, Ed Hagen, Eric Miller, Jennifer Sukow, Kyle Radek, Mark Porter, Mathew Weaver, Michael McVay, Nate Runyan, Rex Barrie, Sean Vincent, and Terry Scanlan.

The authors also thank U.S. Geological Survey colleagues for their contributions. Dave Evetts, Michael Allen, Doug Ott, Alvin Sablan, Connor Molloy, David George, Erin Murray, Greg Pachman, John Carricaburu, Pete Spatz, Paul Schaur, Ryan Moore, Rhonda Fosness, and Sean Patton provided a crucial dataset for this study by planning, installing, and maintaining 10 new streamgages on agricultural drains.

Contents

Figures

Tables

Conversion Factors

U.S. customary units to International System of Units

Multiply	By	To obtain
	Length	
inch (in.)	2.54	centimeter (cm)
foot (ft)	0.3048	meter (m)
mile (mi)	1.609	kilometer (km)
	Area	
square mile (mi^2)	2.590	square kilometer (km^2)
	Volume	
acre-foot (acre-ft)	1,233	cubic meter (m^3)
	Flow rate	
inch per year (in/yr)	25.4	millimeter per year (mm/yr)

International System of Units to U.S. customary units

Multiply	By	To obtain
	Length	
meter (m)	0.3048	foot (ft)

Datums

Vertical coordinate information is referenced to the North American Vertical Datum of 1988 (NAVD 88).

Horizontal coordinate information is referenced to the North American Datum of 1983 (NAD 83).

Altitude, as used in this report, refers to distance above the vertical datum.

Abbreviations

3D HFM	three-dimensional hydrogeologic framework model
DEM	digital elevation model
ET	evapotranspiration
GIS	geographic information system
HFM	hydrogeologic framework model
IDWR	Idaho Department of Water Resources
SDAs	upply and demand areas
TVGWFM	Treasure Valley Groundwater Flow Model
USGS	U.S. Geological Survey
WSRP	western Snake River Plain

Groundwater-Flow Model of the Treasure Valley, Southwestern Idaho, 1986–2015

By Stephen A. Hundt and James R. Bartolino

Abstract

Most of the population of the Treasure Valley and the surrounding area of southwestern Idaho and easternmost Oregon depends on groundwater for domestic supply, either from domestic or municipal-supply wells. Current and projected rapid population growth in the area has caused concern about the long-term sustainability of the groundwater resource. In 2016, the U.S. Geological Survey, in cooperation with the Idaho Water Resource Board and the Idaho Department of Water Resources, began a project to construct a numerical groundwater-flow model of the westernmost portion of the western Snake River Plain aquifer system, called the Treasure Valley.

The development of the model was guided by several objectives, including:

(1) to improve the understanding of groundwater and surface water interactions;

(2) to facilitate conjunctive water management;

(3) to provide a tool for water resources planning; and

(4) to provide a tool for water allocation.

The model was constructed with a spatial scale and level of detail that aimed to meet these objectives while balancing the sometimes-competing goals of fast runtimes, numerical stability, usability, and parsimony.

The Treasure Valley Groundwater Flow Model (TVGWFM) is a three-dimensional finite-difference numerical model constructed using MODFLOW 6 (Langevin and others, 2017, Documentation for the MODFLOW 6 Groundwater Flow Model: U.S. Geological Survey Techniques and Methods, book 6, chap. A55, 197 p., https://doi.org/10.3133/tm6A55). The model covers the westernmost portion of the western Snake River Plain and is discretized into a regular grid of 64 by 65 cells with a side length of 1 mile and 6 layers of varying depth and active area. A historical model period was developed consisting of 360 month-long stress periods for 1986–2015. The model builds upon previous modeling efforts by adding a transient period, incorporating new head and discharge observations to constrain parameters, incorporating information from the hydrogeologic framework model (HFM) of Bartolino (2019, Hydrogeologic framework of the Treasure Valley and surrounding area, Idaho and Oregon: U.S. Geological Survey Scientific Investigations Report 2019–5138, https://doi.org/10.3133/sir20195138) and incorporating refined estimates of evapotranspiration and irrigation classification of lands in the study area.

The TVGWFM includes all significant components of recharge to and discharge from the aquifer. Inflows include canal seepage, irrigation and precipitation recharge, mountain-front recharge, rivers and stream seepage, and seepage from Lake Lowell. Outflows include discharge to agricultural drainage ditches, discharge to rivers and streams, pumping, and discharge to Lake Lowell. Each recharge or discharge component is represented separately using individual MODFLOW 6 packages.

Parameter values were derived with a combination of trial-and-error steps and automated parameter estimation using PEST software (Doherty, J.E., 2005, PEST, model-independent parameter estimation–User manual: Watermark Numerical Computing, https://pesthomepage.org/documentation). Parameter estimates were constrained with several types of observation data, including water levels, water level changes, vertical water level differences, drain discharges, change in drain discharges, river seepage, seepage from Lake Lowell, and change in seepage from Lake Lowell. Material properties from the hydrogeologic framework were also used to assign the minimum and maximum values of some parameters.

A final parameter realization was reached that minimized residuals between the observed and modelled values for the various observation groups. Mean residuals for the observation groups were 15.4 feet (ft) for water levels, 0.2 ft for water level changes, 19.4 ft for vertical water level differences, −3.9 cubic feet per second (ft^3/s) for drain discharges, 0.0 ft^3/s for changes in drain discharge, 45.0 ft^3/s for river seepage, −40.1 ft^3/s for Lake Lowell seepage, and 126.3 ft^3/s for changes in Lake Lowell seepage. The quality of the model's fit to observations varied spatially, with notable areas of under- or over-simulation of water levels present to the northwest and southwest of Lake Lowell, in the foothills along the eastern model boundary, and near the City of Eagle. Trends were observed in the residuals of many of the observation groups, indicating that the model is missing or not fully reproducing some phenomena that are observed in the system.

The TVGWFM can be used as a tool for water resource planning, for understanding the interactions of groundwater and surface water at a basin scale, and for facilitating conjunctive management, but may lack the precision needed for water rights administration at a local scale. Additional sources of uncertainty or limitations of the model are noted. The quantity and spatial distribution of canal seepage and infiltration of irrigation water recharge, the largest sources of recharge to the system, are unknown and approximated indirectly. There is poor understanding of how canal seepage and incidental recharge change as land is converted from agricultural (irrigated) to suburban (semi-irrigated). These uncertainties will affect any scenarios that investigate changes to land use or irrigation practices. Finally, the model has relatively high water-level residuals around and to the southwest of Lake Lowell and should not be used to estimate water level effects in that region.

The model was built with multiple, broadly expressed objectives and did not optimize performance for specific uses. However, the model and the tools included in an associated data release provide ample flexibility to improve the model for future uses. Adjustments and improvements could be made by refining the model in an area of interest, collecting additional calibration data, applying more rigorous boundary conditions, or re-estimating model parameters to optimize model performance for a specific model forecast.

Introduction

The Treasure Valley (fig. 1) is "the agricultural area that stretches west from Boise into Oregon" (U.S. Board on Geographic Names, 2019), although it is commonly referred to as "the lower Boise River watershed" or "the Boise River drainage basin downstream of Lucky Peak Lake"; it lies within the westernmost part of the western Snake River Plain (WSRP). Groundwater withdrawals provide most of the domestic and municipal water in the valley and surrounding area, except for 30 percent of Boise's municipal supply taken from the Boise River (Bartolino, 2019a).

SPF Water Engineering (2016) estimated that the population of the Treasure Valley will increase to about 1.6 million by 2065, resulting in a corresponding increase in domestic, commercial, municipal, and industrial water demand. To address this anticipated demand for water, the Idaho Senate passed Concurrent Resolution 137, which includes a request to "develop a groundwater model, with all necessary measurement networks" for the Treasure Valley (Idaho Senate Resources and Environment Committee, 2016, p. 2). In 2016, the U.S. Geological Survey (USGS), in cooperation with the Idaho Water Resource Board and the Idaho Department of Water Resources (IDWR), began a project to collect additional streamflow data (in the form of 10 new continuous streamgages and 3 additional synoptic streamflow-measurement sites) at 13 ditches and streams that serve as the primary outflow points for the expansive network of agricultural ditches and drains, develop a revised hydrogeologic framework, and create a groundwater-flow model of the Treasure Valley (Hundt, 2023). This is the third USGS report documenting the various components used to develop a groundwater-flow model: the first report described the project and summarized existing studies (Bartolino and Vincent, 2017), and the second report described the process used to build a three-dimensional hydrogeologic framework model (3D HFM) of the WSRP aquifer system (Bartolino, 2019a).

Previous Work

Hundreds of published and unpublished reports on various aspects of the geology and hydrology of the WSRP have been prepared by government agencies, universities, and consultants. Bartolino (2019a) contains a discussion of reports deemed most relevant to preparing the 3D HFM. Most relevant to the current report are eight prior groundwater-flow models of all or part of the WSRP. These models have had varying objectives, details, and model extents (Cosgrove, 2010; Johnson, 2013). Three models include all or most of the current study area: those of Newton (1991), Petrich (2004), and Johnson (2013) (fig. 2). Models by Lindgren (1982), Douglas (2007), Pacific Groundwater Group (2008a, b), Schmidt (2008), and Bureau of Reclamation (2009) had site-specific objectives and covered smaller areas. Cosgrove (2010) evaluated these models (excepting Johnson, 2013), including their suitability for predictive use and the relative strengths and weaknesses of each. Sukow (2016) reviewed various aspects of the Johnson (2013) model.

Purpose and Scope

This report describes the development of a groundwater-flow model for the Treasure Valley located in the westernmost part of the WSRP aquifer system. The Treasure Valley Groundwater Flow Model (TVGWFM) builds upon this previous work with the following new features and data:

(1) a transient historical period;

(2) model layering scheme that allows for vertical water level gradients;

(3) new flux observations in the form of drain discharges;

(4) agricultural pumping, canal seepage, and incidental recharge results from an agricultural and urban water supply and demand model that incorporates new land-use and evapotranspiration (ET) data; and

(5) the newly developed hydrogeologic framework from the 3D HFM (Bartolino, 2019a).

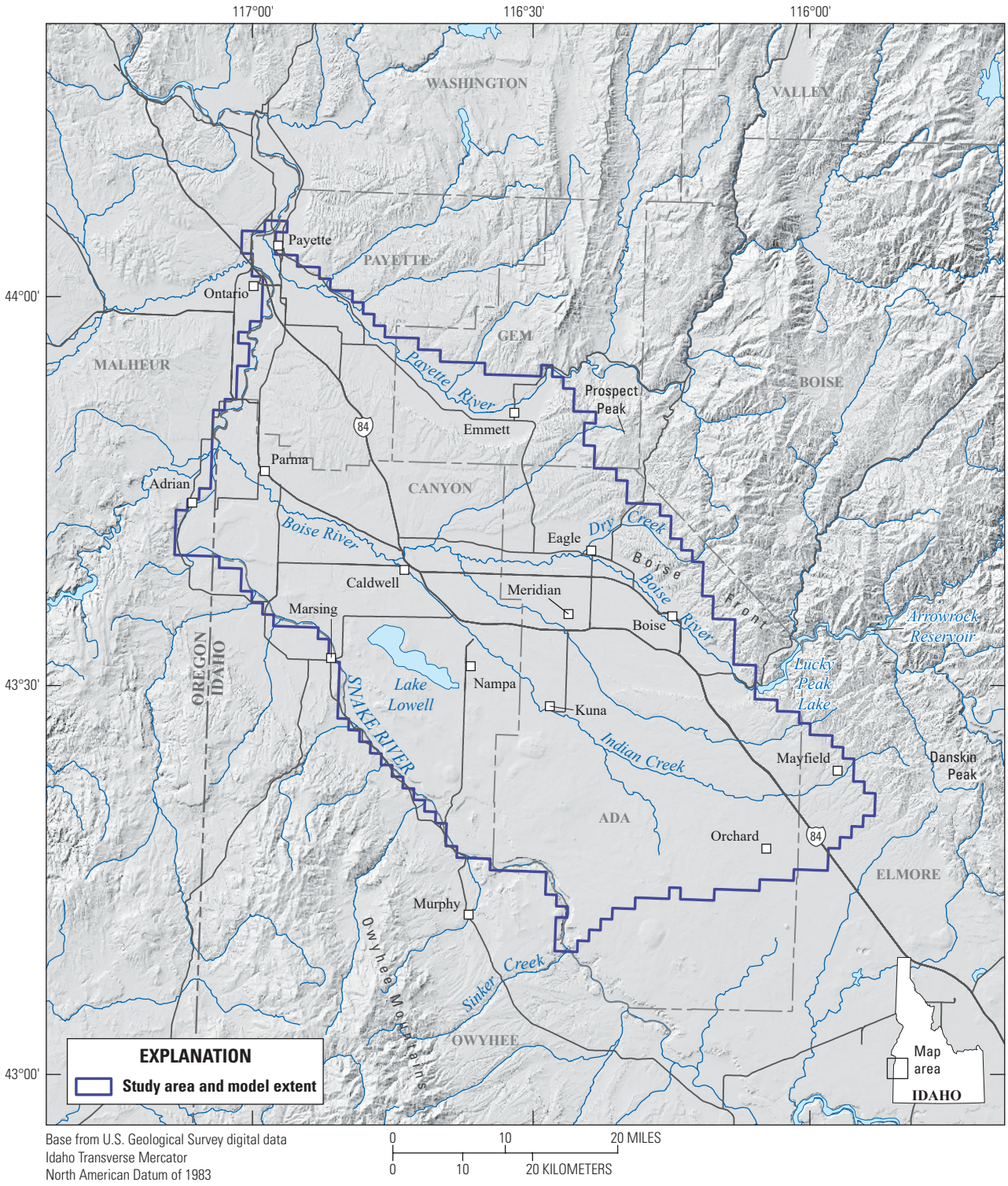

Figure 1. Locations of study areas, communities, streams, and highways in the western Snake River Plain, southwestern Idaho and easternmost Oregon.

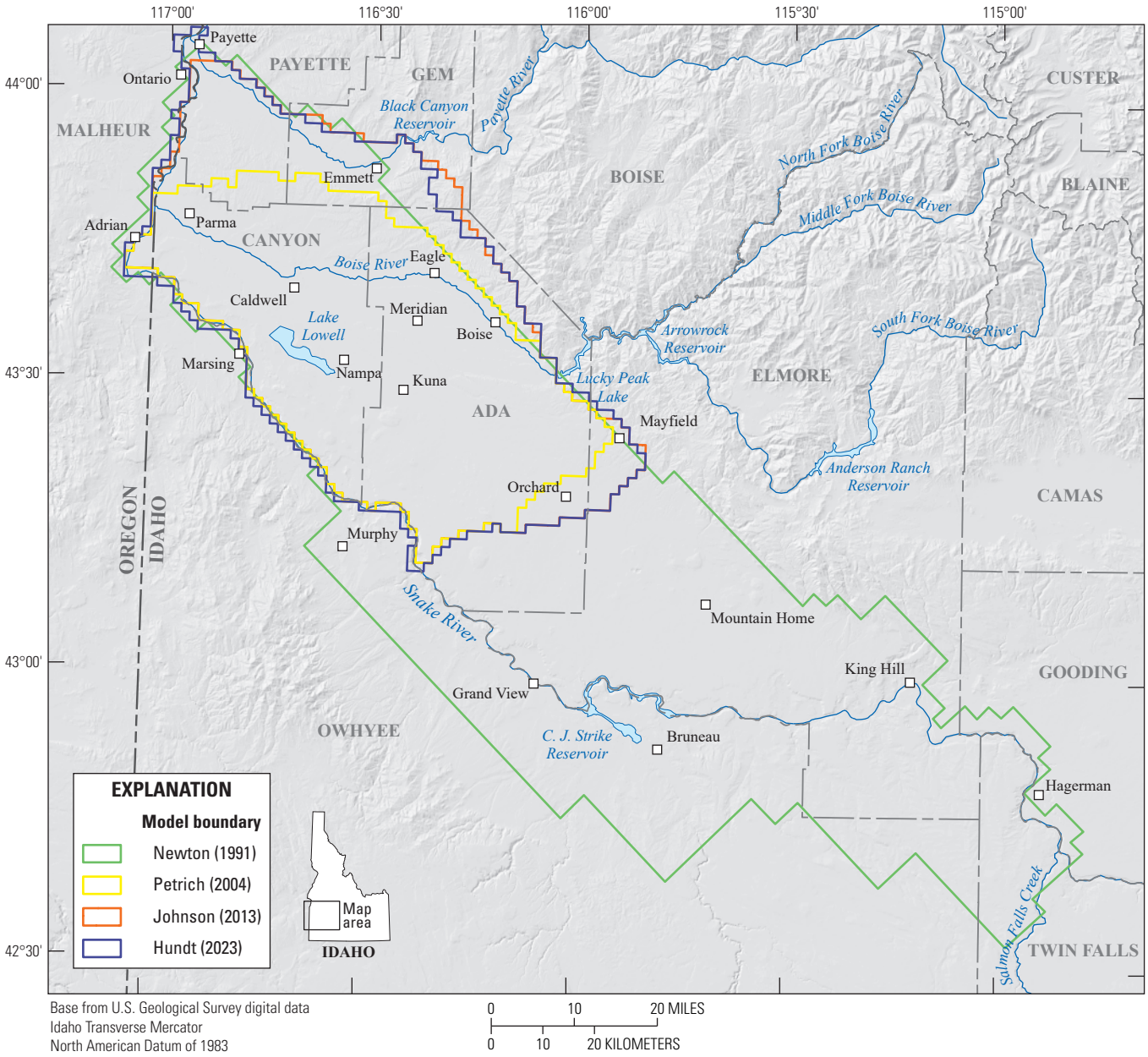

Figure 2. The domains of three past groundwater models (Newton, 1991; Petrich, 2004; Johnson, 2013) and the Treasure Valley Groundwater Flow Model (Hundt, 2023) discussed in this report, western Snake River Plain, southwestern Idaho and easternmost Oregon.

This multi-layer model represents groundwater conditions from 1986 to 2015. An archive of the model and all data used in its development are available in an associated data release (Hundt, 2023).

Description of Study Area

The study area encompasses about 4,160 square miles (mi^2) and is located in the westernmost part of the WSRP. The WSRP is a topographic low in southwestern Idaho and easternmost Oregon (fig. 1) between the Boise and Danskin Mountains to the north (altitude as high as 10,000 feet [ft]) and the Owyhee Mountains to the south (altitude as high as 8,400 ft).

Hydrologically, the study area is bound by the Snake River to the south and west and the hills north of the lower Payette River drainage basin downstream of Black Canyon Reservoir to the north. There is a groundwater divide near the Ada-Elmore County line to the east. About 66 percent of the study area lies within the Boise River drainage basin, 23 percent within the Payette River watershed, and 11 percent drains directly to the Snake River.

The topography across the study area consists of an undulating plain that slopes downwards generally from southeast to northwest. The northern part of the study area is separated by an east-west line of uplands that forms the interfluve between the Boise River watershed to the south and the Payette River watershed to the north. The altitude generally ranges from about 4,810 ft at Prospect Peak along the north-central boundary down to 2,140 ft at the Snake River (Bartolino, 2019a).

Conceptual Model

A conceptual model of the regional aquifer system serves as the basis for the discretization and boundary conditions used in the numerical model. The conceptual model incorporates information about the horizontal and vertical extent of the hydrogeologic units, about how water is thought to flow through the system, and about aquifer properties.

Climate

Eight National Weather Service (NWS) stations and four Bureau of Reclamation AgriMet stations are located within or adjacent to the study area and have data coverage for some or all of the 1986–2015 groundwater-flow model period (Bureau of Reclamation, 2019; National Oceanic and Atmospheric Administration, 2019). Across the study area, the coldest month is January, and the warmest month is July. Mean annual precipitation, which combines rainfall and snowfall (as snow water equivalent), ranges from 7.8 to 19 inches (in.), and mean annual snowfall ranges from 3.9 to 55 in. July and August are typically the driest months; December and January are typically the wettest. Snowfall in the study area typically melts shortly after falling, with the greatest monthly mean snow depth being 1 in. or less (except at the Parma Experiment Station weather station, which has 2 in.) and typically occurring in January (Western Regional Climate Center, 2019). A more complete discussion of the climate of the study area may be found in Bartolino (2019a).

Hydrogeology

Bartolino (2019a, b) created a 3D HFM (fig. 3) of the WSRP to represent the subsurface distribution and thickness of four hydrogeologic units within the groundwater-flow model boundary. These four units include: Coarse-grained fluvial and alluvial deposits, Pliocene-Pleistocene[1] and Miocene basalts, fine-grained lacustrine deposits, and granitic and rhyolitic bedrock. A comparison of the 3D HFM with hydrogeologic frameworks developed by previous authors shows broad agreement and concurs with the general characterization of the aquifer system as coarser-grained alluvial sediments overlying finer-grained lacustrine sediments with some overlying and interbedded basalts.

Bartolino (2019a) details methods, geologic history, and results of the hydrogeologic framework model. The primary source of data for the 3D HFM were lithologic data from 291 well-driller reports taken from the IDWR online database (Idaho Department of Water Resources, 2020a). The resulting model extends from an altitude of 500 ft to land surface (fig. 3).

Vertical Extent of Hydrogeologic Units and Study Area

Along the eastern edge of the study area, the hydrogeologic framework model extends down to the rhyolitic and granitic bedrock that is considered the base of the aquifer. Throughout most of the study area, however, the depth to bedrock beneath the valley unconsolidated material is unknown. In these areas, the bottom of the model was set a distance below the deepest production and monitoring wells. See the numerical model section for details on how the vertical extent was determined.

An important finding of the hydrogeologic framework study (Bartolino, 2019a) is the lack of well-defined and continuous hydrogeologic units across the study area. A notable exception is a pro-delta and deep lake mudstone facies that was mapped throughout much of the study area (Wood, 1997). Despite the lack of continuous geologic units, vertical heterogeneity in aquifer properties and water levels are known to occur at a local scale in the study area.

Direction of Groundwater Flow

As summarized in Bartolino (2019a), previous investigations have identified infiltration of surface-water irrigation as the primary source of recharge and agricultural drains and ditches, rivers, and groundwater pumping as the primary components of discharge. Flow paths generally travel from east to west. The New York Canal forms a local groundwater divide throughout much of the study area, with flow travelling west-southwest on the south side of the canal and west-northwest to the north of the canal. Groundwater near (within 10 ft of) ground surface is observed locally near the Boise River and more extensively in the north-western part of the Boise River Valley and throughout the entire Payette River Valley. Greater depths-to-water are found in the southeastern part of the model area, in local uplands near Lake Lowell, in the uplands between the Boise and Payette River Valleys, and along the eastern edge of the model area.

[1]Hyphens connecting geologic epochs indicate "and." They are presented as hyphens in order to maintain consistency with the hydrogeologic framework report from which they were derived.

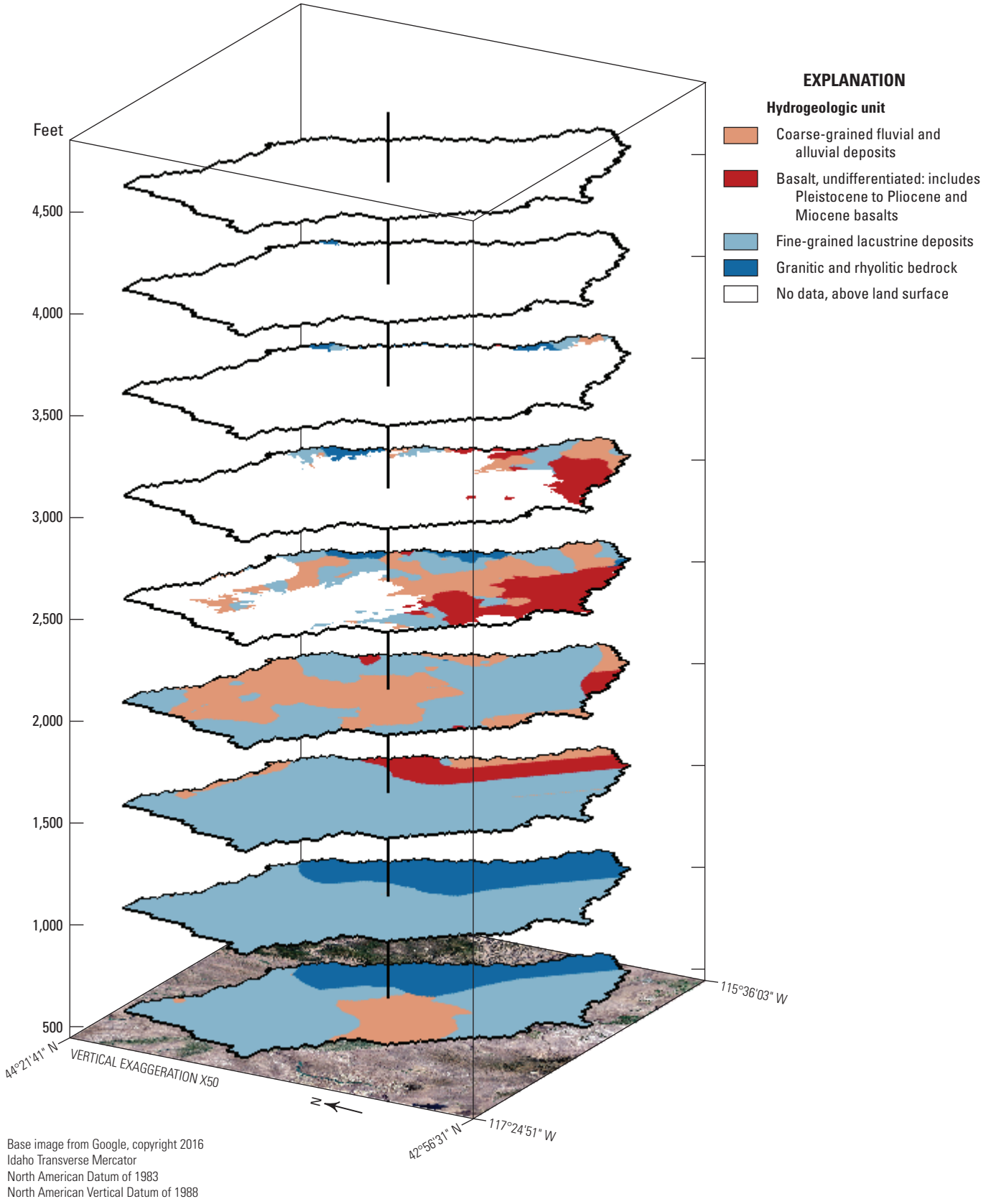

Figure 3. Hydrogeologic framework model of the Treasure Valley, southwestern Idaho and easternmost Oregon. Figure taken from Bartolino (2019b).

Previous Water Budgets

Several previous groundwater budgets have been developed for substantial parts of the WSRP, many from groundwater-flow models. The most relevant to the current report are Newton (1991), Urban (2004), Schmidt and others (2008), and Sukow (2012). The Newton (1991) budget was developed for a groundwater-flow model of the entire WSRP and thus covers a much larger area than the study detailed in this report (fig. 2). Urban (2004) constructed 1996 and 2000 groundwater budgets for the area of Petrich's (2004) groundwater-flow model of the Treasure Valley (fig. 2). Schmidt and others (2008) constructed a combined groundwater/surface-water budget for the Treasure Valley to which Sukow (2012) added data for the Payette River valley and adjoining areas north of the Treasure Valley Hydrologic Project (TVHP) model boundary for use in Johnson's (2013) groundwater-flow model (fig. 2). Table 1 shows the components of the Newton (1991) and Urban (2004) budgets. In table 1, the Schmidt and others (2008) and Sukow (2012) budgets are combined, and only groundwater budget components are shown. Caution is warranted in comparing the budgets because of differing areas, time periods, and how individual budget components are combined. Particularly, the Newton (1991) model domain contains more than twice the land area of the other budgets, including large areas of uncultivated desert and many constant flux boundary cells representing underflow. The reader is referred to the original publications for details (Newton, 1991; Urban, 2004; Schmidt and others, 2008; Sukow, 2012).

Irrigation System and Irrigated Lands

The Treasure Valley has an extensive irrigation system that supports agriculture and urban landscaping. This system allows precipitation that falls primarily in high elevations during the cold season to be stored and delivered to cultivated lands in the Boise and Payette Valleys during the growing season via a series of canals. A large number of datasets were compiled to understand and model irrigation-related water fluxes. These datasets and the routines used to process them are available in the data release associated with this publication (Hundt, 2023).

Irrigated Land Use

In support of the study summarized in this report, contractors to IDWR created eight yearly datasets of irrigated land status across the study area for 1987, 1994, 1997, 2000, 2004, 2007, 2010, and 2015 (Idaho Department of Water Resources, 2020b). These datasets were created using manual interpretation of Landsat imagery and aerial photography. From this imagery, lands are classified as one of three types: irrigated, non-irrigated, or semi-irrigated. Irrigated lands are typically agricultural; non-irrigated lands are typically desert, pavement, or water bodies; and semi-irrigated lands are typically residential. Different terminology is used in this report for the same land use types depending upon the context. The terms "urban" or "urbanized" refer to areas with a land use that is classified as semi-irrigated, and the terms "agriculture" and "agricultural" refer to areas with a land use that is classified as irrigated. Because a given piece of land may fluctuate between irrigated and non-irrigated from year to year, there is some degree of error associated with the datasets. Maps of land irrigation status for 1987 and 2015 are shown on figures 4 and 5.

Figure 6 shows the total area (in square miles) for each irrigation status class over the eight periods sampled. Generally, from 1987 to 2015, the area of irrigated land decreased by 14 percent and the area of semi-irrigated land increased by 67 percent; the non-irrigated land area remained nearly the same.

Water Supply Entities

Water users in the Treasure Valley are served by water supply entities that primarily deliver treated drinking water to residential, commercial, and industrial customers, and untreated irrigation water to agricultural and residential customers. These entities are the basis by which the study area was divided into Supply and demand areas (SDAs) (fig. 7) for the purpose of applying an irrigation supply and demand model.

Irrigation Organizations

Irrigation water in the study area is primarily delivered by organizations that manage water rights and maintain and operate infrastructure for their members. While organizations such as drainage districts perform necessary functions apart from water supply entities, it is the public districts and private companies who divert and deliver irrigation water that were most important in defining SDAs. The State of Idaho stores records of organization boundaries (Idaho Department of Water Resources, 2011), and Water Districts 63 and 65 record monthly diversions for every organization with surface water rights to the Boise and Payette Rivers (Idaho Department of Water Resources, 2018b).

Water Utilities

Treated drinking water is supplied by both private and public providers in the study area. Suez Water is the private water utility that serves Boise. Meridian, Nampa, Caldwell, Eagle, Kuna, Garden City, and other smaller cities are served by municipal utilities. Most urbanized areas fall within the service areas of water utilities. Note that lands that have been converted from agricultural to urban uses often remain members of irrigation organizations and receive untreated water for landscaping. This change in land use is accounted for in the irrigation supply and demand model.

Table 1. Summary of selected western Snake River Plain groundwater budgets by Newton (1991), Urban (2004), Schmidt and others (2008), and Sukow (2012).

[Table taken from Bartolino (2019a). Component names and significant figures are as shown in the referenced reports. **Abbreviations**: acre-ft/yr, acre-feet per year; –, not applicable]

Budget component	Inflows	Percentage of total inflow	Outflows	Percentage of total outflow
	Volume (acre-ft/yr)		Volume (acre-ft/yr)	
Newton (1991), 1980 conditions				
Infiltration from surface-water irrigation	1,400,000	80	–	–
Underflow across boundaries	310,000	18	–	–
Direct precipitation	40,000	2.3	–	–
Groundwater discharge to rivers and drains	–	–	1,450,000	83
Groundwater pumping	–	–	300,000	17
Totals	1,750,000		1,750,000	
Urban (2004), mean of 1996 and 2000 conditions				
Canal seepage	573,750	54	–	–
Flood irrigation and precipitation	353,200	33	–	–
Recharge from precipitation by other land uses	56,850	5.4	–	–
Seepage from rivers and streams	46,500	4.4	–	–
Seepage from Lake Lowell	20,100	1.9	–	–
Rural domestic septic systems	4,800	0.45	–	–
Underflow	4,300	0.41	–	–
Discharge to rivers and drains	–	–	847,800	82
Domestic and industrial withdrawals	–	–	71,400	6.9
Agricultural irrigation	–	–	62,500	6.0
Rural domestic withdrawals	–	–	25,500	2.5
Self-supplied industrial	–	–	14,600	1.4
Municipal irrigation	–	–	10,000	0.97
Stock watering	–	–	3,000	0.29
Totals	1,059,500		1,034,800	
Schmidt and others (2008) and Sukow (2012), mean 1967–97 conditions				
Canal seepage	702,375	48	–	–
Total on-farm infiltration (irrigation and precipitation)	674,699	46	–	–
Tributary underflow (north of Payette River)	59,389	4.1	–	–
Direct precipitation (non-irrigated lands)	23,470	1.6	–	–
Direct precipitation (domestic, commercial, municipal, and industrial lands)	1,793	0.12	–	–
Groundwater discharge to drains	–	–	785,216	51
Groundwater discharge to rivers	–	–	501,802	33
Pumping (irrigation)	–	–	136,147	8.9
Pumping (domestic, commercial, municipal, and industrial)	–	–	85,834	5.6
Aquifer discharge to wetlands	–	–	21,339	1.4
Aquifer discharge to Lake Lowell	–	–	3,752	0.24
Totals	1,461,726		1,534,090	

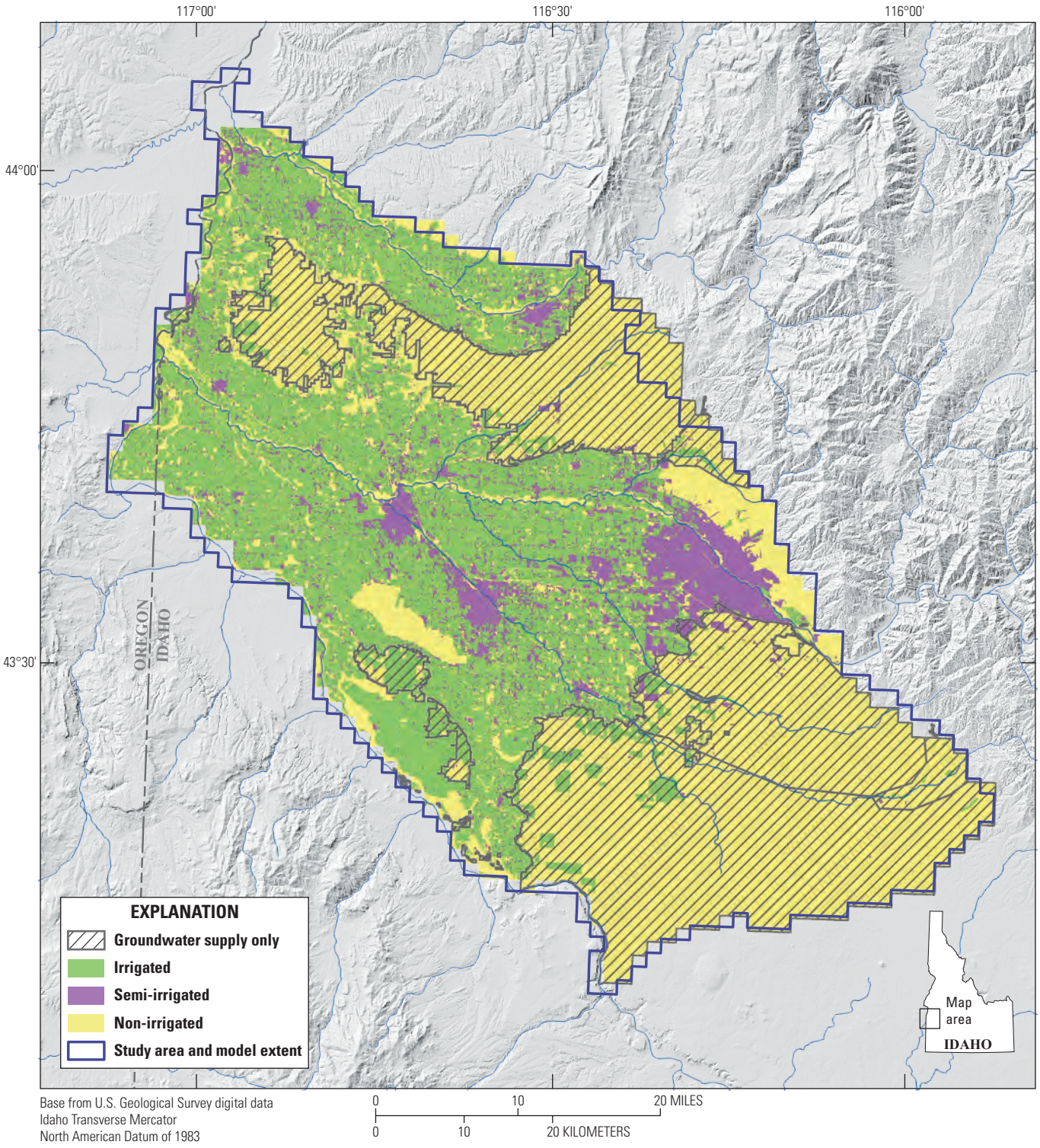

Figure 4. Irrigation status, western Snake River Plain, southwestern Idaho, and easternmost Oregon, 1987 (Idaho Department of Water Resources, 2020b).

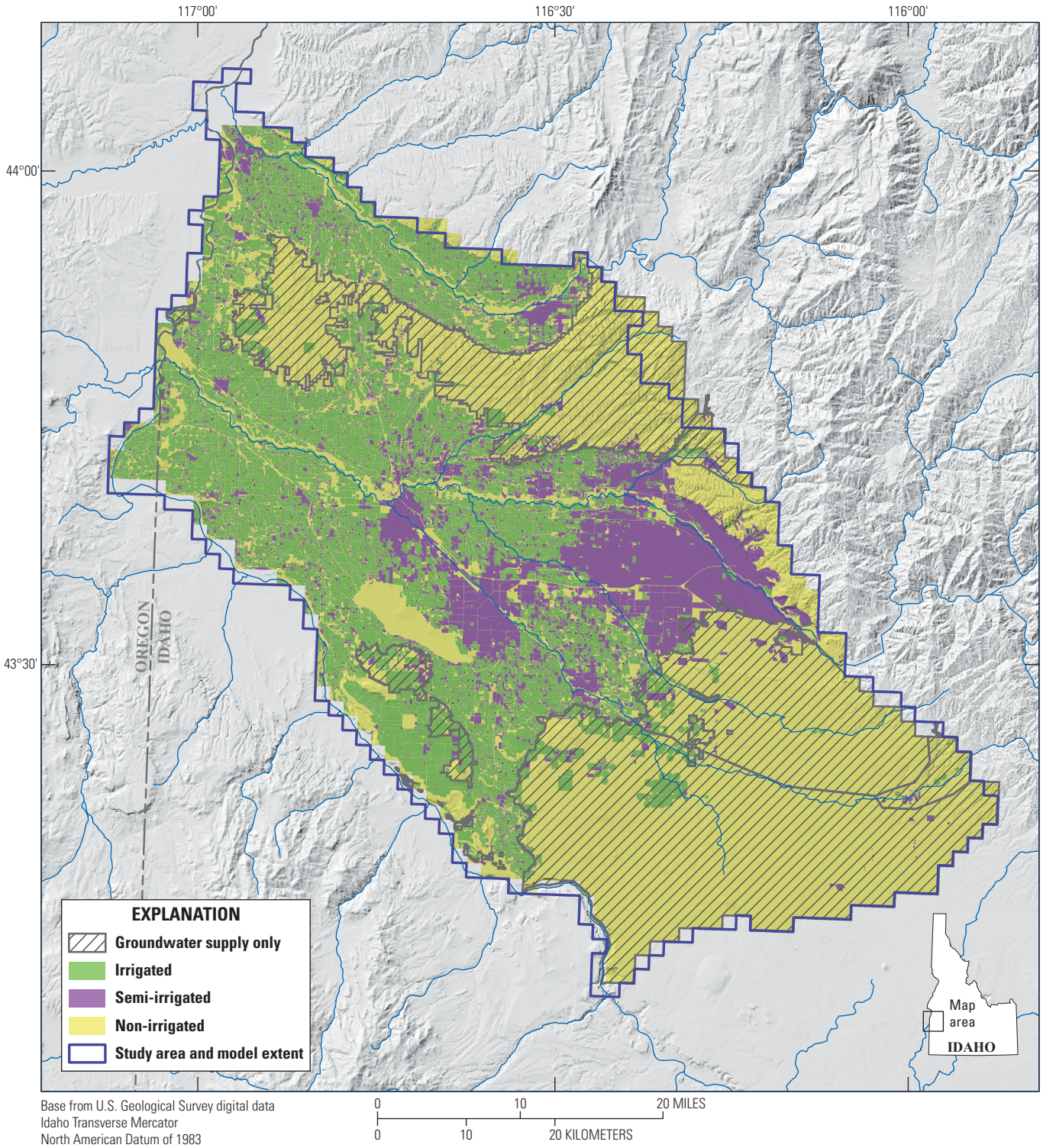

Figure 5. Irrigation status, western Snake River Plain, southwestern Idaho, and easternmost Oregon, 2015 (Idaho Department of Water Resources, 2020b).

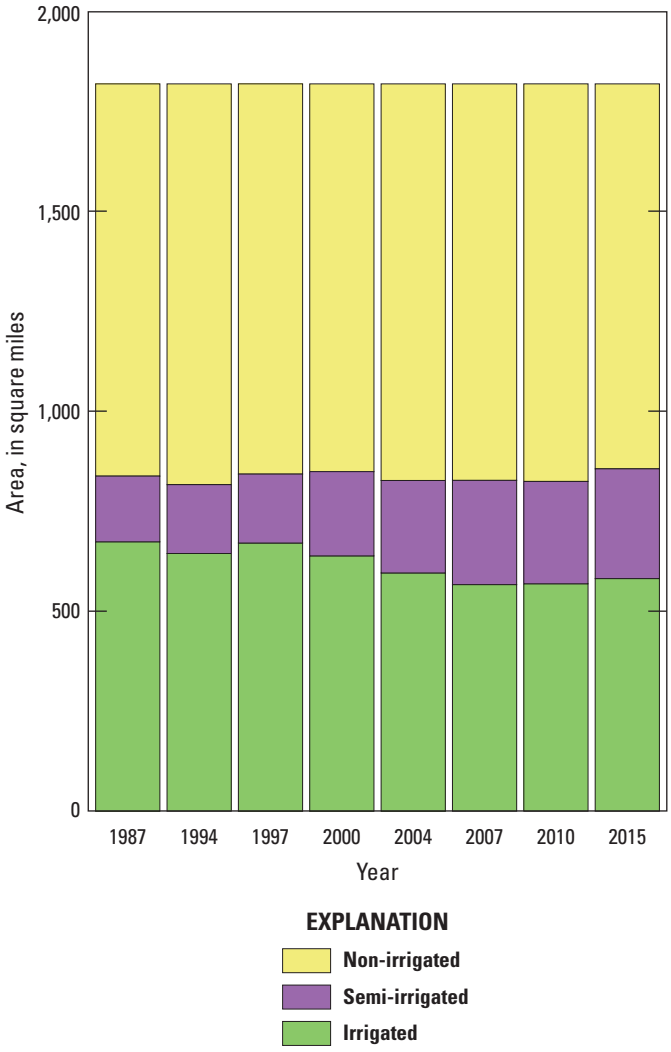

Figure 6. Irrigation status, western Snake River Plain, southwestern Idaho, and easternmost Oregon, 1987–2015 (Idaho Department of Water Resource, 2020b).

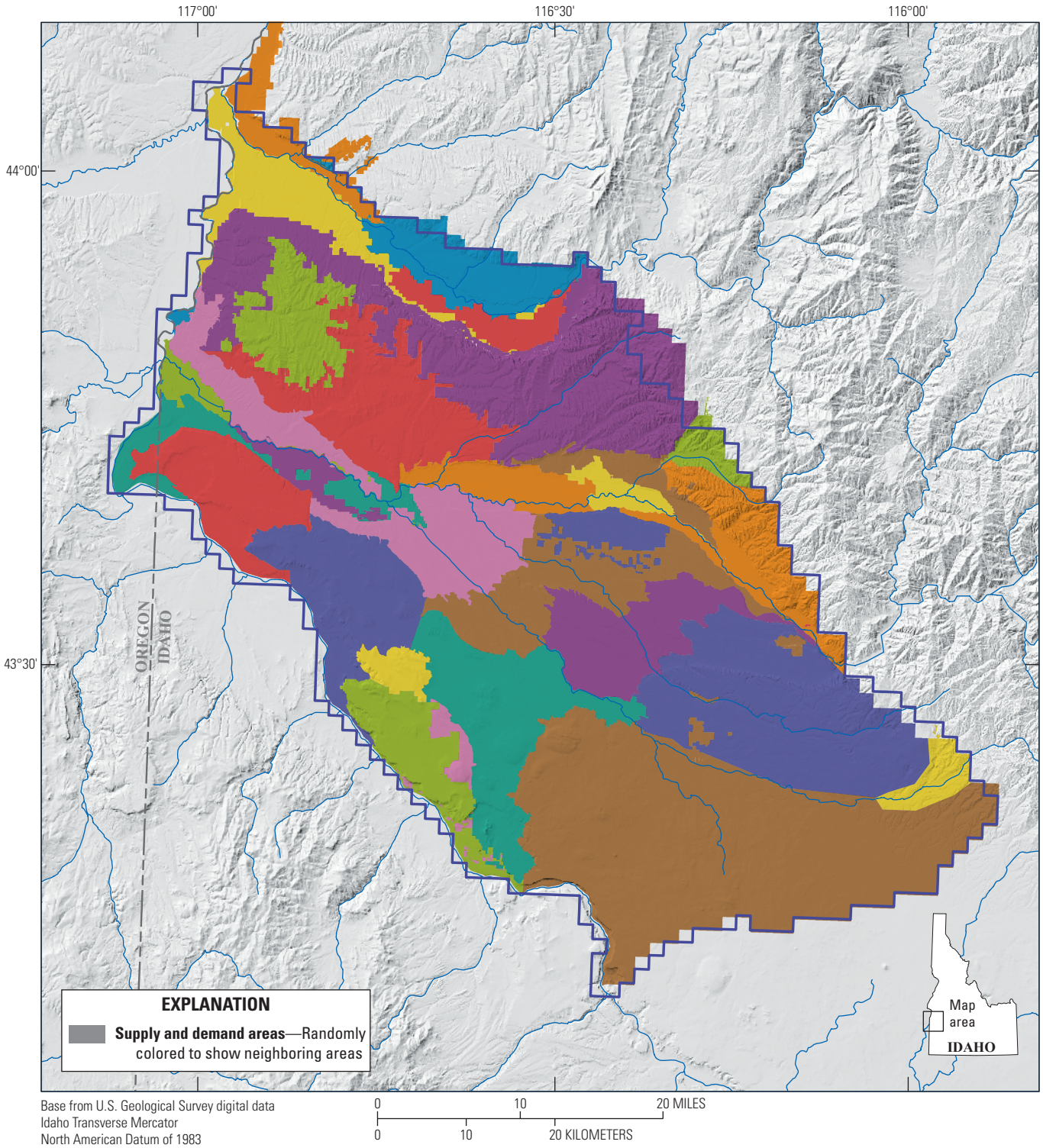

Figure 7. Supply and demand areas used to calculate soil water balance and distribution of recharge and pumping in an irrigation supply and demand model, southwestern Idaho and easternmost Oregon (Hundt, 2023).

The primary consumptive use of water in urban areas of the Treasure Valley is through evapotranspiration (ET) from landscaping. As with irrigated lands, monthly volumetric ET demands are derived from monthly ET and irrigated land area data. Two additional data sources collected or estimated for urban areas were (Hundt, 2023):

- Measured pumping (and surface water diversions)
- Monthly indoor water use (non-consumptive)

Water utilities in the Treasure Valley mostly utilize groundwater. Suez Water also diverts surface water from the Boise River at the Marden treatment plant. Records of groundwater pumping volumes for water utilities are incomplete for the 1986–2015 model period. For periods when groundwater withdrawal records are unavailable, the urban water uses are estimated in the irrigation supply and demand model.

Indoor water use is a non-consumptive urban water demand that is not captured in ET data. Indoor water use was estimated for each municipality as the product of population and the single per-capita indoor use. Population was obtained from the U.S. Census Bureau (1983, 2005, 2019) and the Community Planning Association of Southwest Idaho (2020) and are shown in table 2. The single per-capita use was estimated using (incomplete) records of water utility production. For utilities with available monthly production records, it was assumed that water deliveries in the month of January are entirely for indoor use. These January records were combined with service area population to calculate per-capita use. A single rate of per-capita indoor use was assigned as the average of all such values. Monthly indoor water use is assumed to be constant throughout the year. These demands are included in the "Irrigation Supply and Demand Model" Section (table 3).

Service areas of water utilities may lay within multiple SDAs. In such cases, the supply and demand volumes of each municipality were allocated to SDAs in proportion to the amount of the municipality's area that falls within the SDA.

Private Wells

Small water associations and private wells provide water to residents and businesses both within and outside of water utility service areas. When inside a utility service area, these water users are lumped with water utility customers in the "irrigation supply and demand model." Indoor water use outside of water utility service areas is ignored with the assumption that all indoor water is returned to the aquifer through septic systems. Landscaping ET met by private wells is included as a semi-irrigated ET demand in the "irrigation supply and demand model."

Evapotranspiration Demand and Irrigation Requirements

Transpiration from plants and evaporation from soil, open water, and other surfaces are grouped and referred to as evapotranspiration (ET) in this study. ET from agricultural crops and urban landscaping is the primary driver of water demand in irrigated and semi-irrigated areas, respectively. With little precipitation occurring during the growing season, information about where, when, and how much ET occurs provides an estimate of spatial and temporal distribution of recharge that results from the conveyance and application of irrigation water.

The University of Idaho (UI) produced monthly maps of estimated actual ET during the growing season (March–October) for 1986–2015. Two different algorithms were used. The more sophisticated Mapping EvapoTranspiration at high Resolution and Internalized Calibration (METRIC; Allen and others, 2007) algorithm was used for 1987, 1994, 1997, 2000, 2004, 2007, 2010, and 2015. For the remaining years, a simpler approach was taken that interpolated between the years for which METRIC was applied by developing and applying sets of relationships between METRIC ET rates and Normalized Difference Vegetation Index (NDVI) values. Details regarding the METRIC and NDVI methods are documented separately (Idaho Department of Water Resources, 2020c).

The resulting ET dataset includes monthly estimates of actual ET within 30 by 30 m cells that cover the entire study area for 1986–2015 (Hundt, 2023). These ET data are only used for irrigated and semi-irrigated areas. During 1986–2015, average annual ET was 1,125,000 acre-feet (acre-ft) for irrigated lands and 445,000 acre-feet for semi-irrigated lands; equating to an average of 34 inches per year for irrigated lands and 39 inches per year for semi-irrigated lands.

River Diversions

Irrigation in the Treasure Valley is primarily obtained by the diversion of water from the Boise and Payette Rivers into irrigation canals. These diversions are recorded by publicly elected watermasters who oversee the distribution of water within state-designated districts. These records do not provide the information necessary to resolve where surface water is delivered within an irrigation district or company. Some farmlands along the western border of the study area obtain irrigation water from the Snake River but do not fall within an Idaho water district. Measurements of deliveries are not available for these lands.

River diversions are the largest supply component of the irrigation supply and demand model. During 1986–2015, average annual diversions were 1,120,000 acre-ft from the Boise River and 935,000 acre-feet from the Payette River. Monthly diversions for each irrigation district are available in the associated data release (Hundt, 2023).

Table 2. City and county population in the Treasure Valley, southwestern Idaho and easternmost Oregon, 1980–2020.

City	Population								
	1980	1985	1990	1995	2000	2005	2010	2015	2020
Ada County (unincorporated)	46,637	46,637	46,637	55,765	38,622	49,572	59,731	61,780	61,480
Boise	102,451	119,376	136,300	159,258	195,916	200,728	205,671	223,670	240,380
Caldwell	17,699	18,143	18,586	21,351	27,539	37,614	46,237	51,880	61,210
Canyon County (unincorporated)	35,507	35,507	35,507	43,841	42,705	47,225	50,187	53,800	50,960
Eagle	2,620	3,618	4,616	6,777	12,379	16,209	19,908	24,600	32,560
Emmett	4,605	4,650	4,695	5,266	5,594	6,206	6,557	6,557	6,557
Fruitland	2,496	2,496	2,496	2,998	3,833	4,236	4,684	4,684	4,684
Garden city	4,571	5,762	6,952	8,942	10,656	10,803	10,972	12,060	12,460
Gem County (unincorporated)	7,243	7,243	7,243	8,550	9,621	10,098	10,162	10,162	10,162
Greenleaf	662	662	662	776	858	864	846	860	870
Kuna	2,148	2,148	2,148	2,545	6,457	10,925	15,210	17,320	24,890
Melba	242	242	242	277	453	491	513	570	590
Meridian	6,658	8,483	10,308	17,907	37,264	56,570	75,092	91,310	119,350
Middleton	1,880	1,880	1,880	2,259	3,136	4,425	5,524	7,110	9,780
Nampa	25,112	27,596	30,080	36,974	54,642	69,363	81,557	89,210	106,860
New Plymouth	1,294	1,294	1,294	1,500	1,403	1,461	1,538	1,538	1,538
Notus	363	363	363	394	451	499	531	570	570
Parma	1,607	1,607	1,607	1,721	1,789	1,916	1,983	2,140	2,160
Payette	5,448	5,647	5,846	6,669	7,263	7,295	7,433	7,433	7,433
Payette County (unincorporated)	6,808	6,808	6,808	8,338	8,125	8,492	8,968	8,968	8,968
Star	561	561	561	667	2,034	3,948	5,781	7,930	11,860
Wilder	1,250	1,250	1,250	1,331	1,474	1,527	1,533	1,640	1,810
Ada County Total	165,646	186,584	207,522	251,861	303,328	348,755	392,365	438,670	502,980
Canyon County Total	84,322	87,250	90,177	108,924	133,047	163,924	188,911	207,780	234,810
Gem County Total	11,848	11,893	11,938	13,816	15,215	16,304	16,719	16,719	16,719
Payette County Total	16,046	16,245	16,444	19,505	20,624	21,484	22,623	22,623	22,623
Treasure Valley Total	277,862	301,973	326,081	394,106	472,214	550,467	620,618	685,792	777,132

Table 3. Irrigation Supply and Demand Model components (Hundt, 2023).

Component	Type	Estimation method
Diversion	Input	Measured
Precipitation	Input	Measured
Soil moisture	Storage	Estimated from measured component (precipitation)
Canal seepage	Output	Estimated from measured component (diversion)
Evapotranspiration	Output	Measured
Indoor water use	Output	Estimated from measured component (population; per capita use)
Recharge of applied irrigation (incidental recharge)	Output	Estimated from measured component (evapotranspiration)
Pumping	Output	Residual of water budget equation
Flow through	Output	Residual of water budget equation

Soil Moisture Storage

For this study, water within the shallow subsurface that can be reached by plant roots or is subject to soil evaporation is referred to as "soil moisture storage." Soil moisture is one of the three general parts of the irrigation supply and demand model soil water budget. This water budget is simplified by assuming that soil moisture does not change for most of the year. It is assumed that, from April to November, irrigated soils remain near field capacity, there is no change in soil moisture storage, and inflows exactly balance outflows. A simple model of soil moisture storage change is used to account for years when a wet winter and early spring benefit crops early in the growing season. From December to February, a part of each month's excess inflow (inflow more than outflow) is combined and delivered as an additional inflow source in March.

Recharge

Several main components contribute recharge (or inflow) to the Treasure Valley aquifer system. These include, in decreasing order, seepage from irrigation canals, direct infiltration from excess irrigation water and precipitation, seepage from the Boise and Payette Rivers and Lake Lowell, and mountain-front recharge. The following sections cover sources of recharge and include brief conceptual descriptions, the availability of relevant data, and how recharge was estimated.

Canal Seepage

Seepage from the extensive network of irrigation canals in the Boise and Payette Valleys is a major source of recharge to the Treasure Valley aquifer system, contributing 48–54 percent of total groundwater recharge (Urban, 2004; Schmidt and others, 2008; Sukow, 2012) (table 1). Variation in where and when canal seepage occurs is expected to have a major influence on water levels and seasonal changes in water levels.

Temporal measurements of canal seepage are unavailable at the model scale used in this study. Additionally, few measurements are available of the canal properties that could be used to compute a physically based estimate of seepage in individual canals. These properties would include canal locations, canal widths, water levels in canals, hydraulic properties of canal beds, records of canal lining (where and when), local-scale hydraulic properties beneath canals, and local water levels below and adjacent to canals. The lack of information on the canal seepage is a large source of model uncertainty. Model limitations from the canal seepage uncertainty and possible additional data collection ideas are discussed at the end of this report.

Upper New York Canal

The New York Canal is the backbone of the irrigation system of the Boise Valley and has been identified as one of the most important drivers of water levels and flow paths in the study area (Petrich, 2004). The New York Canal runs from the Boise River Diversion Dam to Lake Lowell and influences the spatial and seasonal variability of groundwater in the adjacent area. Between the Boise River and (roughly) the bifurcation with Indian Creek (near Locust Grove and McDermott Roads), the canal is above the local water table and is assumed to only lose water as seepage. Moving downstream to Lake Lowell groundwater levels are closer to land surface and the New York Canal may act a source or sink of groundwater through this section.

Irrigation on Irrigated and Semi-Irrigated Lands

Previous studies have calculated irrigation to contribute 33–80 percent of total groundwater recharge in the study area (Newton, 1991; Urban, 2004; Schmidt and others, 2008; Sukow, 2012). All irrigation is considered to have some "inefficiency," where water percolates beyond the root zone to become groundwater recharge. Irrigation is applied using several practices and to different land-use and soil types, combining to produce different levels of irrigation (in)efficiency. For example, flood irrigated fields can be expected to have greater groundwater recharge than those with sprinklers. A similar disparity should exist between well-draining and poorly draining soils.

Irrigation practices are not recorded for individual fields, and no attempt was made to infer them from other information. Soil properties were not used to estimate spatial differences in irrigation (in)efficiency. While irrigation practices can have important consequences for many aquifers, for this study area it was instead the differences between urban and agricultural lands and the availability of surface water that were considered more important. These distinctions were partially captured in the irrigation recharge estimates by allowing each SDA to have unique inefficiency factors and by separating irrigated and semi-irrigated land recharge for each SDA.

Mountain-Front Recharge

Because it largely occurs in the subsurface, mountain-front recharge is one of the more difficult water-budget components to quantify. In the current report, it includes tributary underflow (water that enters the WSRP aquifer system as underflow beneath tributary streams at the basin boundary) and mountain-block recharge (flow that enters the aquifer system as underflow from the mountain block across the basin boundary). Mountain-front recharge enters the WSRP aquifer system along the northern boundary of the study area from watersheds tributary to the Payette River and watersheds that drain from the Boise and Danskin Mountains (fig. 8). Previous estimates of this recharge component suggest that it is a minor part of the total recharge to the aquifer system, contributing from less than 1 to 18 percent of total recharge (Newton, 1991; Urban, 2004; Schmidt and others, 2008; Sukow, 2012).

Precipitation on Non-Irrigated Lands

Non-irrigated lands in the study-area are primarily precipitation-limited sagebrush-steppe. It is assumed that all precipitation falling upon these lands are ultimately taken up by ET and that no recharge occurs. Estimates of average annual precipitation excess (precipitation minus actual or potential ET) for sagebrush was collected from ET Idaho, a website with evapotranspiration estimates for weather stations throughout Idaho (Allen and Robison, 2017), for all stations within the model area. These values ranged from −9.4 inches to 0.8 inches, with a median of 0.5 inches. While it may not be strictly true that no recharge occurs in non-irrigated lands for all months, these results are consistent with the understanding that recharge from non-irrigated lands is negligible compared to other sources.

Precipitation on Irrigated and Semi-Irrigated Lands

Infiltration of precipitation to the aquifer is thought to occur primarily in the non-irrigation season when its rate exceeds ET. During the non-irrigation season, precipitation is the only inflow term in the irrigation supply and demand model. During the irrigation season, any precipitation is grouped with irrigation deliveries in the irrigation supply and demand model.

Seepage from Rivers and Streams

The Snake, Payette, and Boise Rivers are all primarily gaining streams throughout the study area. There are several perennial and seasonal streams in the study area (such as Indian Creek, Willow Creek, Dry Creek, and others). Previous studies concluded that these do not provide a significant source of recharge (Newton, 1991; Urban, 2004; Schmidt and others, 2008; Sukow, 2012). No measurements were made on these streams, nor were any attempts made to estimate recharge from these streams.

Seepage from and to Lake Lowell

Seepage from Lake Lowell will occur when lake stage is higher than the adjacent water table. Seepage (recharge and discharge) to/from Lake Lowell is simulated by the model, and estimates are calculated as observations that serve to constrain model parameter estimates. Lake Lowell was identified as a point of net recharge for 119 of 237 months in which calculations were made.

Other

Relatively minor quantities of recharge also occur through injection wells operated by Micron, with quantities available in the data release (Hundt, 2023).

Discharge

There are several main components of discharge (or outflow) from the Treasure Valley aquifer system. These include, in decreasing order, discharge to surface water (rivers, agricultural drains, streams, and Lake Lowell), groundwater pumping, and to a much lesser degree, ET from groundwater in wetlands and riparian areas.

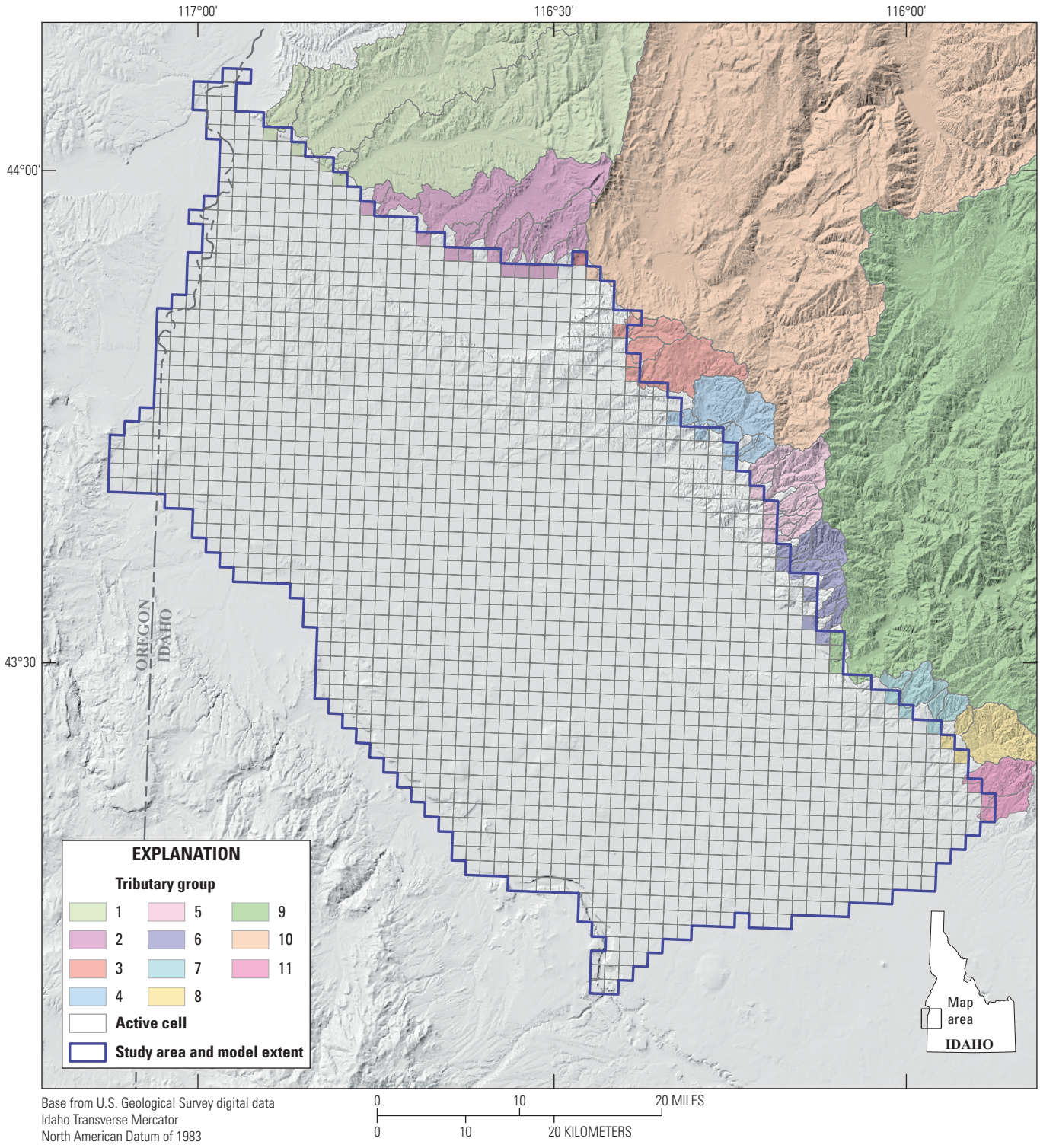

Figure 8. Map showing tributary basins that provide tributary underflow to the western Snake River Plain aquifer system, southwestern Idaho and easternmost Oregon (Moore and others, 2019).

Discharge to Drains

Previous studies have identified agricultural drains and ditches as the primary means by which groundwater discharges from the aquifer. This discharge occurs when the water table rises to the level of the drain or ditch bottom and is carried away as surface flow. Following the recommendation of Petrich (2004), IDWR funded the installation of streamgages on 10 major agricultural drains that discharge to the Boise River, as well as miscellaneous measurements of 3 drains near the confluence of the Boise and Snake Rivers. Idaho Power Company operates an additional streamgage on Indian Creek (fig. 9). For each of these drains, a contributing area was delineated to encompass the network of drains that contribute flow to the measurement location. During the irrigation season water in drains can originate from sources other than groundwater, such as runoff from fields. For this reason, only the drain flow for months outside of the irrigation season, is assumed to represent net groundwater discharge into drains.

Year-round drain measurements began in 2016, with some periodic measurements collected in previous years. As a result, few measurements of drain flow are available for the historical model period of 1986–2015. For each drain measurement location, one or more nearby wells were identified in the IDWR groundwater level database that had regular measurements from 1986 to 2020 and whose water levels fluctuations corresponded to fluctuations in drain flows (fig. 9). Paired measurements of groundwater levels and drain discharge were used to develop regression models, which were then used to estimate drain flows for the historical model period. These models and residual statistics are shown in table 4. For Indian Creek, an additional step was taken to deduct the inflow of treated wastewater from the City of Nampa into the Indian Creek.

Total drain discharges for these areas were simulated by the model and drain discharge estimates served as observations to constrain model parameter estimates. Drain discharge measurements are lacking in several areas with agricultural drains. For these cases, drain discharge could not be differentiated from river seepage, as discussed below.

Discharge to Rivers and Streams

The Snake, Payette, and Boise Rivers all receive discharge from the aquifer throughout all or most of their length within the study area. Groundwater discharge to rivers is simulated by the model, and estimates of discharge are calculated as observations that serve to constrain model parameter estimates. Discharge to the Payette and Boise Rivers are estimated by calculating simple water budgets for reaches between streamgaging locations. These estimates include the minor assumption that there is no change in river storage and the more significant assumption that there is no inflow from natural streams. Additionally, discharge to unmeasured drains was grouped with groundwater discharge to rivers as a single quantity. Figure 9 includes areas for which unmeasured drain flow is grouped with discharge to rivers along with river discharge measurement locations. Discharge was estimated using the following equation (Hundt, 2023):

$$GW_{riv} + GW_{drn;unmeas} = Q_{down} + D - Q_{up} - GW_{drn;meas} \quad (1)$$

where

GW_{riv} is discharge to rivers,
$GW_{drn;unmeas}$ is discharge to unmeasured drains,
Q_{down} is downstream outflow,
D is diversions,
Q_{up} is upstream inflows, and
$GW_{drn;meas}$ is discharge to measured drains.

The ET of groundwater from wetlands and riparian areas was not accounted for in the model nor corrected for in this formula. These estimates of seepage will therefore have a slight upward bias.

Seepage calculations were not made for the Snake River. There is a lack of information about water management within the agricultural and urban areas adjacent to the river, including important measurements of withdrawals from and discharges to the river. This alone could be overcome by lumping unmeasured drain discharges and river seepage together as a single observation target, as is done for parts of the Boise and Payette Rivers. Compounding this challenge, however, is the omission of the land and subsurface to the west of the Snake River from the model area. This area likely contributes a substantial amount of surface discharge and groundwater seepage to the Snake River, but these quantities cannot be distinguished from those that originate from within the model area. Despite these challenges, estimates of seepage to the Snake River from the model area could be worthwhile to pursue as additional work to improve estimates of discharge from the model area. See the “Model Limitations and Suggestions for Additional Work” section for more discussion on this topic.

Pumping

Each of the three classes of water supply entities distinguished in the irrigation supply and demand model–irrigation organizations, water utilities, and private entities–derive some of their supply from pumping wells. Groundwater pumping is the primary source of water for utilities, rural residents, and some industrial and commercial users. While surface water supplies from the Boise and Payette River meet most agricultural needs, agricultural users commonly rely upon groundwater pumping as a supplemental source of water. Additionally, there are several large agricultural areas that rely upon groundwater as their primary source of irrigation water (figs. 4, 5).

Measurements of groundwater pumping are available for some utilities and industrial users (Hundt, 2023) but are incomplete. No pumping records are available for agricultural users.

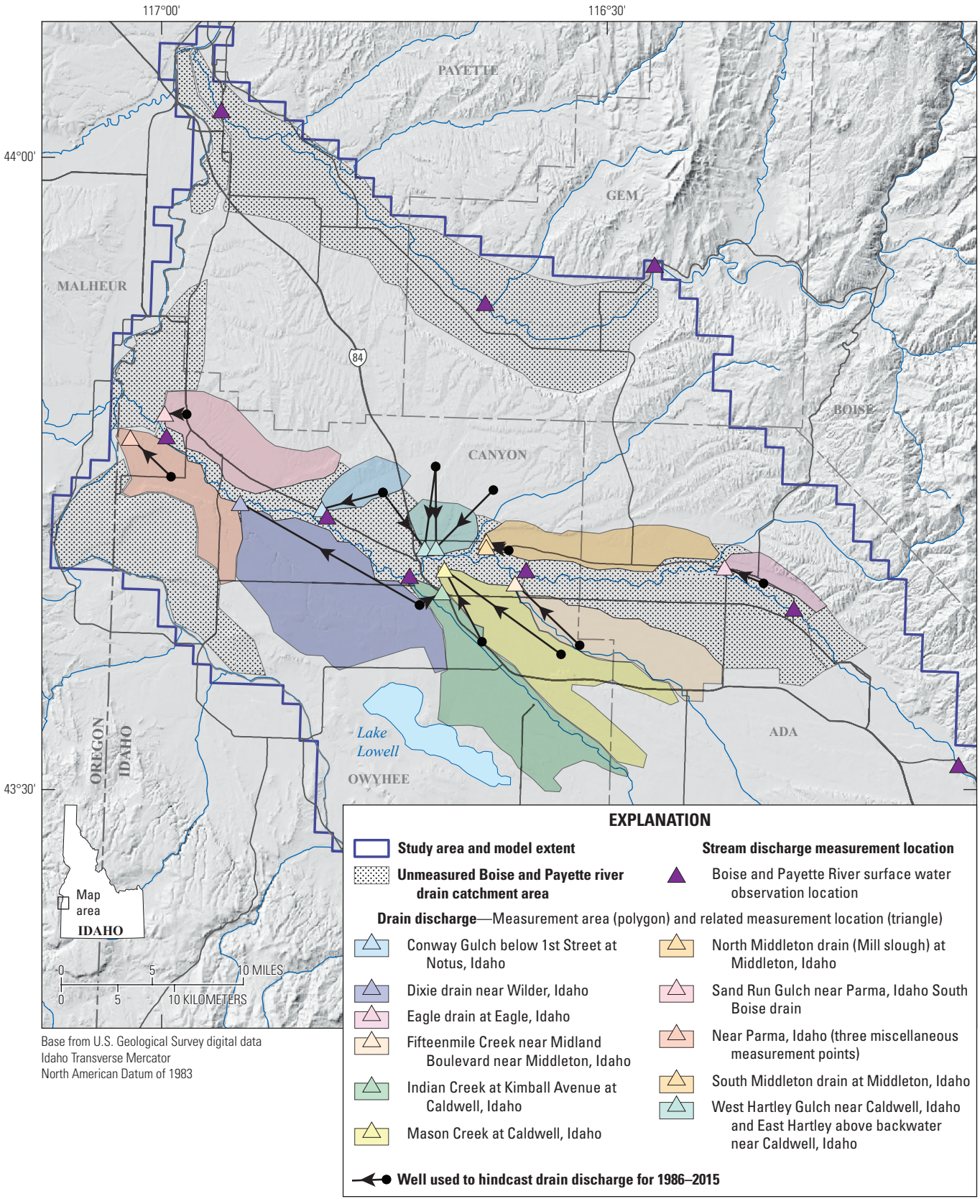

Figure 9. Map showing delineated agricultural drainage networks, drain discharge measurement locations, stream discharge measurement locations, and wells used to hindcast drain discharge for 1986–2015, southwestern Idaho and easternmost Oregon (Hundt, 2023).

Table 4. Regression equations and their significance and coefficient of determination for estimating drain discharge, southwestern Idaho and easternmost Oregon (Idaho Department of Water Resources, 2018a; U.S. Geological Survey, 2021).

[**Abbreviations**: USGS ID, U.S. Geological Survey identifier; R^2, coefficient of determination]

Drain name	USGS ID	Well	Regression equation	p-value	R^2
South Boise	13173630	05N 05W 20CCD1	−4.126X + 83.859	3.56^{-03}	0.52
Eagle	13206400	04N 01E 14CCB4	$27.673X^{-0.901}$ ln(y) = −0.901*ln(X) + ln(27.673)	2.58^{-110}	0.65
Fifteenmile	13210810	03N 01W 06CBBB1	−6.208X + 69.864	1.75^{-107}	0.73
North Middleton	13210824	04N 02W 8ADD1	−10.584X + 48.805	2.80^{-03}	0.24
South Middleton	13210831	04N 02W 8ADD1	−27.405X + 73.369	2.89^{-07}	0.52
Mason	13210980	03N 02W 06ACD1	−18.365X + 386.59	5.38^{-08}	0.70
East Hartley	132109867	05N 03W 15DDC1	−1.092X + 76.68	4.93^{-07}	0.59
West Hartley	13210986	05N 03W 15DDC1	−0.440X + 29.634	3.02^{-14}	0.77
Indian	13211438	04N 03W 27CBAD1	−71.058X + 629.12	2.57^{-16}	0.87
Conway	13212549	05N 04W 35BBB1	−3.251X + 59.738	1.38^{-83}	0.62
Dixie	13212890	04N 03W 27CBAD1	−28.796X + 242.68	1.52^{-06}	0.46
Sand Run	13213072	05N 05W 04BCC1	−6.606X + 154.36	1.03^{-03}	0.37
		05N 05W 13CBC1	−8.705X + 249.58	6.30^{-04}	0.37

Groundwater-Flow Model

A numerical groundwater-flow model of the Treasure Valley aquifer system was developed to better understand hydrologic conditions and to provide water managers a tool that can be used to assess the impact of changing hydrologic stresses.

The Treasure Valley Groundwater Flow Model (TVGWFM; Hundt, 2023) is a three-dimensional finite-difference numerical model constructed with MODFLOW 6 (Langevin and others, 2017). This model builds upon previous modeling efforts by Petrich (2004) and Johnson (2013). This model differs from previous efforts by having a transient historical period, enough vertical model discretization to assess vertical gradients, flux observations from estimated drain discharges; an irrigation supply and demand model that incorporates new land-use and ET data; and a newly developed hydrogeologic framework (Bartolino, 2019a) that informs model discretization and parameter value distribution.

In the development of a groundwater-flow model, assumptions and simplifications are necessary to overcome gaps in data and uncertainty in the conceptual model of the system and to produce a model that can solve quickly enough to be manageable. These assumptions and simplifications can limit how the model should be used. See the "Model Limitations and Suggestions for Additional Work" section for more discussion of this point.

Model Code

MODFLOW 6 (Langevin and others, 2017) has a modular design in which different packages are used to represent the geometry, aquifer properties, solver settings, and boundary conditions used for the model. The packages and package settings used for a MODFLOW 6 model are defined in a collection of ASCII text files. Table 5 shows the boundary types and individual files for the TVGWFM. For information about MODFLOW 6 features and file structure, including any of the packages listed in table 5, please see the official documentation (Langevin and others, 2017).

Discretization

Solving the groundwater-flow equation with a finite-difference approximation requires that the continuous domains of space and time be divided into a grid. The following sections describe how this is implemented for the TVGWFM.

Model Domain

Figure 1 shows the geographic domain of the model. The western boundary of the model domain runs along the Snake River, from the confluence of Sinker Creek downstream to the confluence of the Payette River. The southern boundary aligns with a topographic divide and roughly defined groundwater divide. The northern boundary is delineated where alluvial deposits in the Payette Valley abut alluvium and sedimentary rock at the valley margin, according to a surface geologic map by the Idaho Geological Survey (Lewis and others, 2012). The eastern boundary is where alluvium and sedimentary rock abut the granodiorite and granite of the Boise Front (fig. 1).

Table 5. Treasure Valley Groundwater Flow Model boundaries and representation in MODFLOW 6 (Hundt, 2023).

[**MODFLOW package**: DRN, drain; RIV, river; WEL, well; GHB, general-head boundary]

Boundary	MODFLOW package	Filename
Agricultural drains	DRN	mf6-tv_hist.dis
Boise, Payette, and Snake Rivers	RIV	mf6-tv_hist.riv
Canal seepage (concentrated)	WEL	mf6-tv_hist-canal_leakage-a-canal_dist.wel
Canal seepage (distributed)	WEL	mf6-tv_hist-canal_leakage-b-area_dist.wel
Incidental recharge (irrigated lands)	WEL	mf6-tv_hist-infiltration-irr.wel
Incidental recharge (semi-irrigated lands)	WEL	mf6-tv_hist-infiltration-semi.wel
Lake Lowell	GHB	mf6-tv_hist-lake_lowell.ghb
New York Canal (upper)	WEL	mf6-tv_hist-ny_canal.wel
New York Canal (lower)	RIV	mf6-tv_hist-ny_canal.riv
Groundwater pumpage (irrigated lands)	WEL	mf6-tv_hist-pumping-irr.wel
Groundwater pumpage (semi-irrigated lands)	WEL	mf6-tv_hist-pumping-semi.wel
Groundwater pumpage (municipal)	WEL	mf6-tv_hist-pumping-measured_municipal.wel
Groundwater pumpage (other)	WEL	mf6-tv_hist-pumping-semi-xtra.wel
Tributary underflow (layer 1)	WEL	mf6-tv_hist-tributary_underflow.wel
Tributary underflow (layers 2–6)	WEL	mf6-tv_hist-tributary_underflow-deep.wel

The interface between bedrock and water bearing units was used to define the bottom of the model domain for those locations at which bedrock is present in the hydrogeologic framework model. Elsewhere, the bottom was defined within water bearing materials but at a depth which includes all production and monitoring wells. In these cases, the model bottom was set at the shallower of either 1,200 feet below land surface or 400 feet below the top of the pro-delta and deep lake mudstone facies (Wood, 1997).

Spatial Discretization—Lateral Grid

The model domain is divided laterally into a regular grid of 64 by 65 square cells with side lengths of 1 mile (fig. 10). This grid is aligned closely with previous models (Petrich, 2004; Johnson, 2013). However, the coordinate system of the TVGWFM is defined in the Idaho Transverse Mercator (IDTM), which results in an imperfect alignment with these other grids that are defined in UTM coordinates.

Spatial Discretization—Vertical Layers

Except for the pro-delta and deep lake mudstone facies, model layer elevations in the TVGWFM were defined using water level records. Several multi-level wells and well clusters have been installed throughout the study area with screens or openings that target distinct water bearing zones above or below low-permeability units. Additionally, many pairs of wells can be found that are close geographically but are open to the subsurface at different depths. By looking for instances in which the water levels in these groups of wells differ significantly or where they show different seasonal patterns, one can deduce that a confining unit may be present between the open intervals. Water level records for all pairs of suitable wells were investigated manually to identify these cases.

Confining units that were deduced from water level records were not included as low-permeability model layers. Rather, an effort was made to divide model layers in a way that placed pairs of wells with water level differences in separate layers. Divided as such, the observed vertical differences were included as observation targets in the parameter estimation, and model parameters (notably vertical anisotropy) could be adjusted to reproduce these observations. These model layer divisions were defined manually. Additional objectives for defining layers included having relatively flat (same elevation) layers and limiting the number of layers. Ultimately, not all pairs of water level differences were separated into different layers.

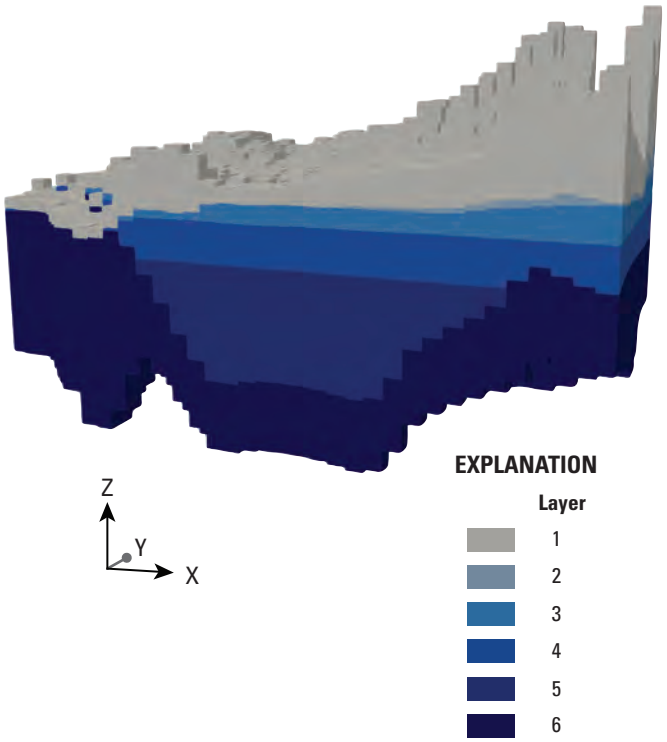

Figure 10. Model cross-section showing layer thickness; clipped at model row 42 and column 45; 50 times vertical exaggeration, southwestern Idaho and easternmost Oregon (Hundt, 2023).

Water level records were used to define six model layers. Below these layers, a final model layer is defined between the pro-delta and deep lake mudstone facies surface and model bottom. The top and bottom layers vary in depth much more than the intermediate layers and intersect with the four other model layers in many areas. Any model cell that had a thickness of less than 10 ft was eliminated as an active model cell, and the cells above and below were connected using a vertical pass-through cell in the structured discretization (DIS) package of MODFLOW 6. Figure 10 shows a cross-section of the model layers. Figures 11–16 show the resulting model layer thicknesses and the location of wells that were used to define layer divisions.

Temporal Discretization

A transient historical simulation was defined for the period 1986–2015 and divided into 360 month-long stress periods. Stress periods were not further subdivided into smaller time-steps. All model inputs with a time dimension were processed into a single constant rate for each stress period. Model outputs are only precise in time to a month.

The transient historical simulation is initiated with a steady-state period. This steady-state period does not represent pre-development conditions. Instead, following the guidance of Anderson and others (2015), a period was defined using the average stresses for a subset of the historical period over which water levels begin and end at roughly the same state. With no (or little) net difference in groundwater levels, the cumulative stresses on the system during this period result in conditions that are, on average, steady. The period 1998–2006 was chosen for calculating average stresses.

Hydraulic Properties

All modeled hydraulic properties of the aquifer and boundaries were set up as parameters whose values were resolved during parameter estimation. Definitions of lithology from the hydrogeologic framework model (Bartolino, 2019b) were used to define upper and lower ranges of properties values as well as their spatial distribution. The hydrogeologic unit properties section below describes how these ranges were calculated. No measurements of local-scale properties, such as from pumping tests, were used to estimate parameter values or ranges.

Pilot-Point Parameterization

A pilot point technique (Doherty and others, 2010) was used to define fields of aquifer properties across the model domain for hydraulic conductivity, storage, and vertical anisotropy. Pilot points enable a collection of sparsely located points of defined parameter values to generate parameter fields that vary smoothly and continuously over the entire model grid. Pilot points were placed in a regular grid, with points located three model cells apart.

Hydrogeologic Unit Properties

The hydrogeologic framework model is a three-dimensional gridded map of hydrogeologic units with a resolution 400 by 400 m laterally and 50 m vertically. The model was used to define the dominant lithology and then set the upper and lower limits of values allowed at each pilot-point. The assigned aquifer properties included hydraulic conductivity, storage, and vertical anisotropy. For each of the four hydrogeologic units from the hydrogeologic framework model–course-grained fluvial and alluvial deposits, Pliocene-Pleistocene and Miocene basalts, fine-grained lacustrine deposits, and granitic and rhyolitic bedrock–values from Freeze and Cherry (1979) were used to assign minimum and maximum values (table 6).

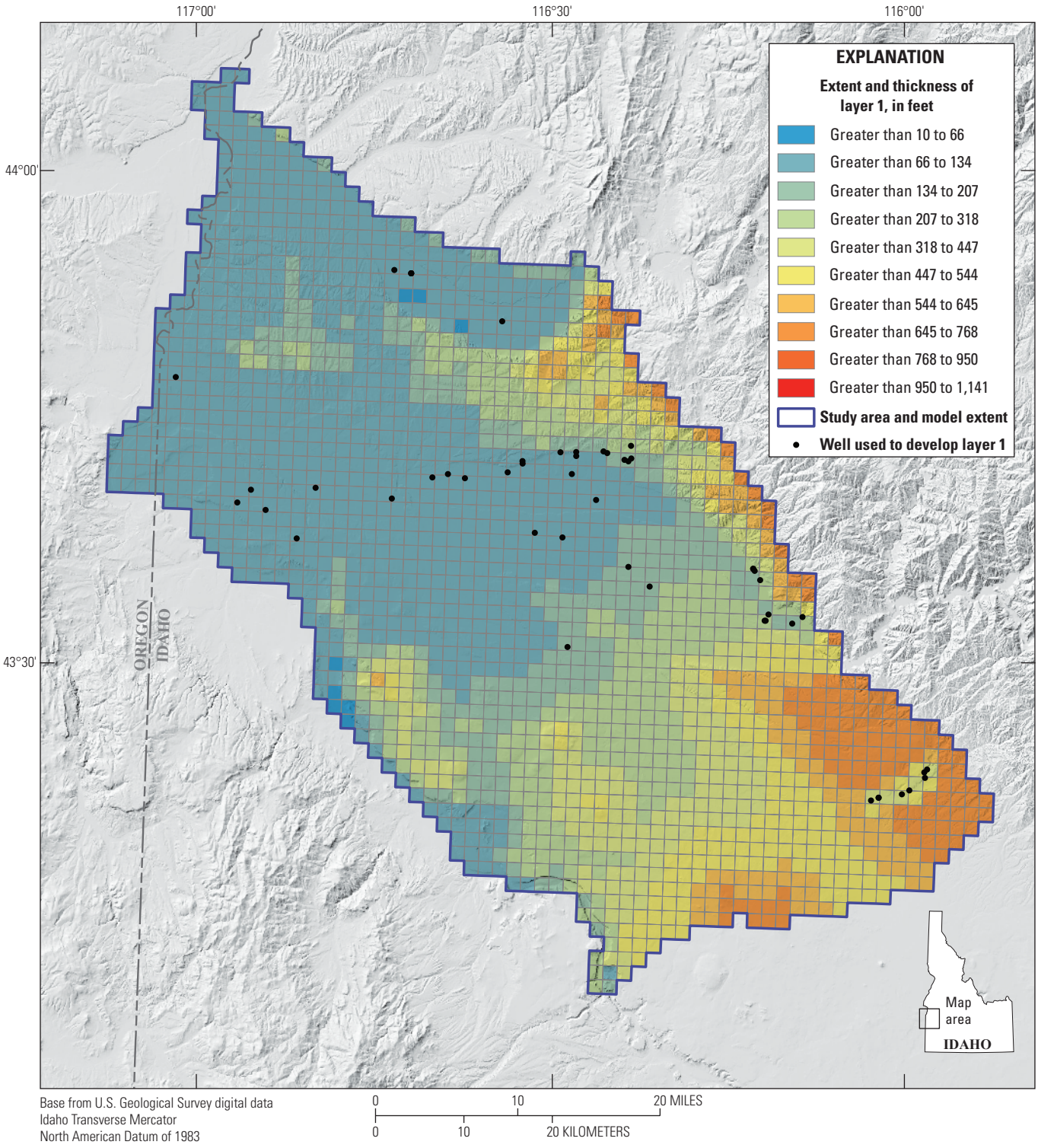

Figure 11. Thickness of model cells in layer 1 and the wells used to define the layer thickness, southwestern Idaho and easternmost Oregon (Hundt, 2023).

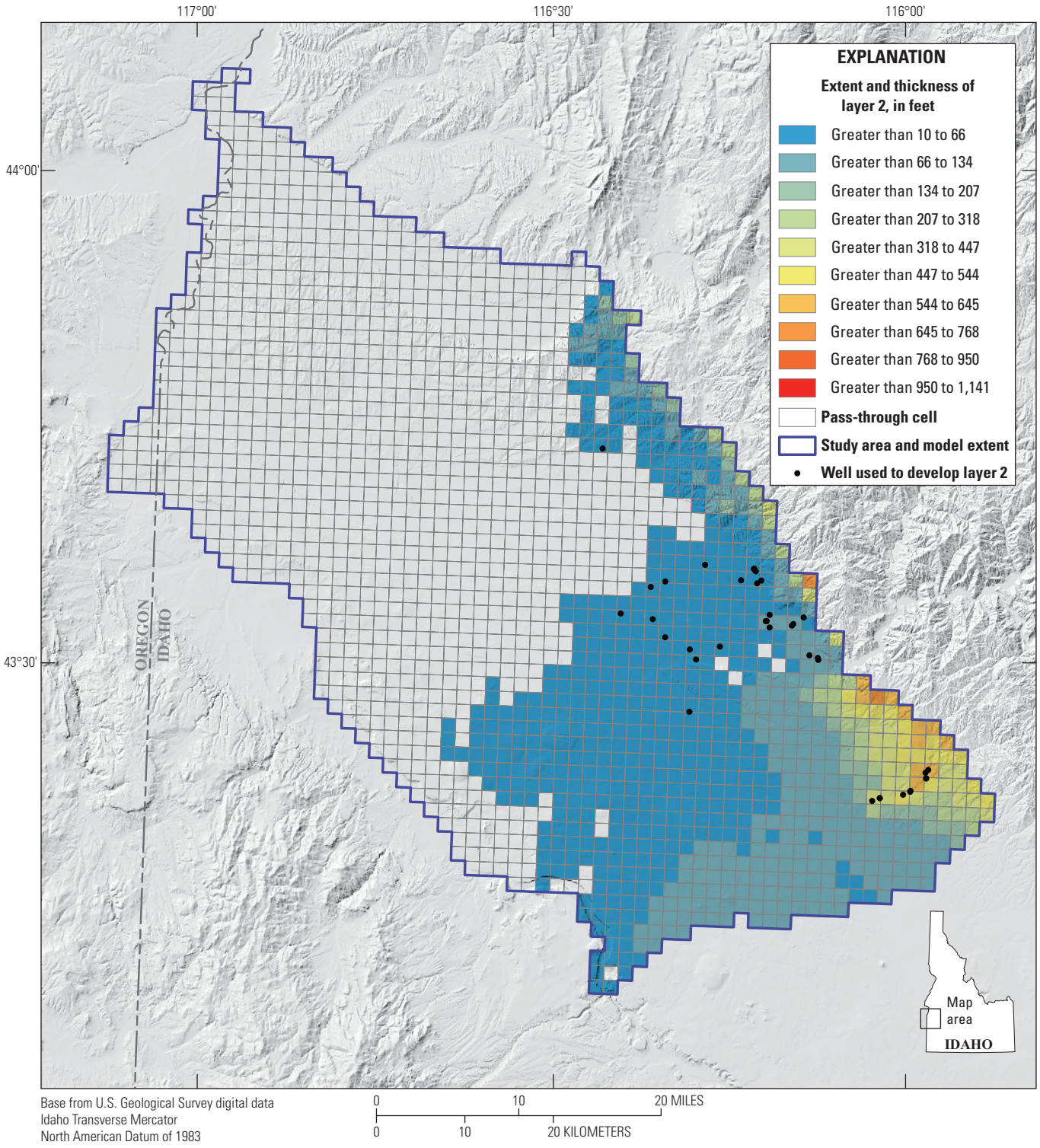

Figure 12. Thickness of model cells in layer 2 and the wells used to define the layer thickness, southwestern Idaho and easternmost Oregon (Hundt, 2023).

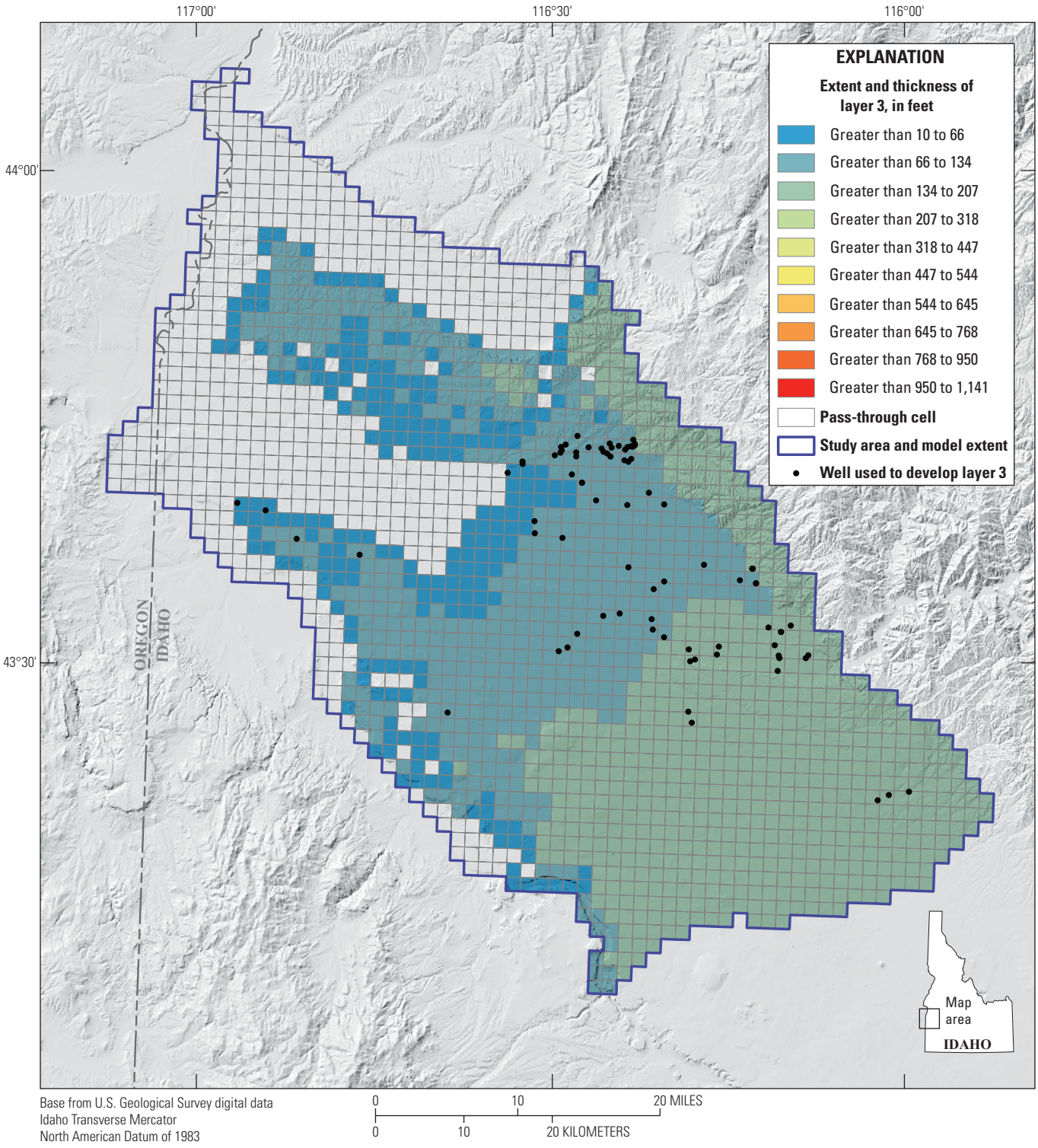

Figure 13. Thickness of model cells in layer 3 and the wells used to define the layer thickness, southwestern Idaho and easternmost Oregon (Hundt, 2023).

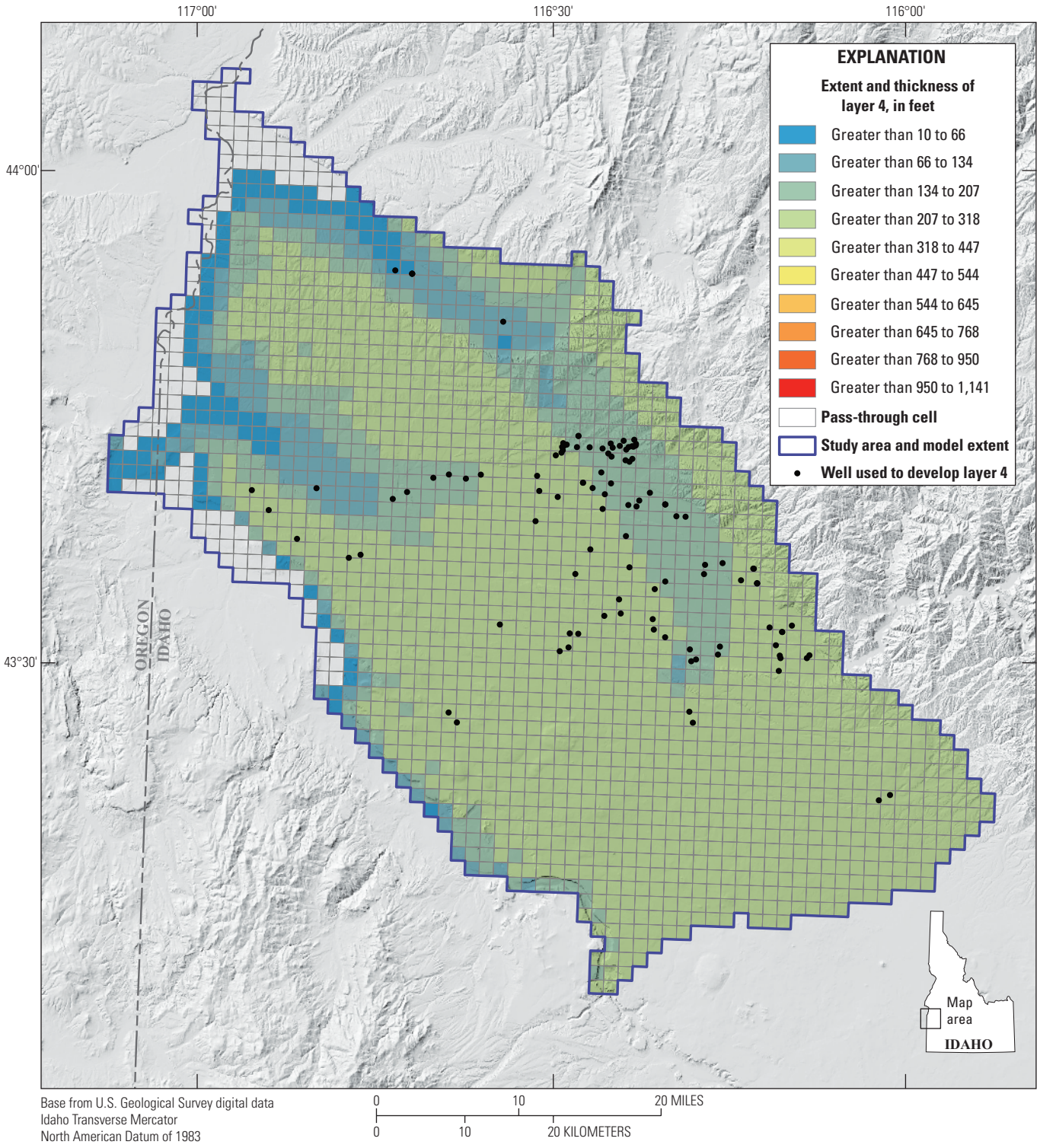

Figure 14. Thickness of model cells in layer 4 and the wells used to define the layer thickness, southwestern Idaho and easternmost Oregon (Hundt, 2023).

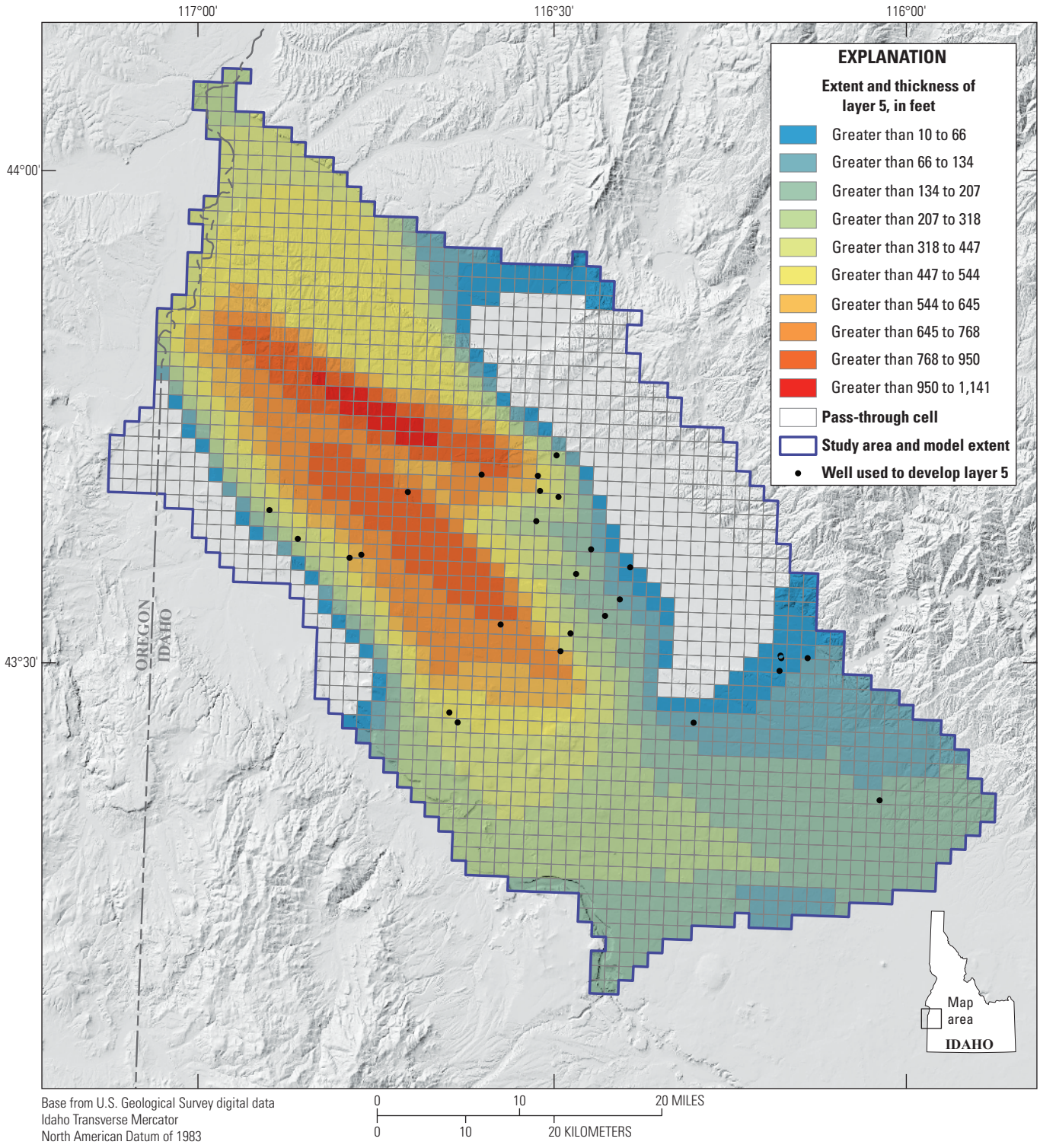

Figure 15. Thickness of model cells in layer 5 and the wells used to define the layer thickness, southwestern Idaho and easternmost Oregon (Hundt, 2023).

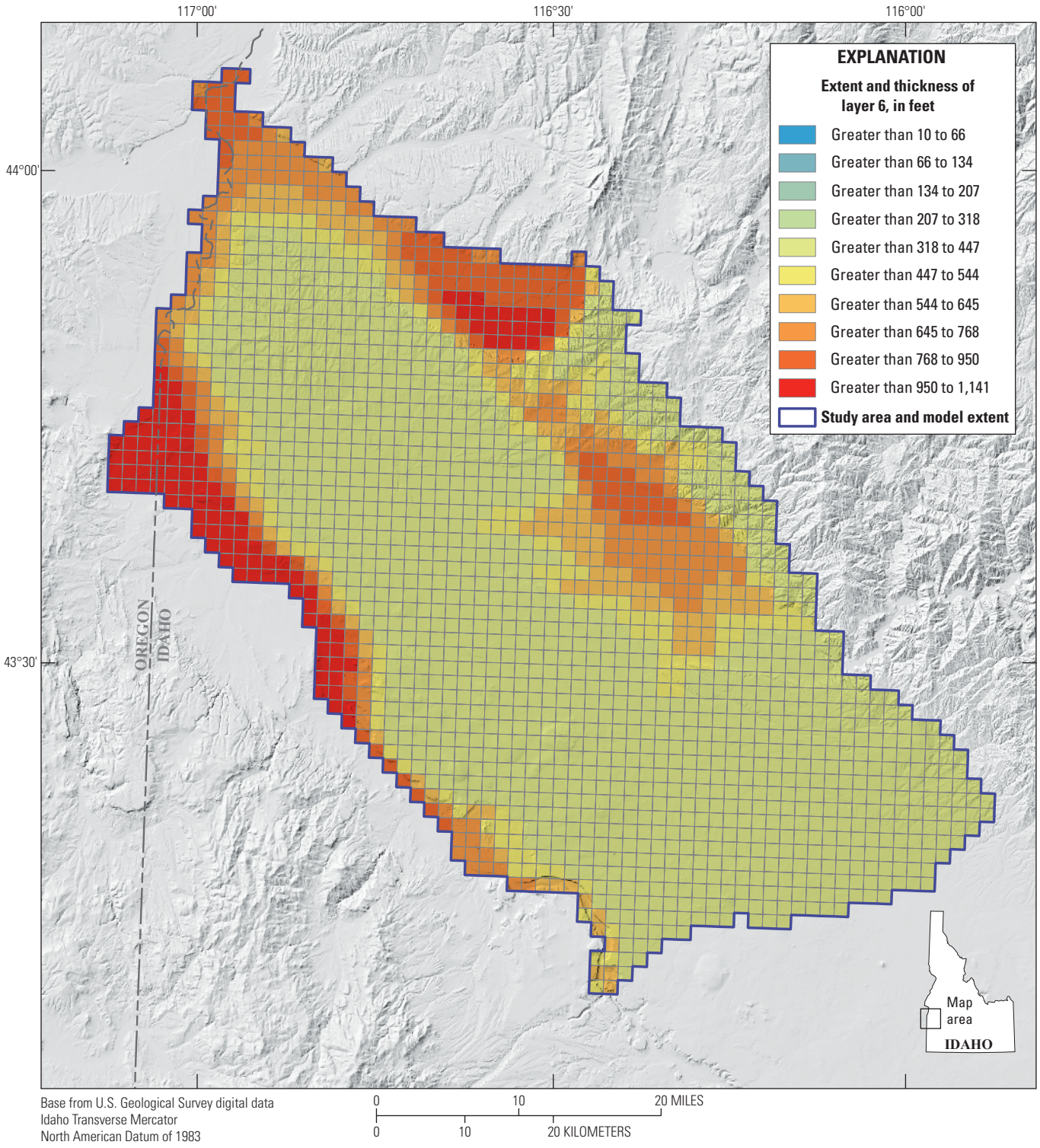

Figure 16. Thickness of model cells in layer 6 and the wells used to define the layer thickness, southwestern Idaho and easternmost Oregon (Hundt, 2023).

Table 6. Initial, minimum, and maximum hydraulic properties assigned to each lithology type (Hundt, 2023).

[**Abbreviations**: feet/day, feet per day; Min, minimum; Max, maximum; cgf, course-grained fluvial and alluvial deposits; bas, Pliocene-Pleistocene and Miocene basalts; fgl, fine-grained lacustrine deposits; grb, granitic and rhyolitic bedrock]

Lithology unit	Lithology unit short name	Hydraulic conductivity (feet/day)			Vertical anisotropy (ratio of vertical to horizontal conductivity–unitless)			Specific storage (feet^{-1})			Specific yield (unitless)		
		Initial	Min	Max	Initial	Min	Max	Initial	Min	Max	Initial	Min	Max
Coarse-grained fluvial and alluvial deposits	cgf	1.00^{3}	1.00^{-2}	2.00^{3}	1.00^{-2}	2.50^{-3}	1.00	1.00^{-3}	1.00^{-4}	1.00^{-2}	1.50^{-1}	5.00^{-2}	3.70^{-1}
Basalt, undifferentiated: includes Pliocene-Pleistocene and Miocene basalts	bas	1.00^{1}	1.00^{-3}	2.00^{1}	1.00^{-3}	2.50^{-4}	1.00	1.00^{-2}	1.00^{-3}	1.00^{-1}	8.00^{-2}	1.00^{-2}	1.80^{-1}
Fine-grained lacustrine deposits	fgl	1.00^{2}	1.00^{-8}	1.00^{-1}	1.00^{-3}	2.50^{-4}	1.00	1.00^{-5}	1.00^{-6}	1.00^{-4}	2.00^{-2}	1.00^{-3}	5.00^{-2}
Granitic and rhyolitic bedrock	grb	1.00	1.00^{-4}	1.00	1.00^{-2}	2.50^{-3}	1.00	1.00^{-6}	1.00^{-7}	1.00^{-5}	1.00^{-3}	1.00^{-4}	1.00^{-2}

Multiple framework model cells fall within each TVGWFM cell (figs. 17–22). For each adjustable parameter within a TVGWFM cell, the range of allowable values was calculated as the weighted mean of the minimum and maximum values assigned to each of the four hydrogeologic units. In this calculation, the weight was equal to each lithology type's proportionate presence within a TVGWFM cell. An arithmetic mean was calculated for hydraulic conductivity and storage, and a geometric mean was calculated for vertical anisotropy.

Vertical Anisotropy

The TVGWFM is modeled as being transversely anisotropic, as is common in sedimentary systems (Anderson and others, 2015). Under this assumption, hydraulic conductivity is isotropic horizontally and anisotropic vertically, or across layers. The TVGWFM uses an anisotropy factor parameter, defined as the ratio of vertical conductivity to horizontal conductivity, to calculate vertical hydraulic conductivity. The storage parameter represents specific yield in model layer one and storativity in model layers two through six.

Boundary Conductance

Several boundaries of the TVGWFM are defined as head-dependent flux boundary conditions where flow is proportional to the difference in head across the boundary. Each of these boundaries includes a conductance parameter that is defined as (Langevin and others, 2017):

$$C = Ak/L \quad (2)$$

where

C is the conductance parameter,
A is cross-sectional area,
k is hydraulic conductivity, and
L is boundary thickness.

The upper and lower limits of conductance were found by choosing realistic ranges of values for A, k, and L and calculating the resulting range of conductance values.

Irrigation Fluxes—Incidental Recharge, Canal Seepage, and Pumping

Incidental recharge from the application of irrigation water, recharge due to seepage from canals, and pumping for irrigation were simulated as specified flux boundaries using the MODFLOW well (WEL) package. Except in those few cases where measurements of irrigation pumping from municipal entities were available, each of these quantities was estimated. Estimates of these flows and the locations at which they occur within the model were framed around two important sources of information: surface water supply in the form of records of diversions, gridded precipitation (PRISM Climate Group, 2020), and crop water demand in the form of gridded estimates of actual ET (Idaho Department of Water Resources, 2020c). The numerical details of this irrigation supply and demand model are described below.

Irrigated Land Use

Lands within the study area were mapped and classified by irrigation status for 1987, 1994, 1997, 2000, 2004, 2007, 2010, and 2015 (figs. 4, 5) (Idaho Department of Water Resources, 2020b). Aerial photographs were used to draw polygons of individual irrigated lands, semi-irrigated (primarily urbanized) lands, and non-irrigated lands. For years without an irrigation status map, the map from the closest year was used. Figure 6 shows the total area of each irrigation status class over the model period.

Irrigation status polygons have a few uses in the irrigation supply and demand model. Monthly precipitation and ET were calculated for irrigation status polygons before being combined and merged with other polygons within the same SDAs. For this purpose, irrigation status polygons that spanned multiple SDAs were divided along SDA boundaries. Irrigation status polygons were also used to define how some recharge and discharge that were calculated for SDAs were distributed to model cells. For this purpose, polygons were overlayed upon the model grid to find the proportion of each irrigation status area that fall within each model cell.

Evapotranspiration Demand and Irrigation Requirements

To calculate the ET of irrigation status polygons, actual ET raster datasets (Idaho Department of Water Resources, 2020c) were overlayed on the polygons, the average actual ET of all raster cells intersecting a polygon was calculated, and this average ET was multiplied by the polygon area. The ET of an SDA was then calculated by summing the ET of polygons within the SDA. The relative amount of ET in model cells of an SDA was calculated by intersecting the polygons with the model grid and summing the ET of all parts of the irrigation status polygons that fall within each model cell. Each of these steps were performed separately for irrigated lands and semi-irrigated lands.

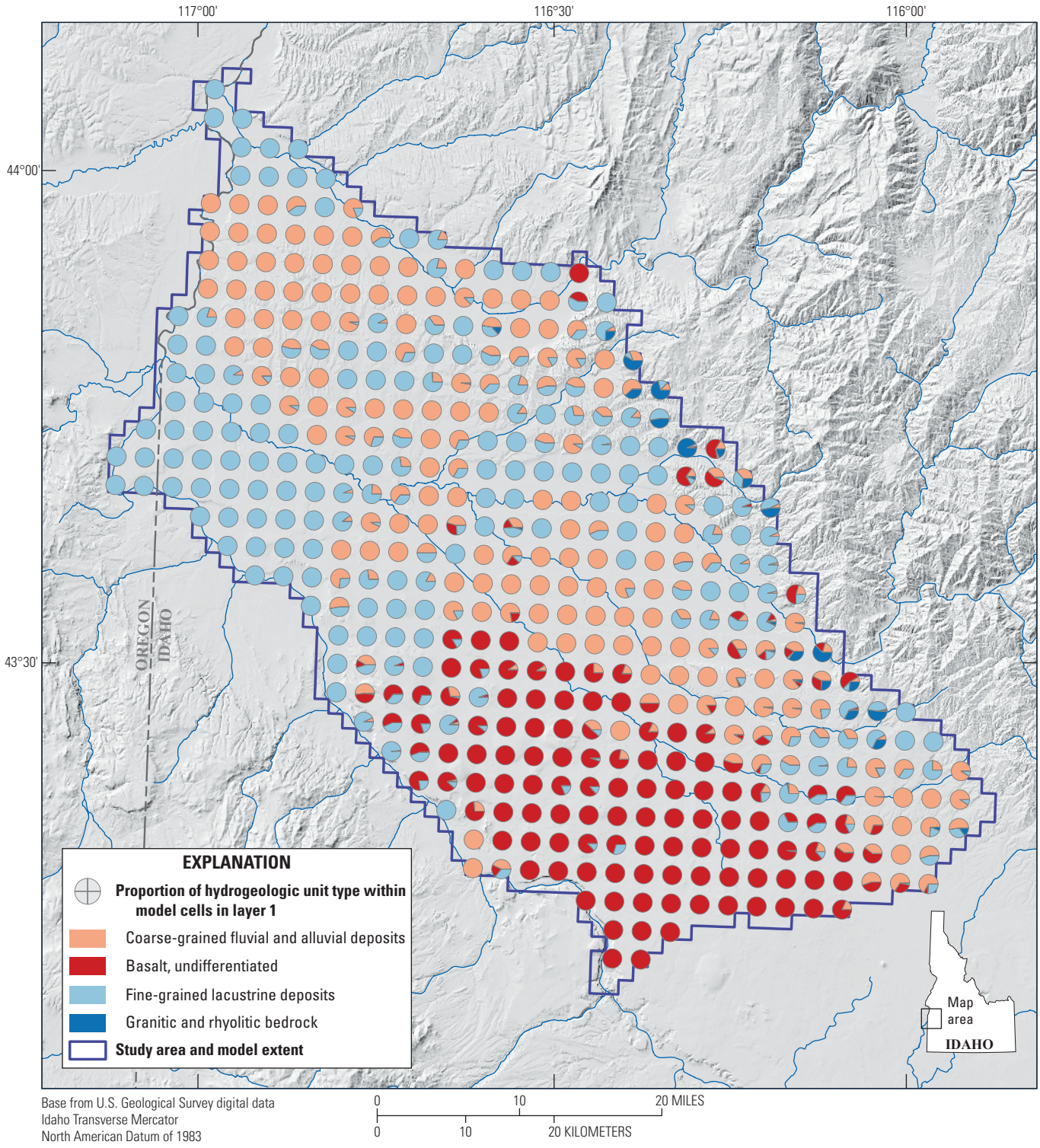

Figure 17. Proportion of hydrogeologic unit type within model cells in layer 1, southwestern Idaho and easternmost Oregon. Not all cells shown (Hundt, 2023).

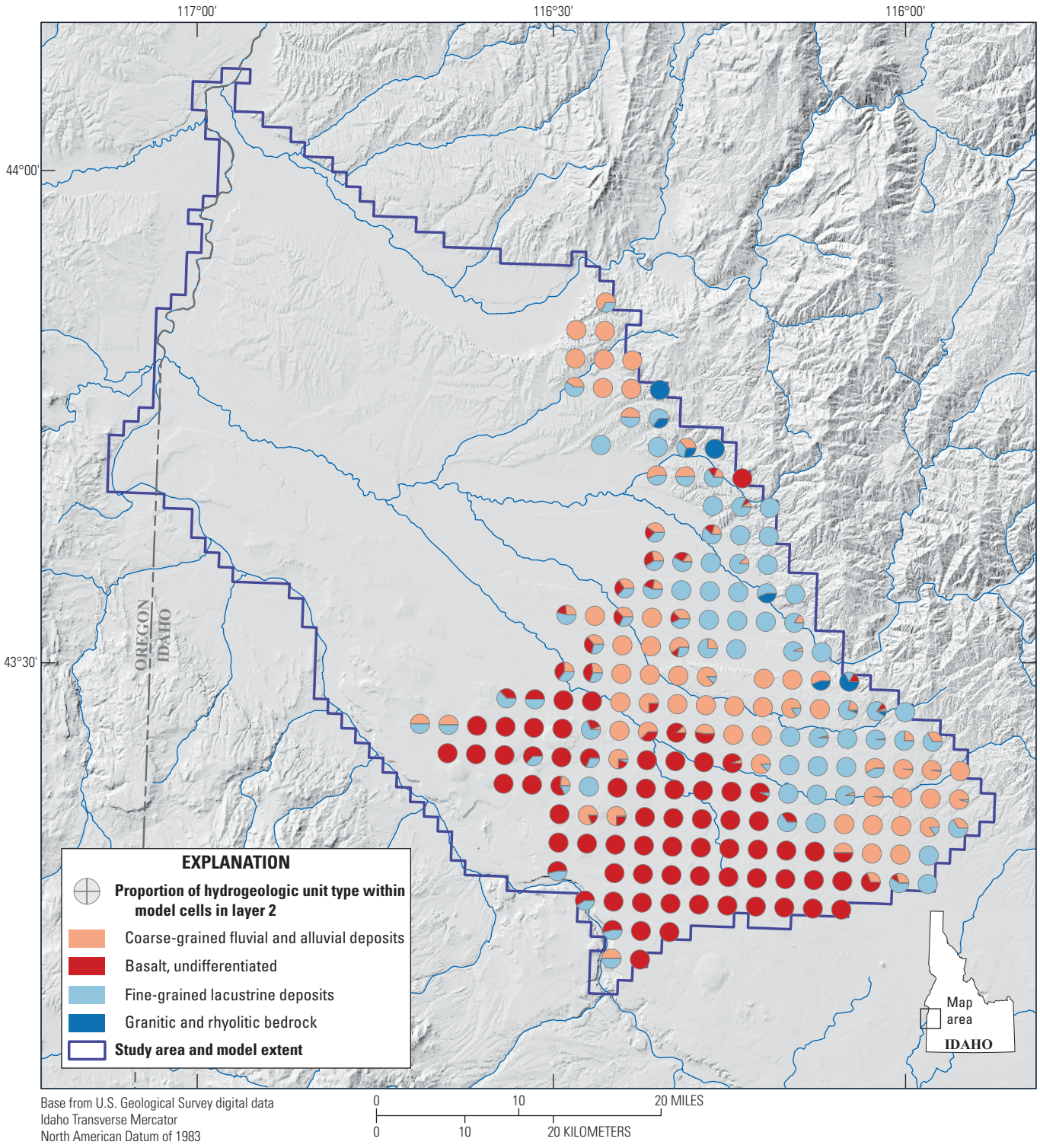

Figure 18. Proportion of hydrogeologic unit type within model cells in layer 2, southwestern Idaho and easternmost Oregon. Not all cells shown (Hundt, 2023).

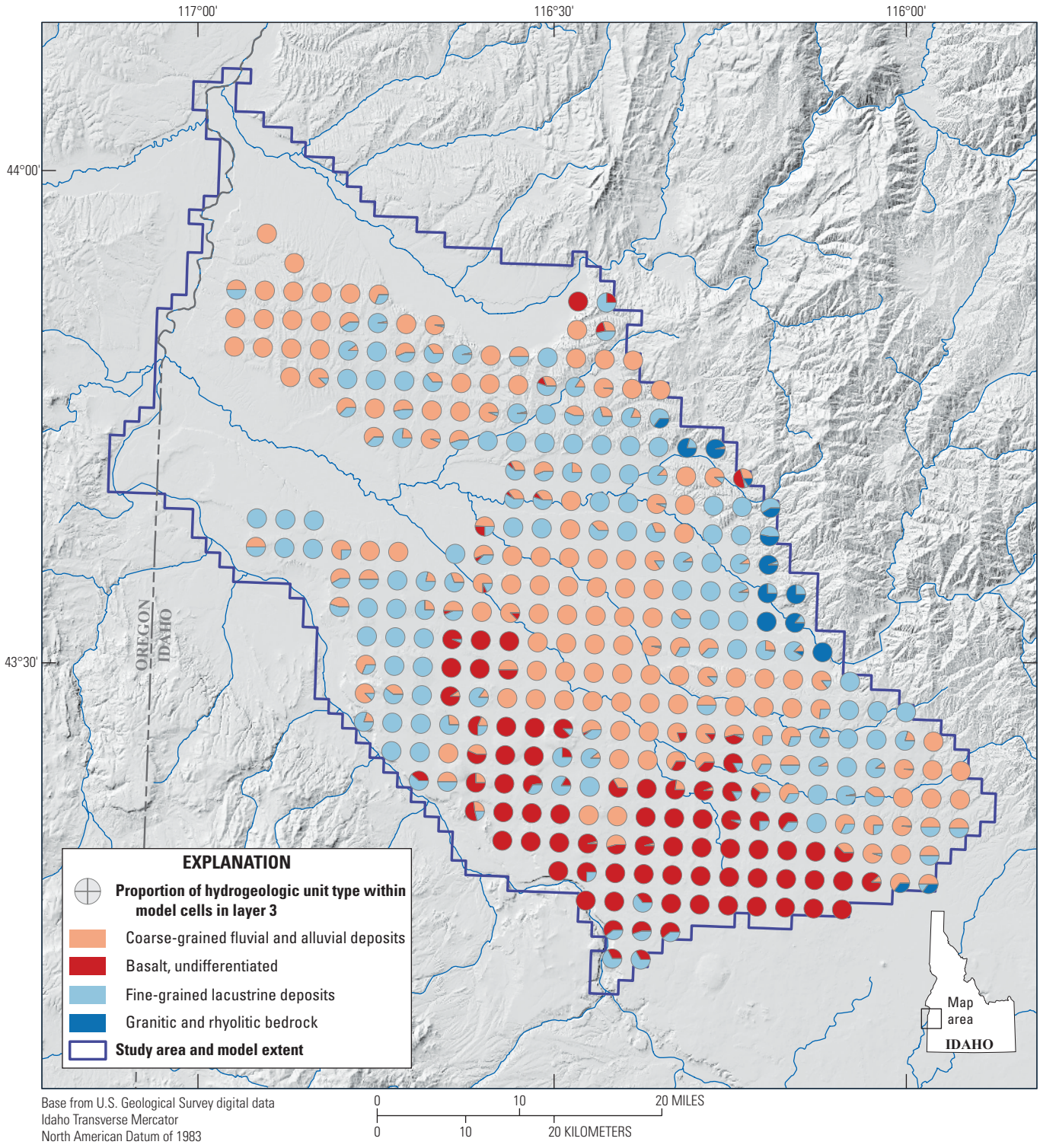

Figure 19. Proportion of hydrogeologic unit type within model cells in layer 3, southwestern Idaho and easternmost Oregon. Not all cells shown (Hundt, 2023).

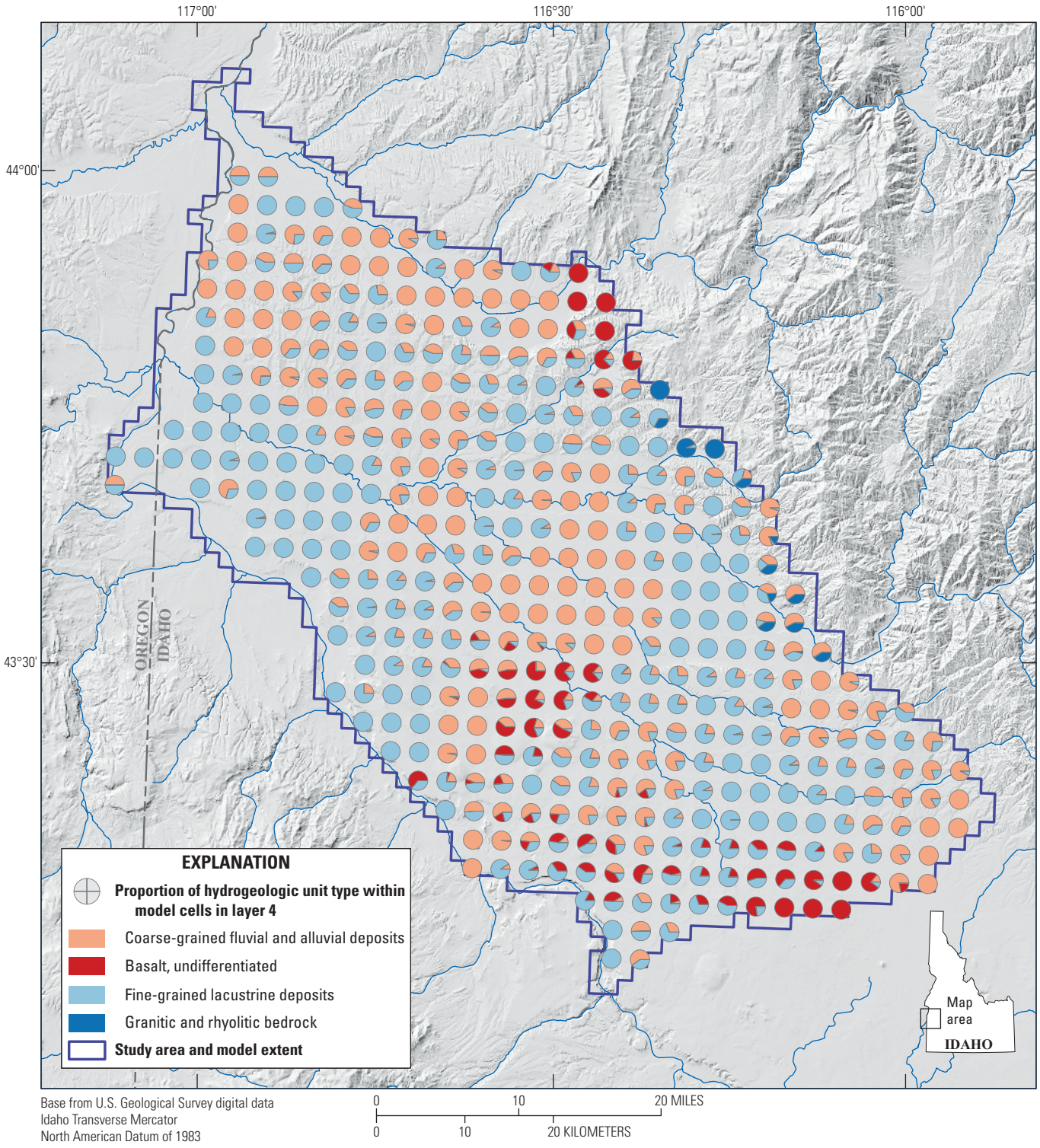

Figure 20. Proportion of hydrogeologic unit type within model cells in layer 4, southwestern Idaho and easternmost Oregon. Not all cells shown (Hundt, 2023).

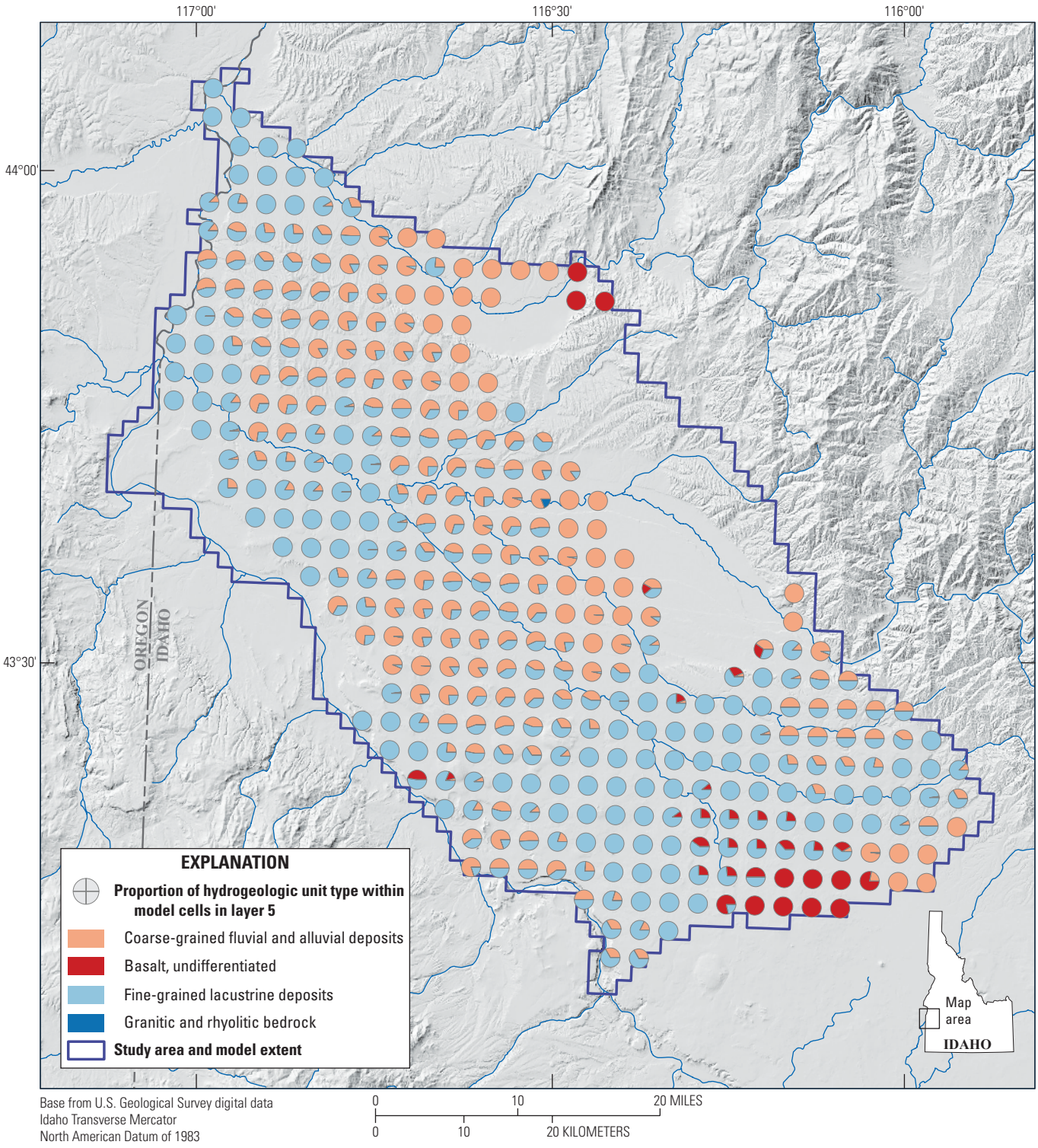

Figure 21. Proportion of hydrogeologic unit type within model cells in layer 5, southwestern Idaho and easternmost Oregon. Not all cells shown (Hundt, 2023).

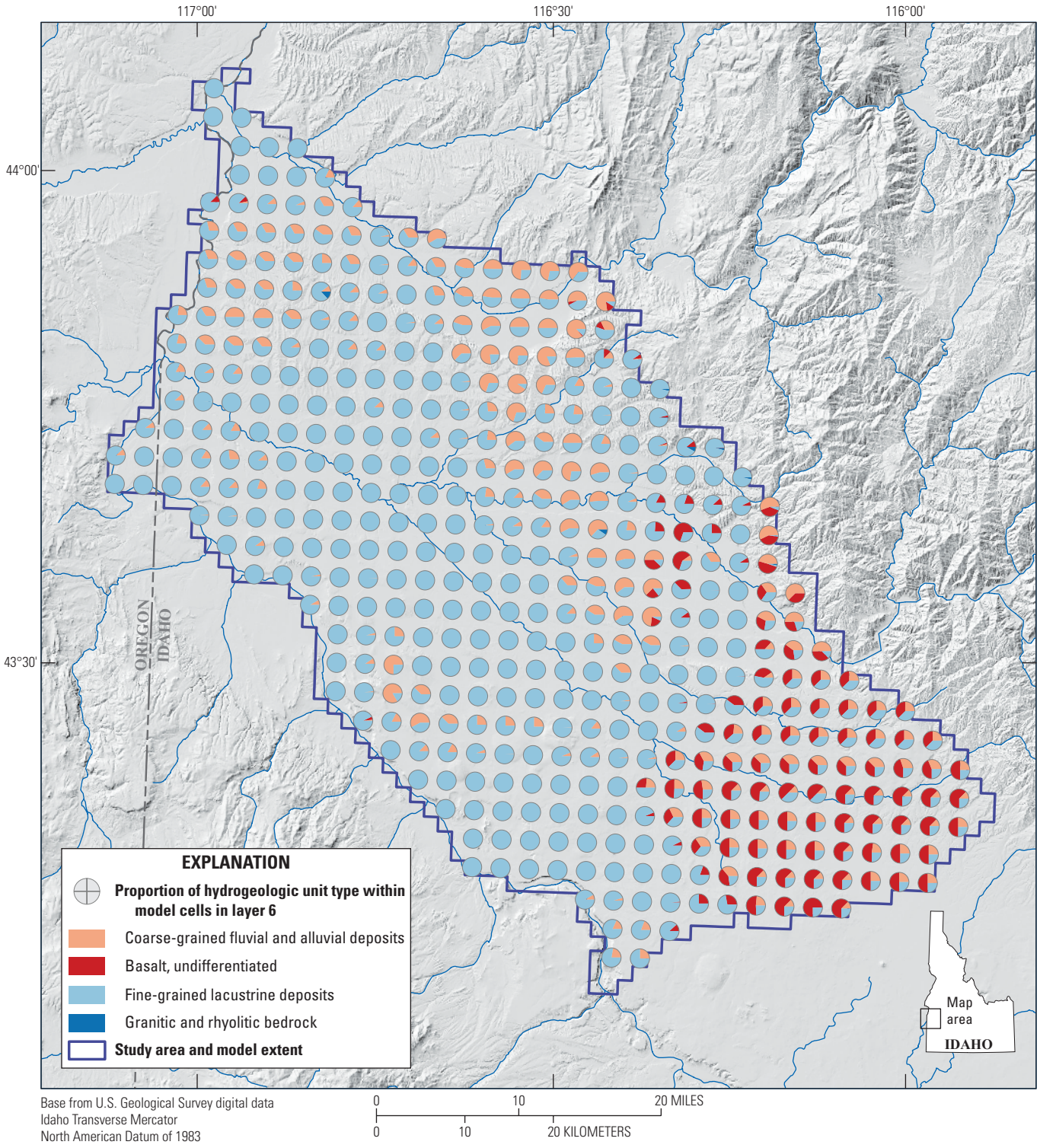

Figure 22. Proportion of hydrogeologic unit type within model cells in layer 6, southwestern Idaho and easternmost Oregon. Not all cells shown (Hundt, 2023).

Irrigation Supply and Demand Model

The calculation of incidental recharge, canal seepage, and pumping begins with a simple soil water balance of the form:

inflow (supply) – outflow (demand) = change in soil storage (3)

This calculation is applied individually to every SDA and every month of the model period. Additionally, these calculations are made separately for irrigated and non-irrigated areas. Inflows (supplies) are calculated as:

$$Supply = P + D_{sw} \times \left(1 - f_{seep}\right) + GW_{irr} \quad (4)$$

where

P is precipitation,
D_{sw} is diversions,
f_{seep} is canal seepage, and
GW_{irr} is groundwater irrigation.

Inflows include precipitation (P), surface-water irrigation, and groundwater irrigation ($GWirr$). Surface-water irrigation is set equal to diversions (D_{sw}) minus a constant percentage lost to canal seepage (f_{seep}). This is split between irrigated and semi-irrigated areas in proportion to the total ET demand of each irrigation class within an SDA for that month. In cases where surface water irrigation exceeds demands the excess water is split as a fixed proportion (f_{xinf}) between additional infiltration and flow that continues through the canal system undelivered. This proportion is adjusted during parameter estimation. Groundwater pumping to meet agricultural and urban landscaping irrigation demands (GW_{irr}) is estimated by the irrigation supply and demand model. This pumping is assumed to make up the difference in the water balance in cases where precipitation and surface-water irrigation are insufficient to meet demands. Unless there is a deficit from the combined precipitation, soil moisture, and delivered surface water, groundwater pumping for irrigation is assumed to be zero. Groundwater pumping for irrigation is calculated separately for irrigated and semi-irrigated lands. Groundwater pumping to meet indoor municipal demands is not considered as a part of the irrigation supply and demand model.

Outflows (demands are calculated as):

$$Demand = f_{ET} \times ET \times \left(1 + f_{inf}\right) \quad (5)$$

where

f_{ET} is factor adjusted during parameter estimation,
ET is evapotranspiration, and
f_{inf} is base amount representing irrigation (in) efficiency calculated as a fixed factor of ET.

Outflows include ET and infiltration. ET from gridded datasets is multiplied by a factor (f_{ET}) that was adjusted during parameter estimation. This factor was added to account for uncertainty in the ET dataset. A base amount of infiltration that represents irrigation (in)efficiency is calculated as a fixed factor (f_{inf}) of ET. Separate infiltration factors are defined for irrigated and semi-irrigated lands. Additional infiltration occurs when surface water supplies exceed demands, but this is not considered a demand in the irrigation supply and demand model.

From December through February, it is assumed that soil moisture storage (S) increases, with 50 percent of December precipitation, 75 percent of January precipitation, and 100 percent of February precipitation contributing to a buildup of soil moisture during the winter months. This winter buildup is assumed to all be released in March when it is treated as an additional source of water. In all other months, the change in soil storage is assumed to be zero.

The soil water balance thus becomes:

$$\overbrace{P + D_{sw} \times \left(1 - f_{seep}\right) + GW_{irr}}^{supply} - \overbrace{f_{ET} \times ET \times \left(1 + f_{inf}\right)}^{demand} = \Delta S \quad (6)$$

In cases where surface water supplies and precipitation are insufficient to meet demand, groundwater pumping and infiltration are:

$$GW_{irr} = \overbrace{f_{ET} \times ET \times \left(1 + f_{inf}\right)}^{demand} + \Delta S - P - D_{sw} \times \left(1 - f_{seep}\right) \quad (7)$$

$$Infiltration = base\ infiltration = f_{inf} \times ET \quad (8)$$

In cases where surface water supplies and precipitation meet or exceed demand, groundwater pumping and infiltration are:

$$GW_{irr} = 0 \quad (9)$$

$$Infiltration = \overbrace{f_{inf} \times ET}^{base\ infiltration} + \overbrace{f_{xinf} \times \left(P + D_{sw} \times \left(1 - f_{seep}\right) - f_{ET} \times ET \times \left(1 + f_{inf}\right) - \Delta S\right)}^{surplus\ infiltration} \quad (10)$$

Finally, in either case recharge from canal seepage is:

$$canal\ seepage = D_{sw} \times f_{seep} \quad (11)$$

Spatial Allocation of Irrigation and Precipitation on Irrigated and Semi-Irrigated Lands

Recharge resulting from precipitation and applied irrigation water on irrigated and semi-irrigated lands were simulated as specified flux boundaries using the well (WEL) package. All recharge was in layer 1. Recharge on irrigated and semi-irrigated lands were each defined in their own WEL package file.

Recharge from the infiltration of applied irrigation water is distributed to model cells within a SDA in proportion to the ET demand within each model cell. This process is done separately for irrigated and semi-irrigated lands in an SDA to account for differences in irrigation efficiency.

Spatial Allocation of Canal Seepage

Seepage from other canals was simulated as a specified flux boundaries using the well (WEL) package. All recharge was in layer 1. Two WEL package files were used for recharge from canal seepage: one for concentrated recharge and one for distributed recharge.

Recharge from canal seepage is divided between recharge that is concentrated at major canals and recharge that is distributed throughout the irrigated area. For recharge concentrated at canals, recharge is placed only in those cells of an SDA which contain major supply canals or laterals. This recharge volume is divided amongst these cells in proportion to the relative length of major supply canals and laterals that fall within each cell. Distributed canal recharge represents seepage that occurs in the parts of the water conveyance system that connect major canals to individual fields. This part of canal seepage is distributed to model cells within an SDA in proportion to the relative amount of irrigated or semi-irrigated lands that fall within each cell. The split between concentrated and distributed canal recharge is solved through parameter estimation and fixed throughout the model period and is the same for all SDAs. For SDAs without a mapped major canal, all canal seepage is distributed.

Spatial Allocation of Pumping

Groundwater pumping is simulated as a specified flux boundary condition using the well (WEL) package. Separate WEL package files are included for unmeasured pumping for irrigated areas, unmeasured pumping for semi-irrigated areas, measured or estimated pumping from municipal wells, and pumping from other measured wells.

The lateral distribution of groundwater pumping to model cells is calculated in two steps. First, pumping is distributed to model cells in proportion to the relative quantity of water rights for wells that fall within each cell. The IDWR water rights database (Idaho Department of Water Resources, 2019) was queried to locate all groundwater rights within the study area along with their points of diversion locations and water volume. Second, these proportions were adjusted to ensure that the ratio of pumping in those cell(s) with the most and least amount of water rights did not exceed 20. This was a manual adjustment made during parameter adjustment to improve model performance. This adjustment includes all model cells in an SDA, even those without groundwater points of diversion.

For each model cell with groundwater pumping for irrigation, pumping is further distributed among model layers. A sample of 7,019 well logs were examined to identify altitude intervals over which each well is open to the aquifer. Using this sample, a synthetic well – representing not any single well but a grouping of wells with approximated construction and pumping characteristics - was developed for each model cell located at the cell center, with the top and bottom of the open interval calculated by averaging the intervals of all inspected wells within 3 miles of the cell center. Irrigation, municipal, and commercial well logs were used to generate synthetic wells for irrigated lands and semi-irrigated lands falling within city boundaries. Domestic well logs were used for semi-irrigated lands falling outside of city boundaries. Figures 23 and 24 show how the open intervals of synthetic wells are distributed among model layers. Finally, pumping was assigned to individual layers in proportion to the product of open interval length and hydraulic conductivity.

Simulation of Non-Irrigation Recharge and Discharge

New York Canal

The upper New York Canal was simulated as a specified flux boundary using the well (WEL) package. The cells representing this boundary were chosen by selecting all model cells that contain a canal segment and then manually eliminating some cells to minimize the effective width of the canal boundary. The total monthly seepage from the upper New York Canal is estimated using the following formula:

$$f_{ny} \times (div - del - I_{Lowell}) \quad (12)$$

where

f_{ny} is a factor that is adjusted during parameter estimation (final value of 1.03).
div is the diversion into the canal,
del is the deliveries to Boise Project irrigators, and
I_{Lowell} is the flow into Lake Lowell.

This total seepage is distributed to cells in proportion to the length of the canal contained within them. The model cells representing the upper New York Canal are shown on figure 25.

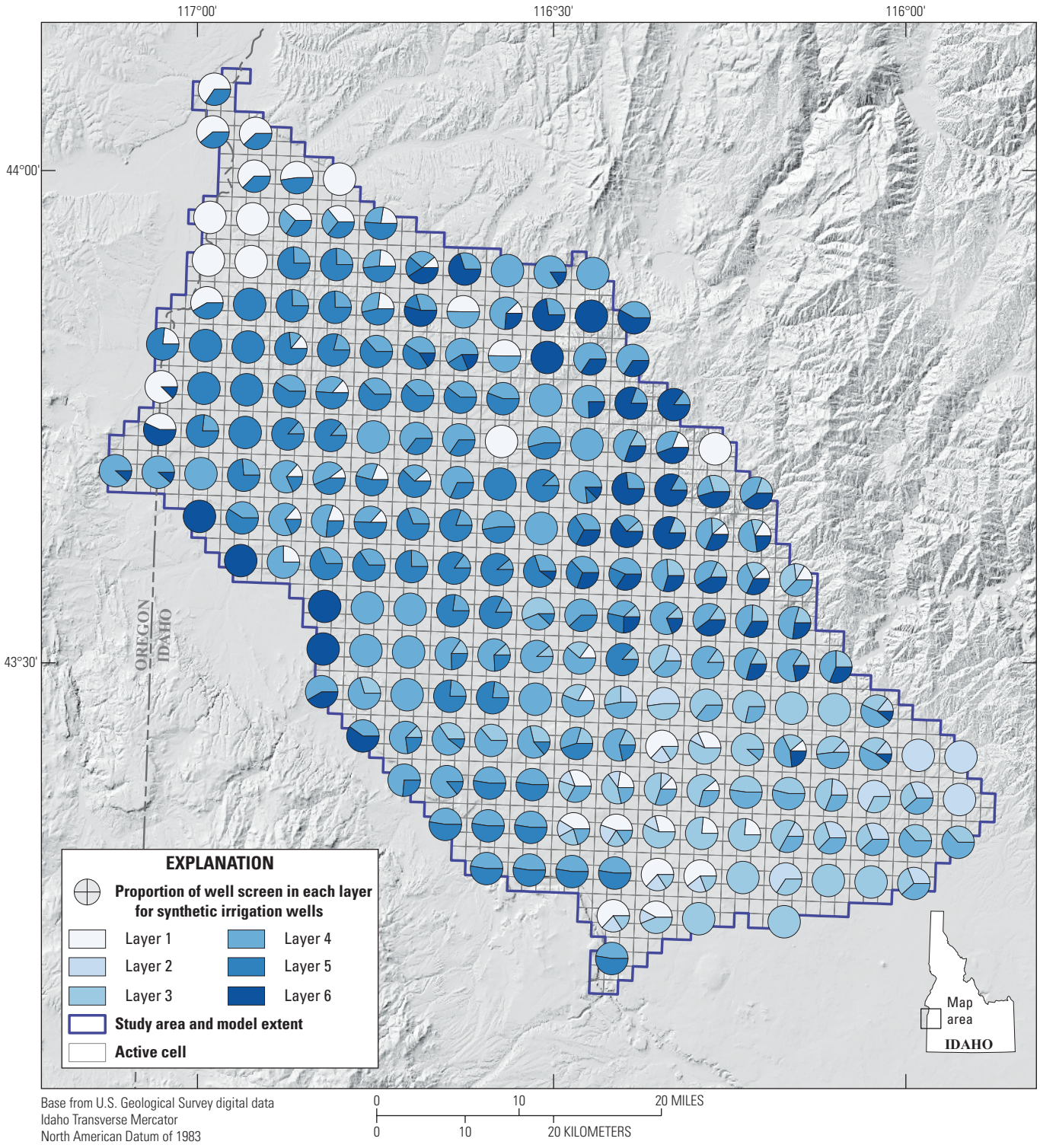

Figure 23. Proportion of open well interval in different layers for synthetic irrigation wells, southwestern Idaho and easternmost Oregon (Hundt, 2023).

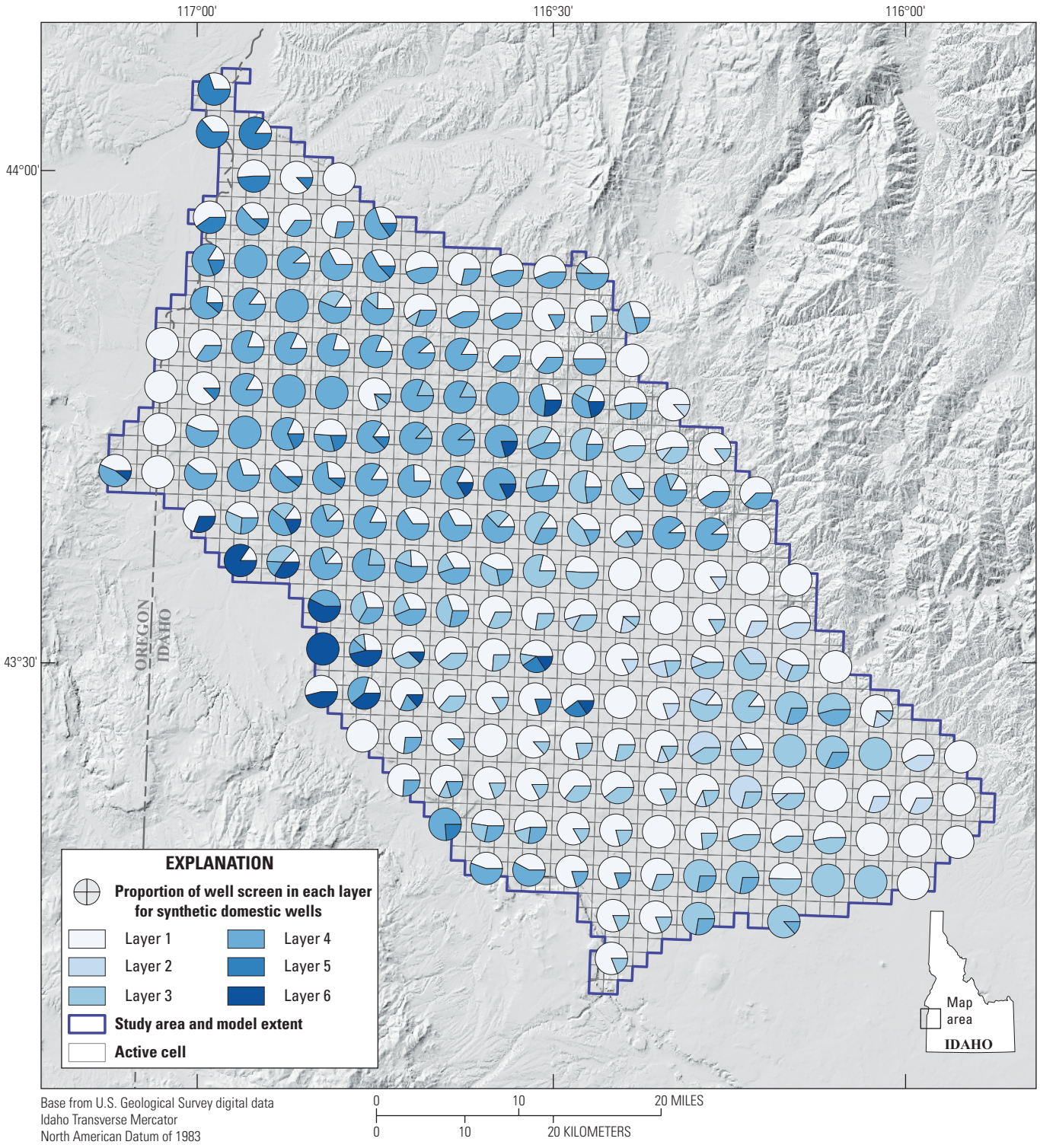

Figure 24. Proportion of open well interval in different layers for synthetic domestic wells, southwestern Idaho and easternmost Oregon (Hundt, 2023).

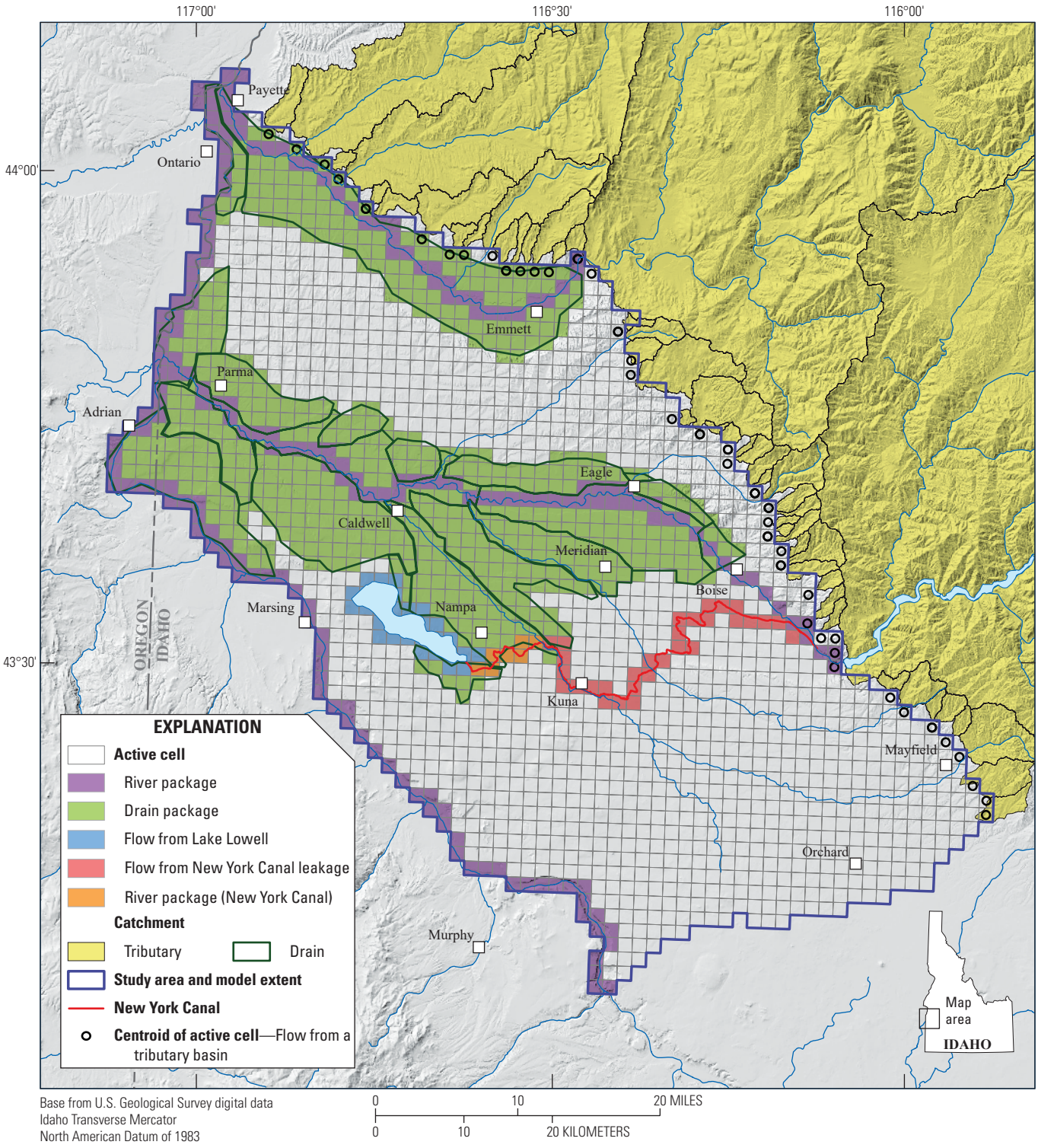

Figure 25. Locations of boundary cells representing drains, rivers, Lake Lowell, New York Canal, and tributary underflow, southwestern Idaho and easternmost Oregon (Hundt, 2023).

The lower New York Canal was simulated as a head-dependent flux boundary using the river (RIV) package. The cells representing this boundary were chosen by selecting all model cells that contain a canal segment and then manually eliminating some cells to minimize the effective width of the canal boundary. The conductance value does not change over time and was included in the parameter estimation. A multiplier variable was used to adjust the relative conductance of cells to be proportional to the length of the canal contained within them. The RIV river bottom variable is set equal to the 2.5th percentile of the ground surface altitudes within the model cell (Gesch and others, 2018). During the irrigation season, the stage of the boundary is set 2 ft above the river bottom. In the non-irrigation season, the stage is set equal to the river bottom. This restricts the boundary to only receive discharge during the irrigation season stress-periods.

Mountain-Front Recharge

Mountain-front recharge was simulated as a specified flux boundary condition using the well (WEL) package. Mountain-front recharge for watersheds that enter the model domain on the northern and eastern boundaries (fig. 19) was calculated using a process based on groundwater-recharge estimates for the entire Dry Creek Experimental Watershed by Aishlin (2006) and Aishlin and McNamara (2011). They found that recharge ranged from 0 to 11 percent of the annual precipitation; the mean of the range is 5.5 percent.

Mountain-front recharge for the groundwater-flow model was determined by a several step process. This process aimed to apply the recharge estimates from the Dry Creek Watershed (Aishlin, 2006; Aishlin and McNamara, 2011) to the remaining small watersheds along the eastern and northern boundary of the model using the area, altitudes, and precipitation of each watershed. The following steps were taken:

1. Tributary basins along the northern model boundary (16 along the Payette River and 30 along the Boise and Danskin Mountains) were delineated using a geographic information system (GIS) by applying flow-accumulation routines to a 30-m digital elevation model (DEM) (U.S. Geological Survey, 2020).

2. The average infiltration rate of the tributary basins was scaled compared to Dry Creek based upon their altitude, with greater infiltration rates at high altitude and lesser at low altitude. The average altitude of the basin above its intersection with the model boundary was determined and multiplied by the mean recharge of 5.5 percent of the precipitation in the Dry Creek Experimental Watershed to obtain an “infiltration scalar” value for each tributary basin.

3. The altitude of each DEM raster cell within the delineated tributary basin was divided by the infiltration scalar to calculate the “infiltration fraction” for each DEM raster cell in the basin.

4. Monthly precipitation for the 360-month model period was determined using the monthly PRISM precipitation datasets with a raster size of 4 kilometers (2.5 mi) (PRISM Climate Group, 2020). The “monthly infiltration rate” for each raster cell of the DEM was then calculated by multiplying the monthly precipitation value from the PRISM raster by the infiltration fraction.

5. The monthly mean infiltration rate for the entire tributary basin is then calculated from the DEM raster values and multiplied by the basin area to get a “monthly infiltration volume” for each tributary basin.

6. The monthly infiltration volume for each tributary basin was assigned to the boundary cell at each basin outlet as a specified groundwater flow (some boundary cells sum the monthly infiltration volumes for several tributary basins).

7. Finally, estimates of mountain-front recharge were further modified by including an adjustable multiplier in the parameter estimation that scales rates upward or downward for the entire model period.

For 11 groups of watersheds (fig. 8), 11 factors were defined.

Precipitation on Non-Irrigated Lands

Non-irrigated lands in the study-area are primarily precipitation-limited sagebrush-steppe. It is assumed that all precipitation falling upon these lands are ultimately taken up by ET by native vegetation during the summer months and that no recharge occurs (Schmidt and others, 2008).

Seepage from Rivers

The Snake, Boise, and Payette Rivers were simulated as head-dependent flux boundaries using the RIV package. The RIV variable of conductance is constant over prescribed reaches of each river (fig. 26). The Boise River is divided into reaches of constant conductance values at the New York Canal diversion dam, Glenwood Street in Boise, Middleton, Parma, and the Snake River. The Payette River is divided into reaches of constant conductance values at Emmett, Letha, Payette, and the Snake River. The Snake River is divided into reaches of constant conductance values at Murphy, Noble Island, Given’s Hot Springs, Marsing, Homedale, Nyssa, and Weiser. A multiplier was applied to the conductance of each RIV cell that is proportional to the relative length of river that falls within a model cell. The RIV variable of river bottom is set equal to 20 ft less than the 2.5th percentile of the ground surface altitude within a cell. This value was arrived at through a combination of trial-and-error and guidance from Gesch and others (2018). The RIV variables of stage varies throughout the simulation period. The river stage is measured at gaged locations on the rivers. These stages were averaged for each month and converted to a water depth. These depths were linearly interpolated between measurement locations and extrapolated upstream and downstream of the upper and lower measurement locations. Finally, the stage at all river cells was calculated by adding these depths to the river bottom.

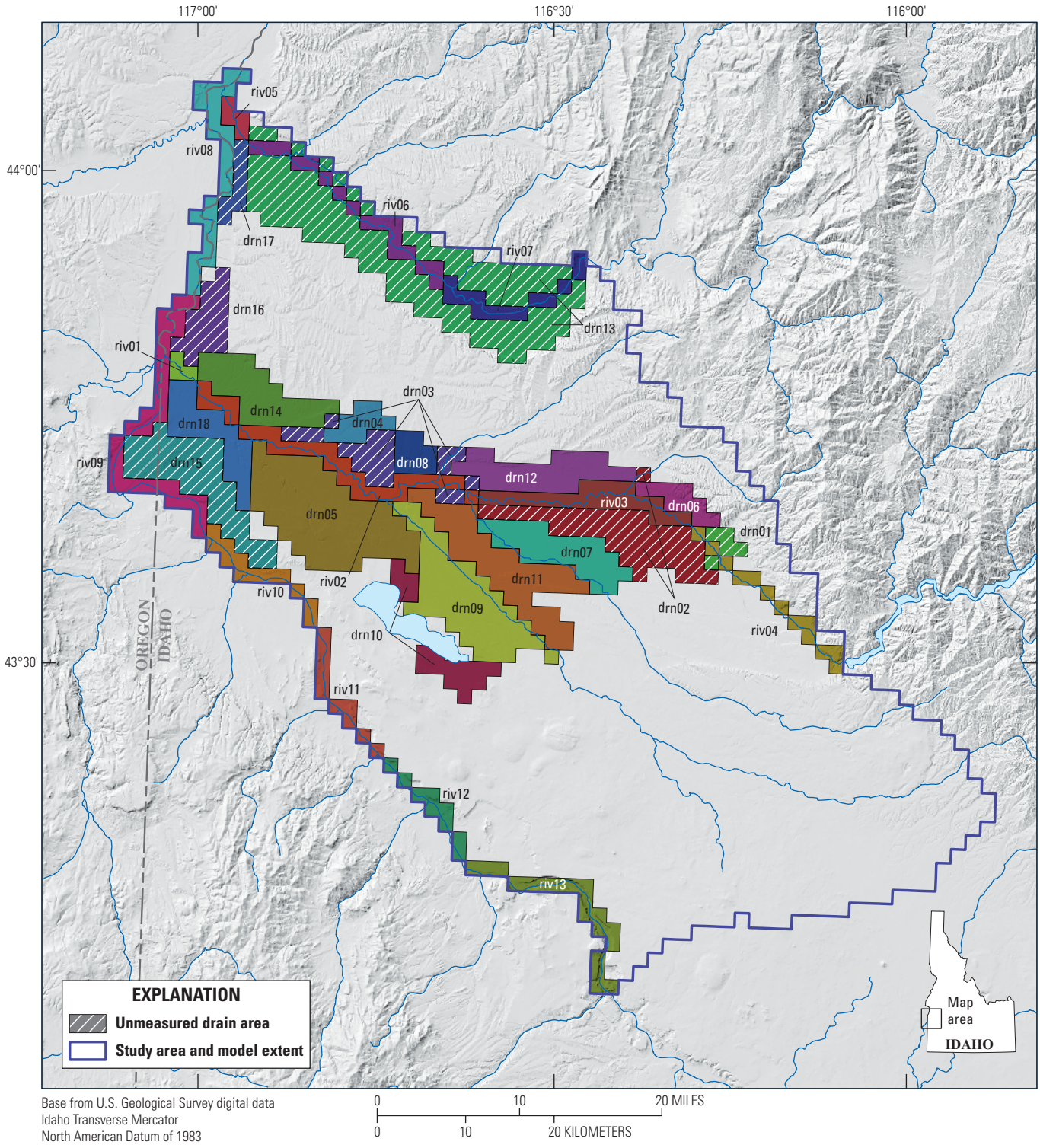

Figure 26. Zones of uniform conductance for drain and river boundary cells, southwestern Idaho and easternmost Oregon (Hundt, 2023).

Seepage from Lake Lowell

Lake Lowell was simulated as a head-dependent flux boundary using the general-head boundary (GHB) package. The GHB variables of boundary head and conductance both varied throughout the simulation period. The boundary head was set equal to the average lake stage (Bureau of Reclamation, 2020a) in a stress period. The final conductance is calculated as the product of a constant base conductance variable and a time-varying multiplier variable. Multipliers were calculated by first finding a lake surface area for each stress period using a bathymetric contour map (Ferrari, 1995) to relate lake stage to lake area. The monthly multiplier was then set equal to the proportion of the cell covered by the lake; from 0 to 1. The base conductance was set the same for all cells and times and is solved by parameter estimation.

Discharge to Drains

The network of agricultural drains in the Treasure Valley are simulated as head-dependent boundary conditions using the drain (DRN) package. The DRN elevation is set equal to 15 ft below the 5th percentile of the ground surface altitude within a cell (Gesch and others, 2018). The model area with drains is divided into zones of constant conductance (fig. 26). These zones represent the catchment areas of the drain network above discharge measurement locations or areas for which drain discharge is unmeasured (fig. 9). Unlike the other head-dependent boundary conditions used in the model, the DRN boundary can only be a source of discharge. When aquifer head is less than boundary head, no flow occurs across the boundary.

Parameter Estimation and Model Performance

The following section discusses the software and techniques used to estimate parameters, the observations and weights that comprise the objective function, a summary of residuals, and model output. The software and techniques used are standard and thus are discussed only briefly. The scope of this study consisted of a historical period created for the purpose of parameter estimation. For this reason, model output is also only discussed briefly.

Parameters were estimated using a combination of automated and manual adjustments. Parameter adjustments were automated using the PEST (Doherty, 2005) software, in which a quantitative measure of model misfit is defined and minimized. Adjustments were also made manually before and after running PEST by assessing multiple qualitative and quantitative measures of parameter suitability and model performance. These measures were not formally incorporated into the nonlinear least-squares regression implemented by the PEST software.

Nonlinear Least-Squares Regression Method

The PEST version 12 software was used for automated parameter adjustments. Optimal parameters are found using a nonlinear least-squares regression method to minimize the sum of squared weighted residuals:

$$\phi = \sum_{i=1}^{N} (w_i r_i)^2 \tag{13}$$

where

N is the number of measurements,
w_i is the weight for the i^{th} measurement quantity,
r_i is the i^{th} residual, or difference between the i^{th} observed and simulated quantities, and
ϕ is the sum of squared weighted residuals also known as the objective function.

The objective function is minimized using a Gauss-Levenberg-Marquardt algorithm with Tikhonov regularization. See the PEST documentation for more details (Doherty, 2005).

Weights applied to residuals determine the relative importance that each residual applies to the objective function and thus on the derived set of parameters that minimize the objective function. The determination of weights is detailed below. The full set of weights can be found in the data release (Hundt, 2023).

Software Tools

Multiple tools were used in the process of estimating parameters. PEST was the core software tool and served many functions to enable automated parameter estimation. The PEST-HP version was used to orchestrate parallel computations across multiple computing resources. Three small custom applications were developed to (1) run the irrigation supply and demand model, (2) develop weighting factors used to calculate water levels for multi-level observation wells, and (3) calculate pumping rates for multi-layer pumping wells. Source code is in the data release (Hundt, 2023).

Observation Targets

Automated parameter estimation seeks to minimize the difference between modeled and observed values for provided model targets. Targets for this model included observed aquifer heads and fluxes to agricultural drains, rivers, and seepage from Lake Lowell. Table 7 lists each observation target group and the total number of observations within.

Table 7. Observation target group residual summary (Hundt, 2023).

[**Abbreviations**: No., number; Min, minimum; Max, maximum; MAE, mean absolute error; ft, foot; ft^3/s, cubic foot per second]

Observation group	Units	No.	Min	Max	Range	Mean absolute error	MAE/range (percent)	Mean residual	Root-mean-square error	Residual percentiles						
										5	10	25	50	75	90	95
Water levels	Water level altitude, in ft	15,101	2,161	3,450	1,289	33.4	2.6	15.4	84.8	–49	–27	–12	7	23	45	70
Temporal water level differences	Difference in water level altitude, in ft	3,008	–79	37	116	4.1	3.5	0.2	6.4	–9	–6	–2	0	3	7	10
Vertical water level differences	Difference in water level altitude, in ft	2,224	–135	199	334	29.1	8.7	19.4	41.3	–31	–21	0	8	39	69	88
Drain discharge	Discharge, in ft^3/s	449	–219	–5	214	8.4	3.9	–3.9	13.7	–36	–19	–7	–1	3	6	11
Temporal drain discharge difference	Difference in discharge, in ft^3/s	174	–57	60	117	5.4	4.6	0.0	7.8	–14	–9	–3	0	3	11	13
River (and unmeasured drain) seepage	River (and ungaged drain) discharge, in ft^3/s	432	–1,143	7,069	8,212	133.7	1.6	45.0	658.8	–174	–112	–47	–11	14	60	129
Lake Lowell Seepage	Discharge, in ft^3/s	117	–312	171	483	49.3	10.2	–40.1	78.8	–162	–82	–42	–30	–18	11	35
Lake Lowell seepage difference	Difference in discharge, in ft^3/s	18	–54	317	371	95.4	25.7	86.3	126.3	–32	–9	24	83	122	223	238

Water Levels

Measurements of water levels were retrieved primarily from IDWR databases (Idaho Department of Water Resources, 2018a). The well target set was reduced further when developing water level observation targets. Wells whose water levels appeared anomalous compared to other nearby wells were removed. Wells that appeared within the cone of depression of nearby pumping were removed because the 1-mi grid cell of the TVGWFM should not be expected to reproduce such local drawdown. Wells in the foothills on the eastern side of the model were removed where the simple representation of the local hydrogeology and tributary underflow were determined to be incapable of reproducing observed water levels. Finally, wells close to other wells with water level targets were removed to better balance the spatial influence of observation target wells. A total of 15,101 water level targets from 507 wells remained.

Absolute Water Levels

A water level target for each well was calculated on a monthly time-step. Water levels at the end of each month, rather than a mean or median monthly value, were estimated or retrieved where possible. When water level measurements were 15 or fewer days apart, water levels at the end of each month were calculated with linear interpolation. In other cases, the final water level measured in a month was selected.

Simulated equivalents to water level observations were calculated using the PEST utility mf6mod2obs (Doherty, 2005). Water levels for locations between cell centers were calculated with bilinear interpolation. Equivalent water levels for wells that are open or screened across multiple model layers were calculated as a weighted mean of those model layers, with the weight equal to the product of hydraulic conductivity and screen or open borehole length within that layer relative to the total screen or borehole length.

Temporal Difference of Water Levels

Observations of changes in water level over time were calculated for all instances in which water levels in a well were collected 12 or fewer months apart.

Vertical Difference of Water Levels

Observations of vertical head differences between water levels in different model layers were calculated using the same pairs of wells used to define model layers. Vertical water level differences were used for any such pair of wells where both wells had greater than 10 water level observations and where water levels in both wells were measured in the same month. Differences between simulated equivalents of absolute water levels were calculated for the same cases.

Drain Discharge

Measurements of discharge at 13 drain locations began in November 2016. Streamgages with continuous (15 minute) discharge estimates were available at nine streamgages in agricultural drainage areas (fig. 9), and monthly to bimonthly measurements are made at the remaining three in the Ross, South Boise, and Alkali Drains near Parma, Idaho. No measurements of drain discharge were collected in the Payette Valley nor for smaller areas of agricultural drains near the Boise River.

Absolute Drain Discharge

Monthly volumes of drain discharge were back-cast for 1986–2015 by developing relationships between drain discharge and water levels in wells. For each drain measurement point, one or two wells (fig. 9) were selected that were located near the drainage area and had regular water level measurements from 1986 to 2021. Separate relationships were developed for each drain using coincident measurements of water levels and discharge during 2016–21. These relationships were then used to estimate discharge for 1986–2015. Table 4 provides information on these relationships. Drain discharge was only estimated in this way for months outside of the irrigation season, when discharge of groundwater is assumed to be the sole source of water to agricultural drains unless precipitation or snowmelt runoff occurs.

Model cells containing drain boundaries were grouped into zones that align with the drain network upstream of each drain measurement point (fig. 20). Simulated equivalents to the estimated drain discharge were calculated as the total of all discharge through drain boundaries in these zones.

Temporal Difference of Drain Discharge

Observations of changes in drain discharge over time were calculated for all instances in which discharges were estimated 12 or fewer months apart. Differences between simulated equivalents of absolute drain discharge were calculated for the same cases.

Lake Lowell Seepage

Absolute Lake Lowell Seepage

Monthly values of Lake Lowell seepage to or from groundwater were calculated by defining a water budget of Lake Lowell and populating it with existing data. This water budget has the form:

$$inflow - outflow = change\ in\ storage \quad (14)$$

Inflow includes inflow through canals (C_{in}), precipitation (P), and inflows from groundwater (GW_{in}). As Lake Lowell is an artificial impoundment with a small natural watershed, it is assumed that the lake does not receive natural streamflow. Outflow includes outflow through canals (C_{out}), evaporation (E), and outflow to groundwater (GW_{out}). Change in storage (ΔS) occurs when the lake level rises or falls. The water budget is then:

$$\overbrace{C_{in} + P + GW_{in}}^{inflow} - \overbrace{C_{out} - E - GW_{out}}^{outflow} = \Delta S \quad (15)$$

And the net groundwater seepage is:

$$GW_{net} = GW_{in} - GW_{out} = \Delta S + C_{out} + E - C_{in} - P \quad (16)$$

The Boise Project Board of Control provided monthly records of the volumes of flows into and out of the lake via canals in addition to monthly changes in lake storage since 1994 (Hundt, 2023). Evaporation and precipitation were calculated using daily measurements from the Nampa, Idaho, AgriMet (nmpi) weather station (Bureau of Reclamation, 2020a). These rates were multiplied by the lake surface area of the median water level during a month to arrive at a monthly volume.

Simulated equivalents to monthly net seepage to and from Lake Lowell are produced by calculating the sum of all fluxes across the lake boundary for a stress period.

Temporal Difference of Lake Lowell Seepage

Observations of changes in seepage in Lake Lowell over time were calculated for all instances in which seepage was estimated 3, 6, 9, or 12 months apart, using only the months of January, April, July, and October. Differences between simulated equivalents of absolute Lake Lowell seepage were calculated for the same cases.

River and Unmeasured Drain Seepage

Measurement from continuous streamflow gaging stations on the Boise and Payette Rivers (fig. 9) were used to estimate the combined seepage to or from rivers and unmeasured drains. The calculation of seepage is derived from a simple water budget of a river reach that takes the form:

$$inflow - outflow = change\ in\ storage \quad (17)$$

Typical inflow sources may include streamflow at the upstream end of the reach (Q_{up}), agricultural drains (D_{meas} and D_{unmeas}), streams, groundwater (GW_{in}), precipitation, wastewater treatment plant releases (W), and other inflow sources (overland flow and sewer returns). Within the study reaches, stream inflow, precipitation, and other inflows were assumed to be zero or negligible. Typical outflow sources may include streamflow at the downstream end of the reach (Q_{down}), diversions, groundwater (GW_{out}), evaporation, transpiration from riparian vegetation, and other withdrawals. Evaporation, transpiration from riparian vegetation, and other withdrawals were assumed to be zero or negligible. Calculations were not performed during the irrigation season to assume that agricultural drain flows are made up entirely of groundwater discharge. Additionally, change in storage and wastewater discharge in those cases where data are unavailable are also assumed to be zero. The water budget then becomes:

$$\overbrace{Q_{up} + D_{meas} + D_{unmeas} + GW_{in} + W}^{inflow} - \overbrace{Q_{down} - GW_{out}}^{outflow} = 0 \quad (18)$$

The net groundwater seepage is:

$$GW_{net} = GW_{in} - GW_{out} + D_{unmeas} = Q_{down} - Q_{up} - D_{meas} - W \quad (19)$$

Simulated equivalents to monthly net seepage to and from rivers and unmeasured agricultural drains are produced by calculating the sum of all fluxes across the corresponding of river and drain boundary cells (fig. 26).

Parameter Regularization

Regularization was added to the objective function to help overcome the challenge that parameter correlation and non-uniqueness would otherwise present to the automated parameter estimation algorithm. Regularization is accomplished by defining expressions in which the values of parameters, or the difference of two parameters, are compared to a target value. The objective function is penalized when parameter values depart from this target value. For distributed physical parameters hydraulic conductivity, hydraulic conductivity anisotropy ratio, specific yield, and storativity regularization formulae were developed to prefer a parameter value distribution that balances lateral uniformity with a distribution derived from the hydrogeologic framework model. For river conductance, regularization formulae prefer similarity between values in adjacent reaches. For all other parameters, regularization formulae prefer similarity between values of the same type. A combination of automated and manual steps was taken to adjust the relative weights of regularization.

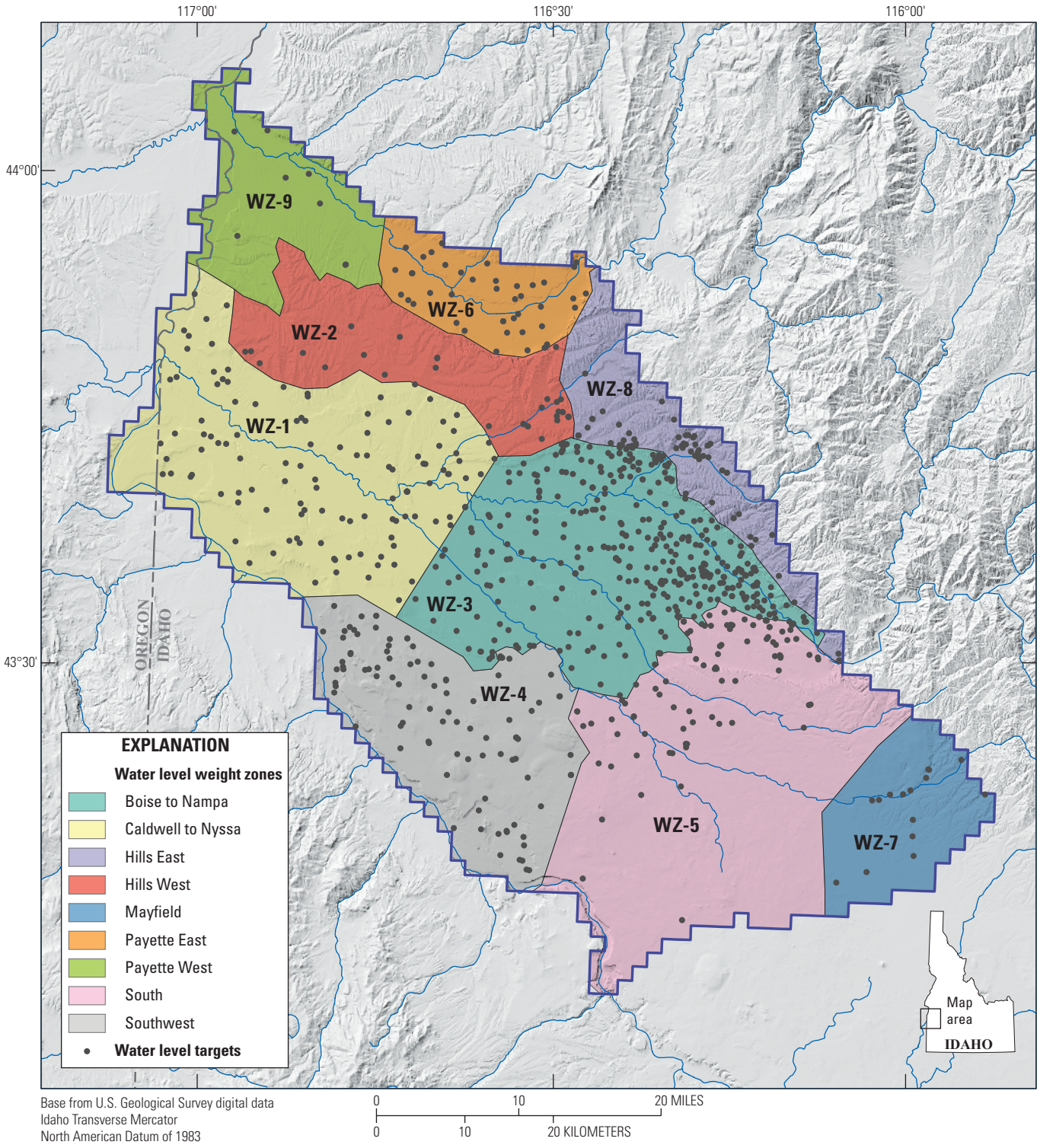

Figure 27. Water level observation target weighting zones, southwestern Idaho and easternmost Oregon (Hundt, 2023).

Informal Targets

Several additional criteria that were not included in the objective function were used to judge the suitability of parameter sets and to guide manual adjustments of parameters. Efforts were made to reduce spatial anomalies in fields of aquifer hydraulic parameters; decrease the presence of cells with simulated water levels above the land surface ("flooded" cells); roughly match previous water budget estimates; reduce bias in flux targets; and ensure accuracy in the amplitude of seasonal variations of fluxes in all rivers and drain areas that have observation targets.

Observation Weights

The PEST software employs a weighted least-squares minimization technique to estimate parameters. Each residual, or difference between an observation target and its model-simulated equivalent, is multiplied by a weight that alters the residual's contribution to the objective function, and thus the observation's influence on parameter estimates. These are referred to as "observation weights," and they were assigned in this study using multiple information sources and strategies.

In the study summarized in this report, parameters were estimated with a combination of automated and manual adjustments, and therefore the observation weights were not a strict determinant of final parameter estimates. Nonetheless, the observation weights strongly affected the relative influence of observations, particularly within observation groups.

While measurement quality is variable, weights were not assigned based upon measurement error variance. Rather, relative observation weights within groups were adjusted to improve the performance of the model with respect to informal criteria. First, a relative weight was assigned to observations of a given location equal to the inverse of its total number of observations. For drain and river flux targets, weights were further altered manually to seek a similar magnitude of residuals among the different observation locations. The water level observations were further adjusted by defining weighting zones (fig. 27) and assigning different weight factors (table 8) to wells within each zone. Finally, weights for all members of an observation group were adjusted manually to achieve a desirable balance with respect to each group's contribution to the objective function (fig. 28). Final weights can be found in the data release (Hundt, 2023).

Estimated Parameters

In most cases, final parameter estimates are best understood by viewing the full set of values contained in the data release (Hundt, 2023). A summary of values for each parameter group is shown in table 9. Figures are included for those parameters defined with pilot points to display the spatial distribution of estimated values. These include hydraulic conductivity (figs. 29–34), vertical anisotropy (figs. 35–40), specific yield (fig. 41), and storativity (figs. 42–46).

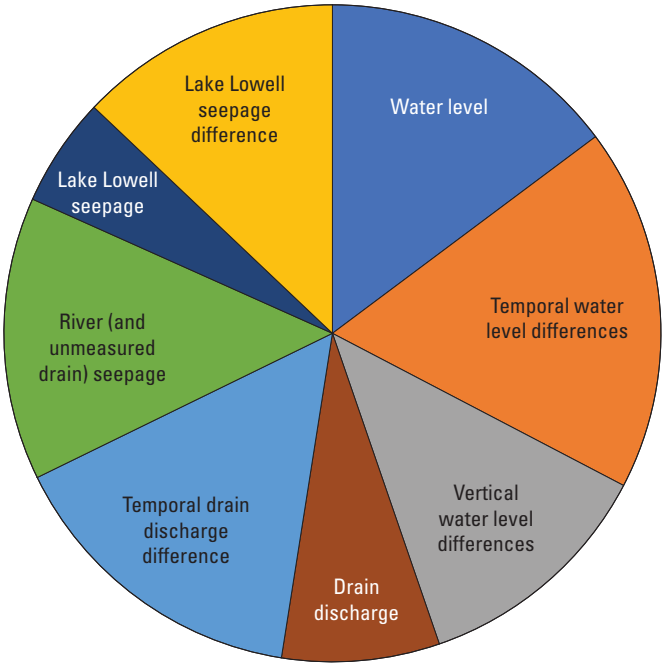

Figure 28. Relative objective function contribution from each observation group, southwestern Idaho and easternmost Oregon (Hundt, 2023).

Table 8. Water level observation target weight zone factors, southwestern Idaho and easternmost Oregon (Hundt, 2023).

Weight zone	Weight zone identifier	Weight multiplier
Caldwell to Nyssa	WZ-1	3
Hills West	WZ-2	1.5
Boise to Nampa	WZ-3	3
Southwest	WZ-4	3
South	WZ-5	2
Payette East	WZ-6	2
Mayfield	WZ-7	0.05
Hills East	WZ-8	1.5
Payette West	WZ-9	2

Table 9. Parameter groups used in the Treasure Valley Groundwater Flow Model (Hundt, 2023).

[**Abbreviations**: ID, identifier; ft/d, feet per day; ft²/d, square feet per day; Dim., dimensionless; ny, New York; ET, evapotranspiration; –, not applicable]

Parameter group ID	Parameter name	Units	Layer	Count	Median	Mean	Minimum	Maximum
Hk	Horizontal hydraulic conductivity	ft/d	All	1,040	7.53[1]	1.48[2]	2.84[−03]	1.76[3]
			1	212	2.88[1]	7.88[1]	4.98[−02]	1.34[3]
			2	92	1.07[2]	1.11[2]	5.10	6.47[2]
			3	154	9.14[1]	1.22[2]	3.07[−02]	1.67[3]
			4	199	5.22[1]	1.11[2]	2.84[−03]	1.76[3]
			5	171	8.29[1]	1.01[2]	2.88[−02]	1.38[3]
			6	212	3.06[1]	5.22[1]	5.09[−03]	1.34[3]
Ss	Storativity	Dim.	All	1,040	1.53[3]	3.21[−02]	4.24[−04]	3.38[−01]
			1	212	1.35[1]	1.38[−01]	4.24[−04]	3.38[−01]
			2	92	4.66[3]	4.68[−03]	3.39[−03]	7.48[−03]
			3	154	2.88[3]	2.89[−03]	2.19[−03]	5.65[−03]
			4	199	1.35[3]	1.39[−03]	7.07[−04]	4.62[−03]
			5	171	2.62[3]	2.87[−03]	5.48[−04]	9.54[−02]
			6	212	1.31[3]	1.46[−03]	9.91[−04]	7.79[−03]
Vk	Vertical conductivity anisotropy	Dim.	All	1,040	3.01[3]	5.23[−03]	2.78[−04]	3.27[−01]
			1	212	3.43[3]	5.37[−03]	3.94[−04]	3.27[−01]
			2	92	3.09[3]	4.09[−03]	4.21[−04]	1.21[−01]
			3	154	4.01[3]	5.32[−03]	1.83[−03]	7.74[−02]
			4	199	3.40[3]	4.38[−03]	3.68[−04]	6.94[−02]
			5	171	2.62[3]	2.87[−03]	5.48[−04]	9.54[−02]
			6	212	1.27[3]	1.30[−03]	2.78[−04]	1.59[−02]
drncnd	Drain conductance	ft²/d	–	20	1.18[4]	3.05[4]	1.96	1.66[5]
rivcond	River conductance	ft²/d	–	13	2.05[5]	3.00[5]	8.92[3]	9.47[5]
lowellcond	Lake lowell conductance	ft²/d	–	1	8.94[3]	8.94[3]	8.94[3]	8.94[3]
nycanalcnd	Lower ny canal conductance	ft²/d	–	1	1.45[4]	1.45[4]	1.45[4]	1.45[4]
nyleakfac	Upper ny canal leakage factor	Dim.	–	1	1.03	1.03	1.03	1.03
leakfac	Canal leakage factor	Dim.	–	26	1.26	1.04	0.20	1.51
leakdistprop	Canal leakage spatial Distribution proportion	Dim.	–	1	0.20	0.20	0.20	0.20
Etfac	ET adjustment factor	Dim.	–	39	0.94	0.96	0.94	1.01
tribmult	Tributary factor	Dim.	–	12	1.11	1.25	0.00	2.51

Table 9. Parameter groups used in the Treasure Valley Groundwater Flow Model (Hundt, 2023).—Continued

[**Abbreviations**: ID, identifier; ft/d, feet per day; ft^2/d, square feet per day; Dim., dimensionless; ny, New York; ET, evapotranspiration; –, not applicable]

Parameter group ID	Parameter name	Units	Layer	Count	Median	Mean	Minimum	Maximum
infacirr	Irrigated lands infiltration factor	Dim.	–	37	0.80	0.73	0.20	1.33
infacsem	Semi-irrigated lands infiltration factor	Dim.	–	39	1.00	0.94	0.38	1.26
mxfacirr	Irrigated lands maximum excess infiltration factor	Dim.	–	37	1.00	1.15	0.74	1.67
mxfacsem	Irrigated lands maximum excess infiltration factor	Dim.	–	39	1.01	1.14	0.78	1.67
ssfac	Steady-state boundary flux adjustment factors	Dim.	–	4	1.28	1.19	0.69	1.51

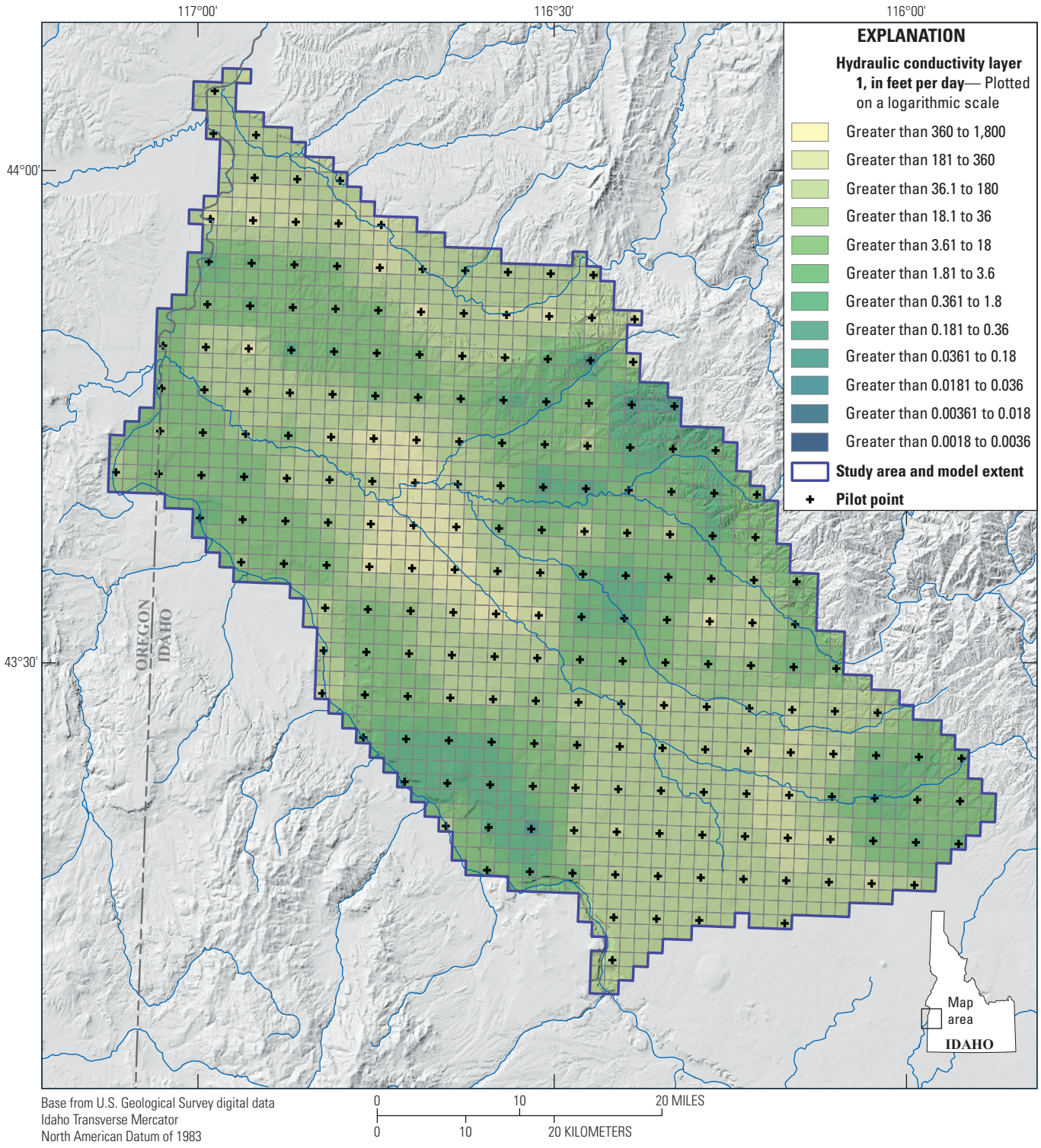

Figure 29. Hydraulic conductivity in layer 1 of the Treasure Valley Groundwater Flow Model, southwestern Idaho and easternmost Oregon (Hundt, 2023).

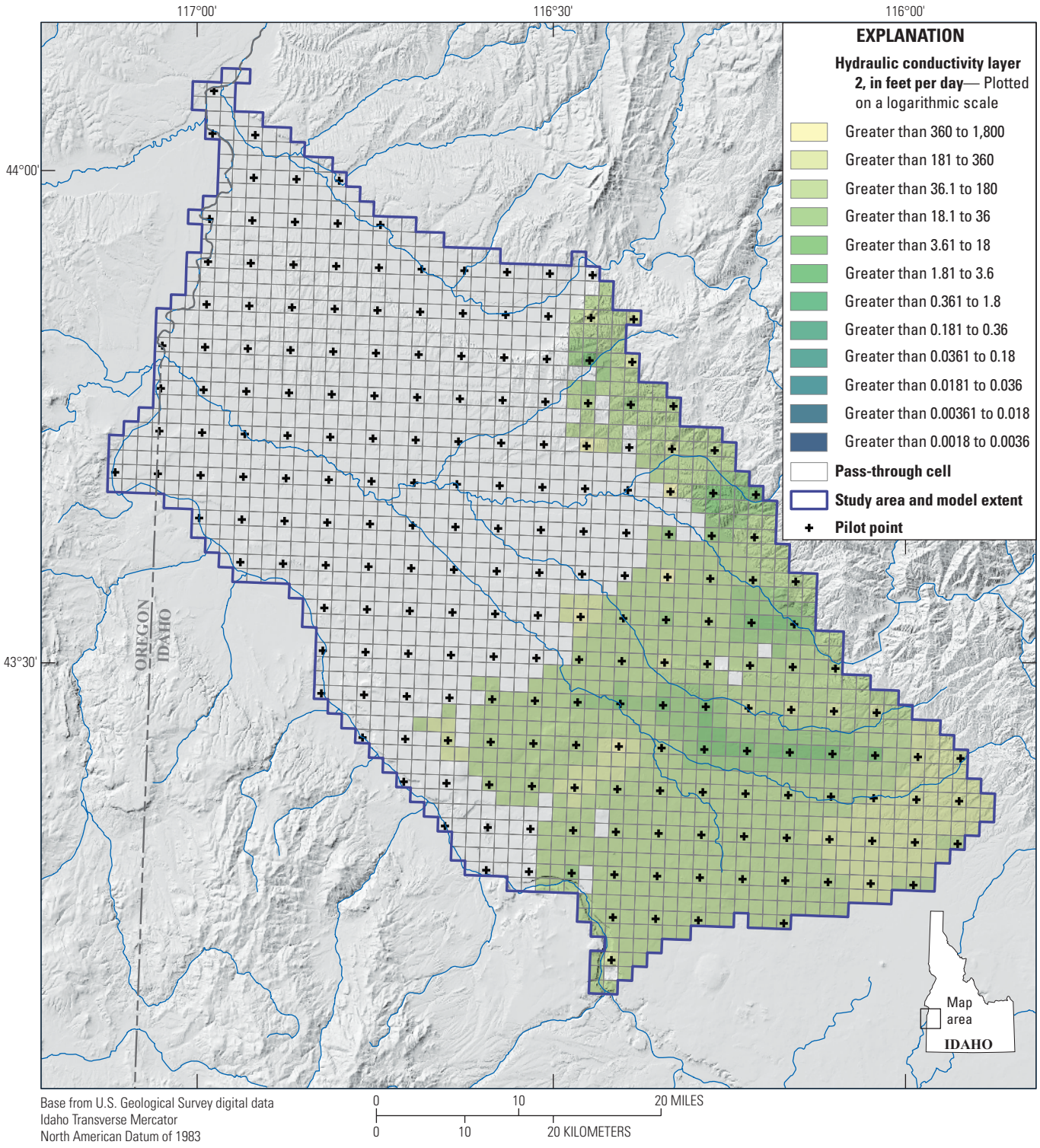

Figure 30. Hydraulic conductivity in layer 2 of the Treasure Valley Groundwater Flow Model, southwestern Idaho and easternmost Oregon (Hundt, 2023).

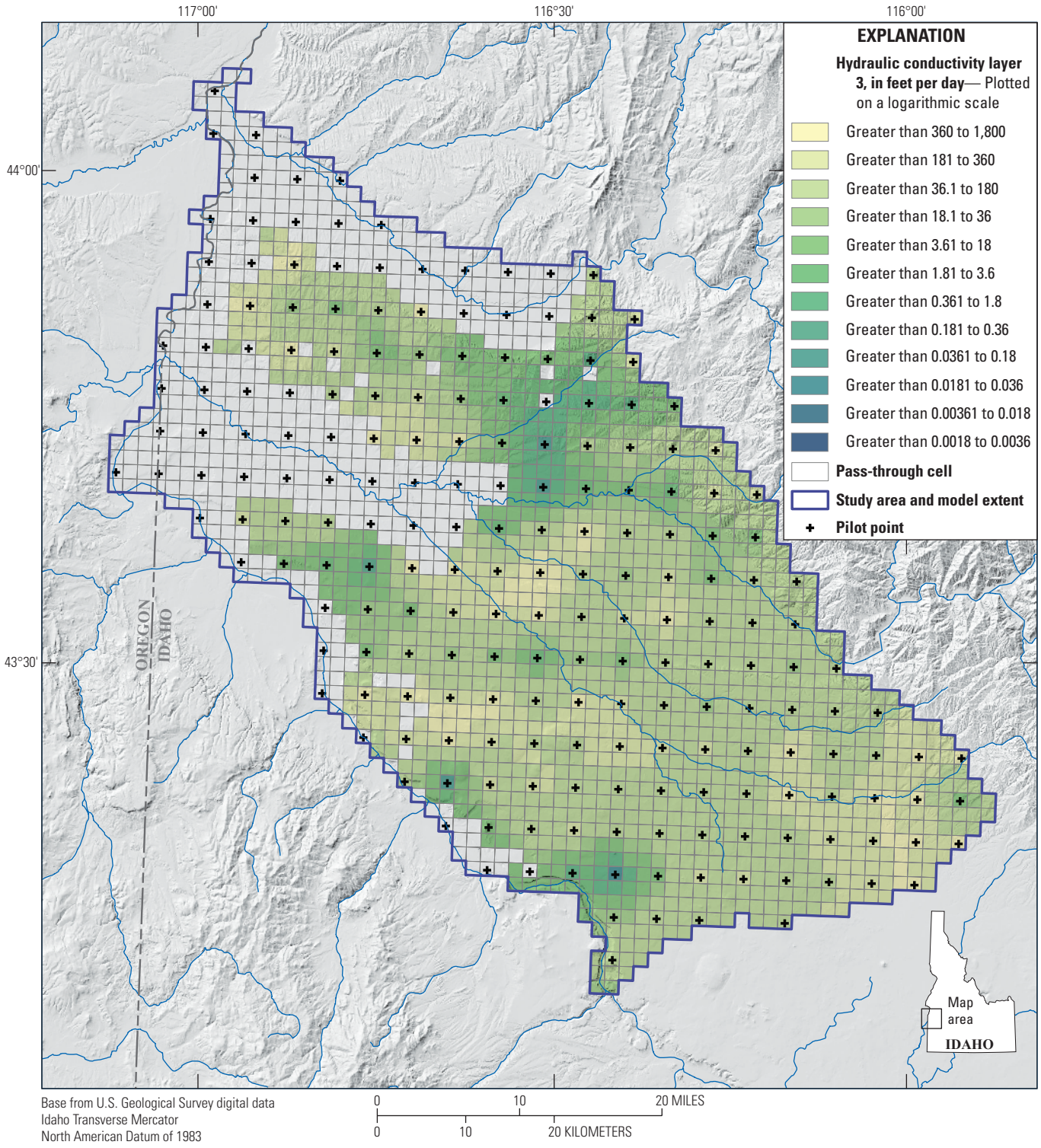

Figure 31. Hydraulic conductivity in layer 3 of the Treasure Valley Groundwater Flow Model, southwestern Idaho and easternmost Oregon (Hundt, 2023).

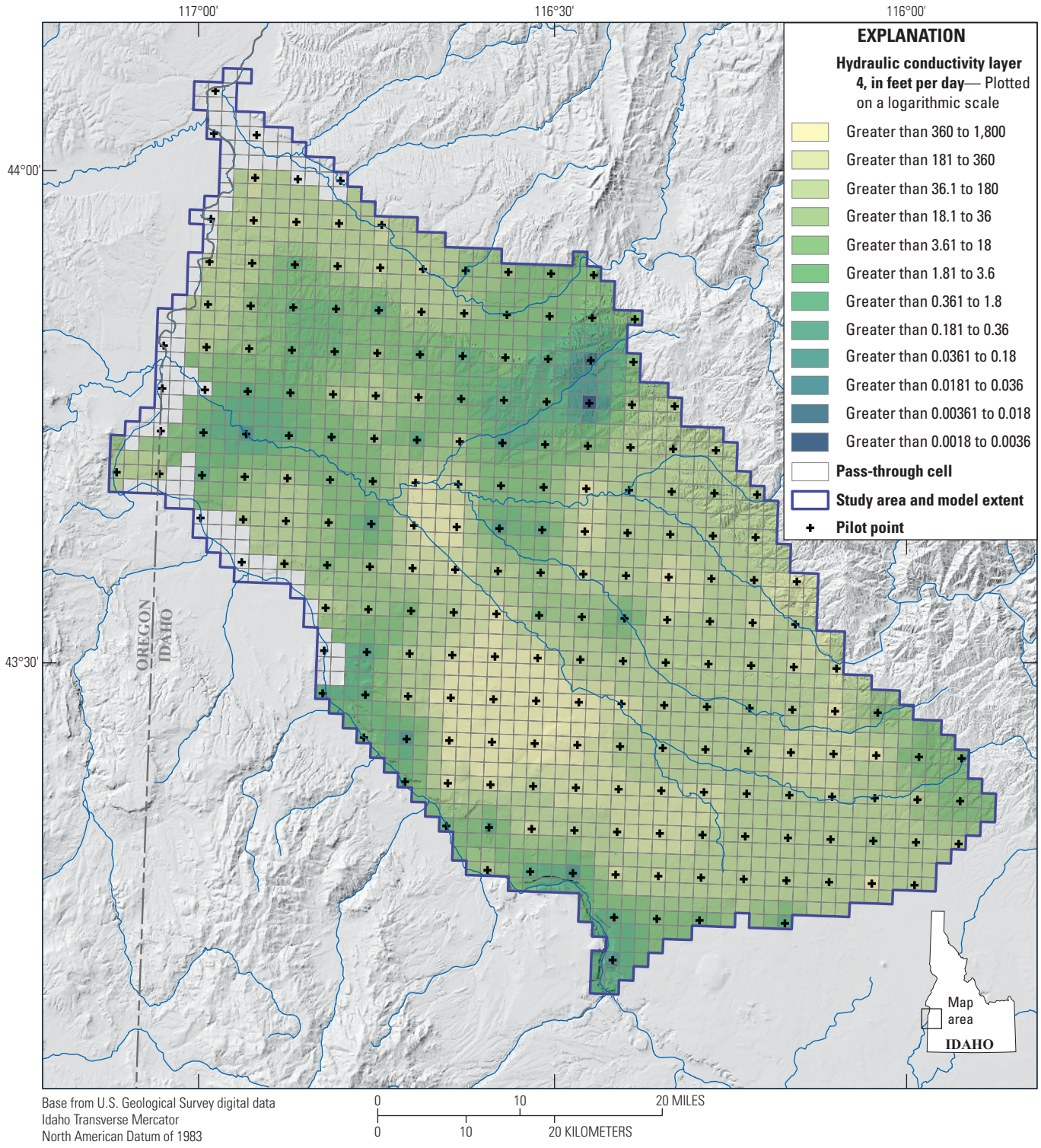

Figure 32. Hydraulic conductivity in layer 4 of the Treasure Valley Groundwater Flow Model, southwestern Idaho and easternmost Oregon (Hundt, 2023).

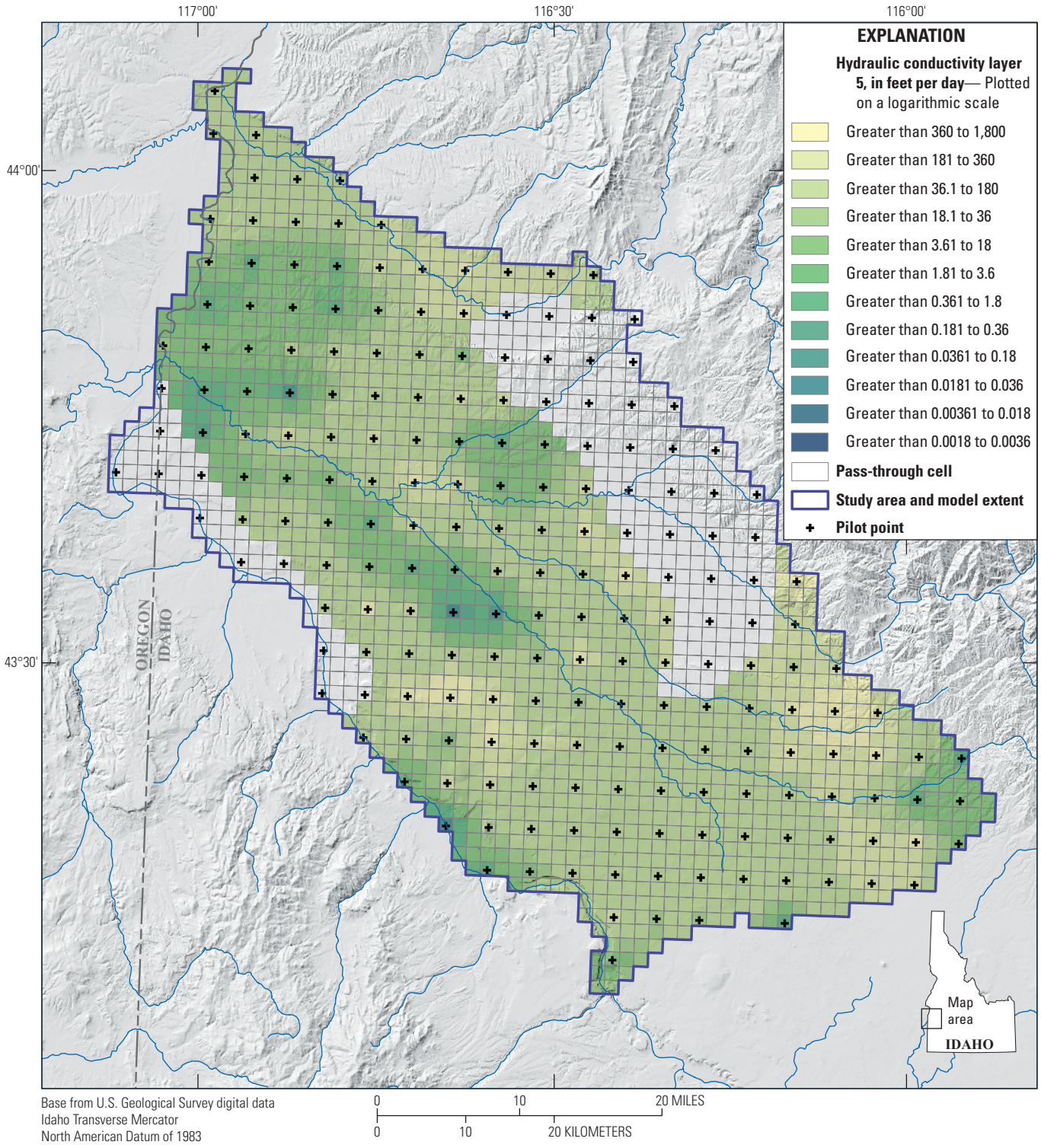

Figure 33. Hydraulic conductivity in layer 5 of the Treasure Valley Groundwater Flow Model, southwestern Idaho and easternmost Oregon (Hundt, 2023).

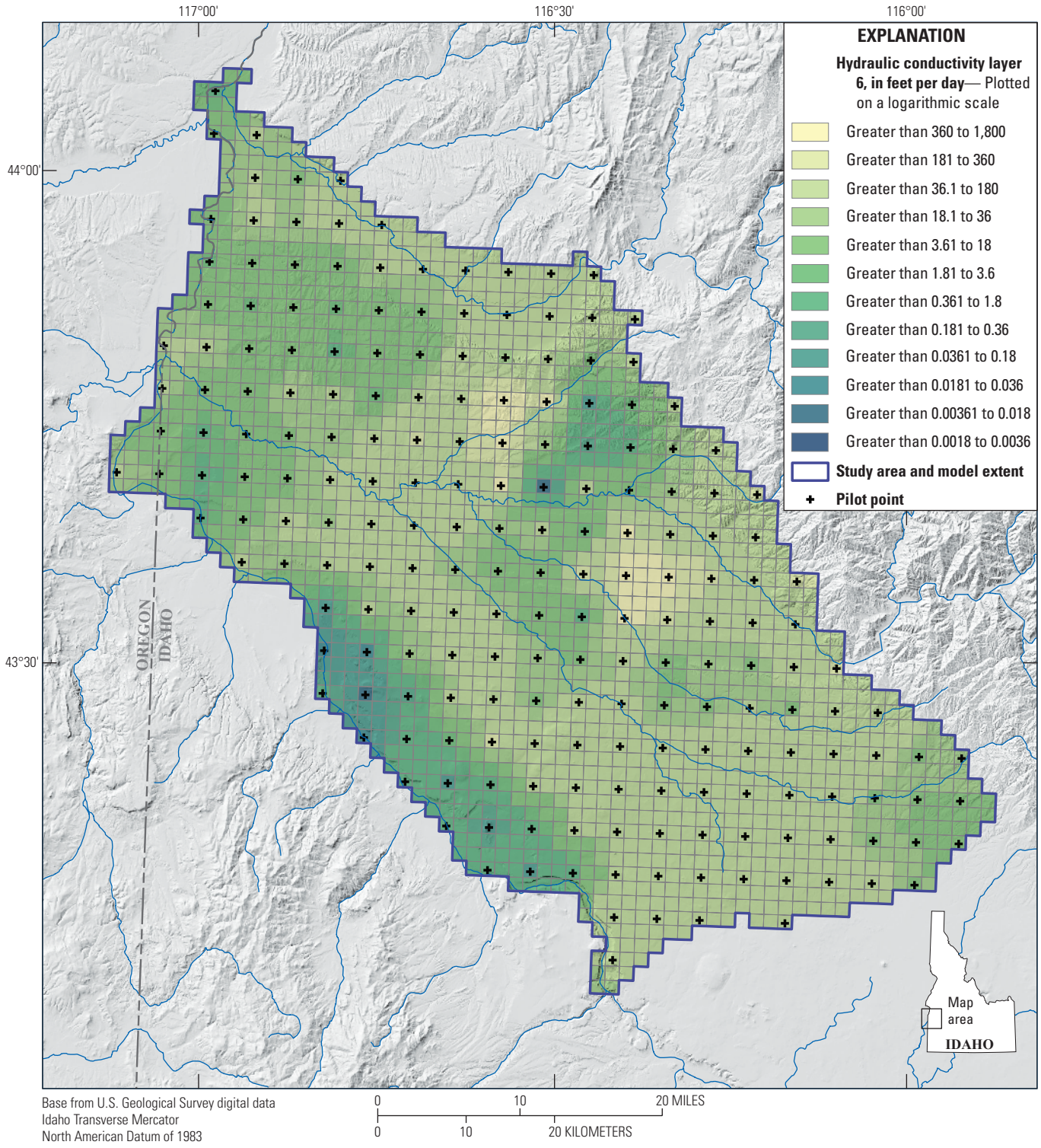

Figure 34. Hydraulic conductivity in layer 6 of the Treasure Valley Groundwater Flow Model, southwestern Idaho and easternmost Oregon (Hundt, 2023).

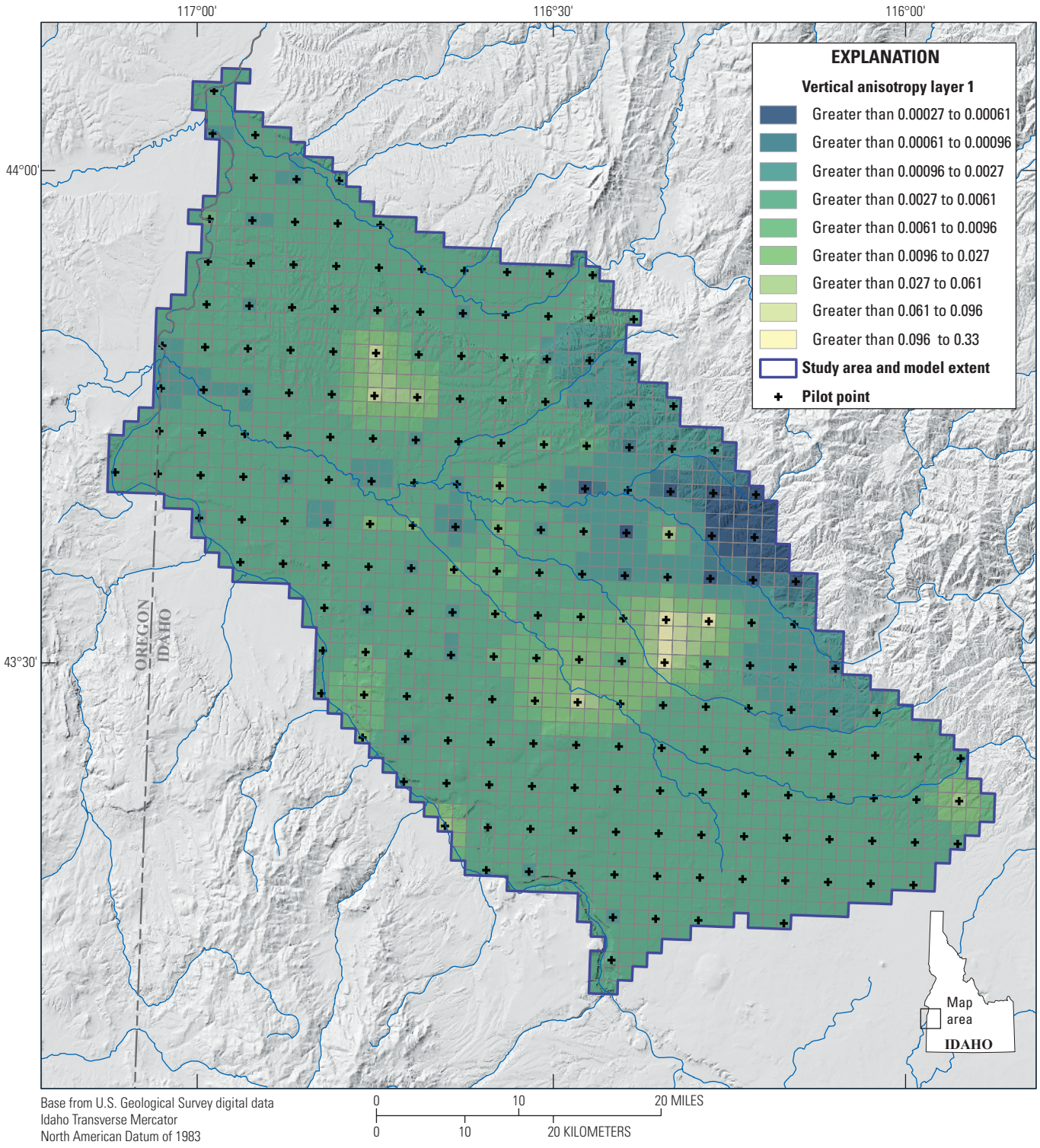

Figure 35. Vertical hydraulic conductivity anisotropy ratio in layer 1 of the Treasure Valley Groundwater Flow Model, southwestern Idaho and easternmost Oregon (Hundt, 2023).

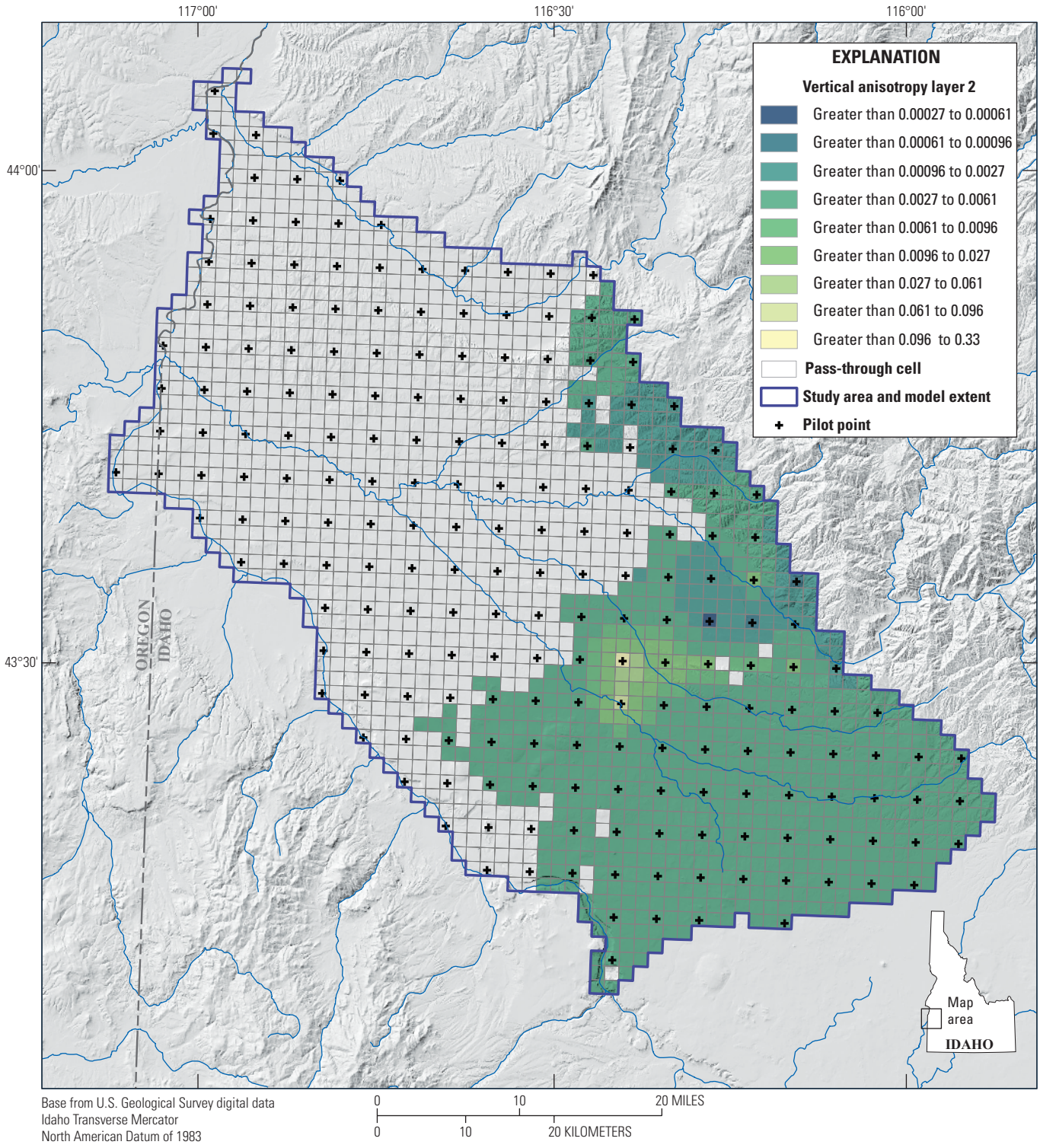

Figure 36. Vertical hydraulic conductivity anisotropy ratio in layer 2 of the Treasure Valley Groundwater Flow Model, southwestern Idaho and easternmost Oregon (Hundt, 2023).

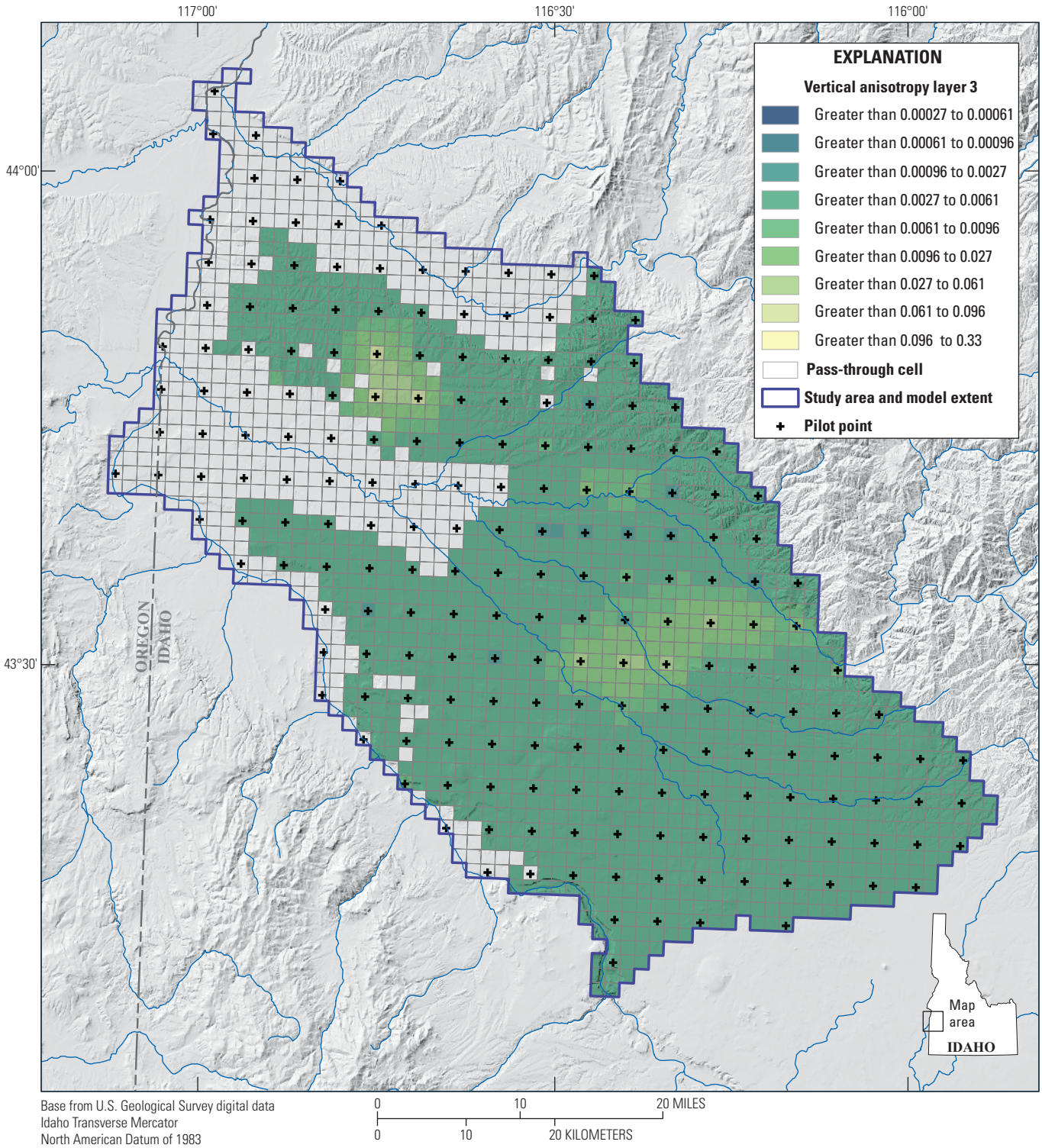

Figure 37. Vertical hydraulic conductivity anisotropy ratio in layer 3 of the Treasure Valley Groundwater Flow Model, southwestern Idaho and easternmost Oregon (Hundt, 2023).

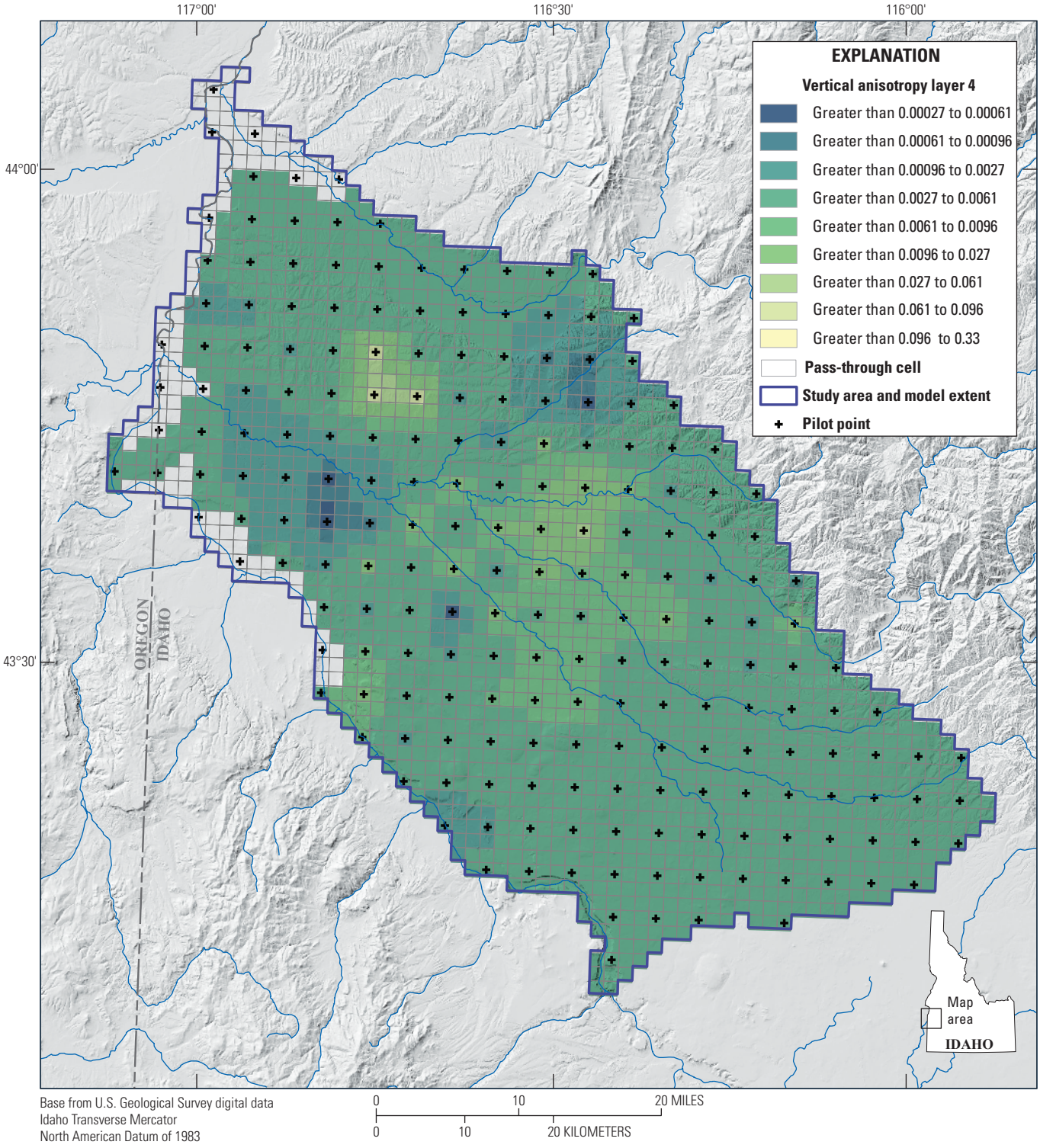

Figure 38. Vertical hydraulic conductivity anisotropy ratio in layer 4 of the Treasure Valley Groundwater Flow Model, southwestern Idaho and easternmost Oregon (Hundt, 2023).

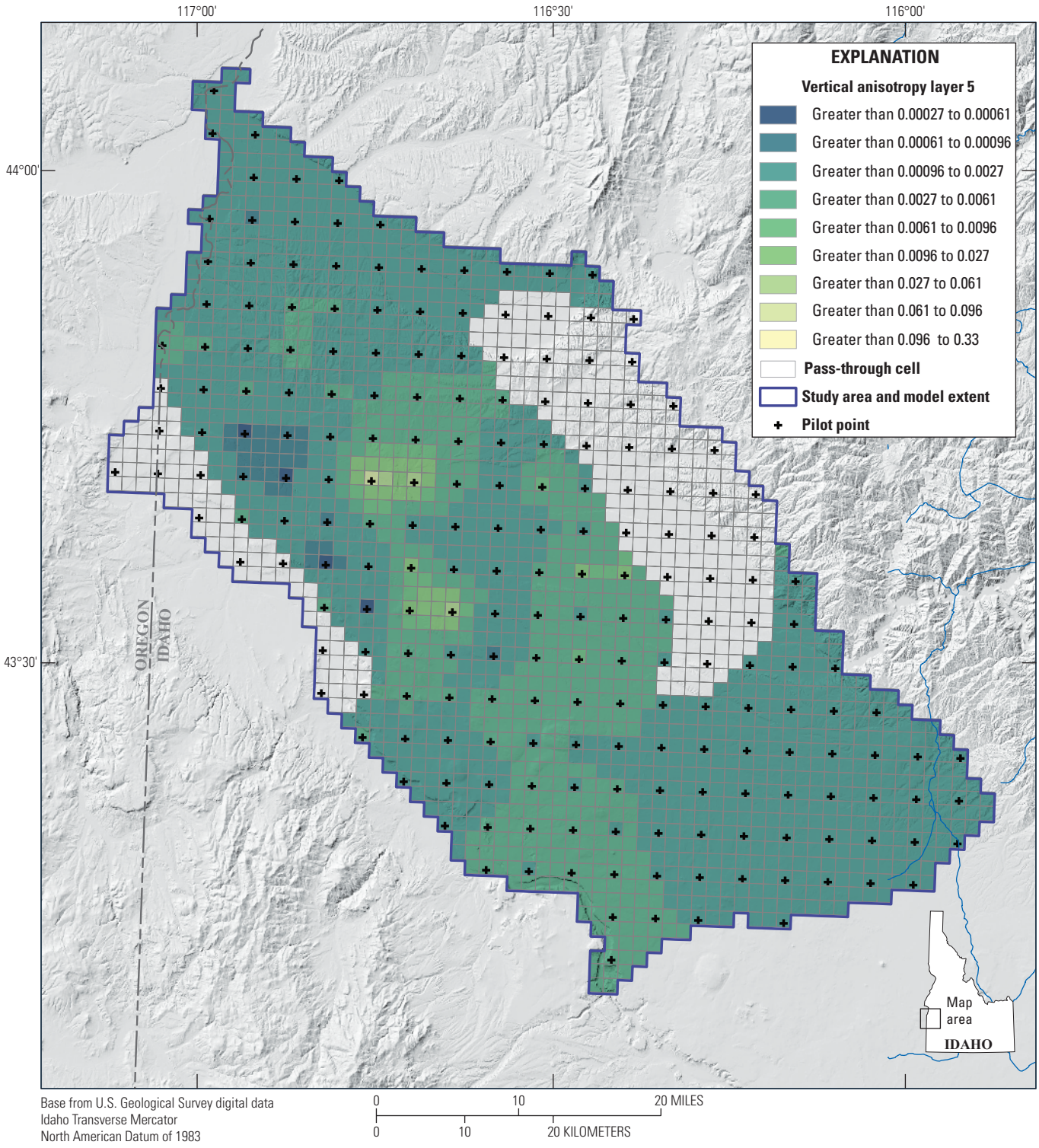

Figure 39. Vertical hydraulic conductivity anisotropy ratio in layer 5 of the Treasure Valley Groundwater Flow Model, southwestern Idaho and easternmost Oregon (Hundt, 2023).

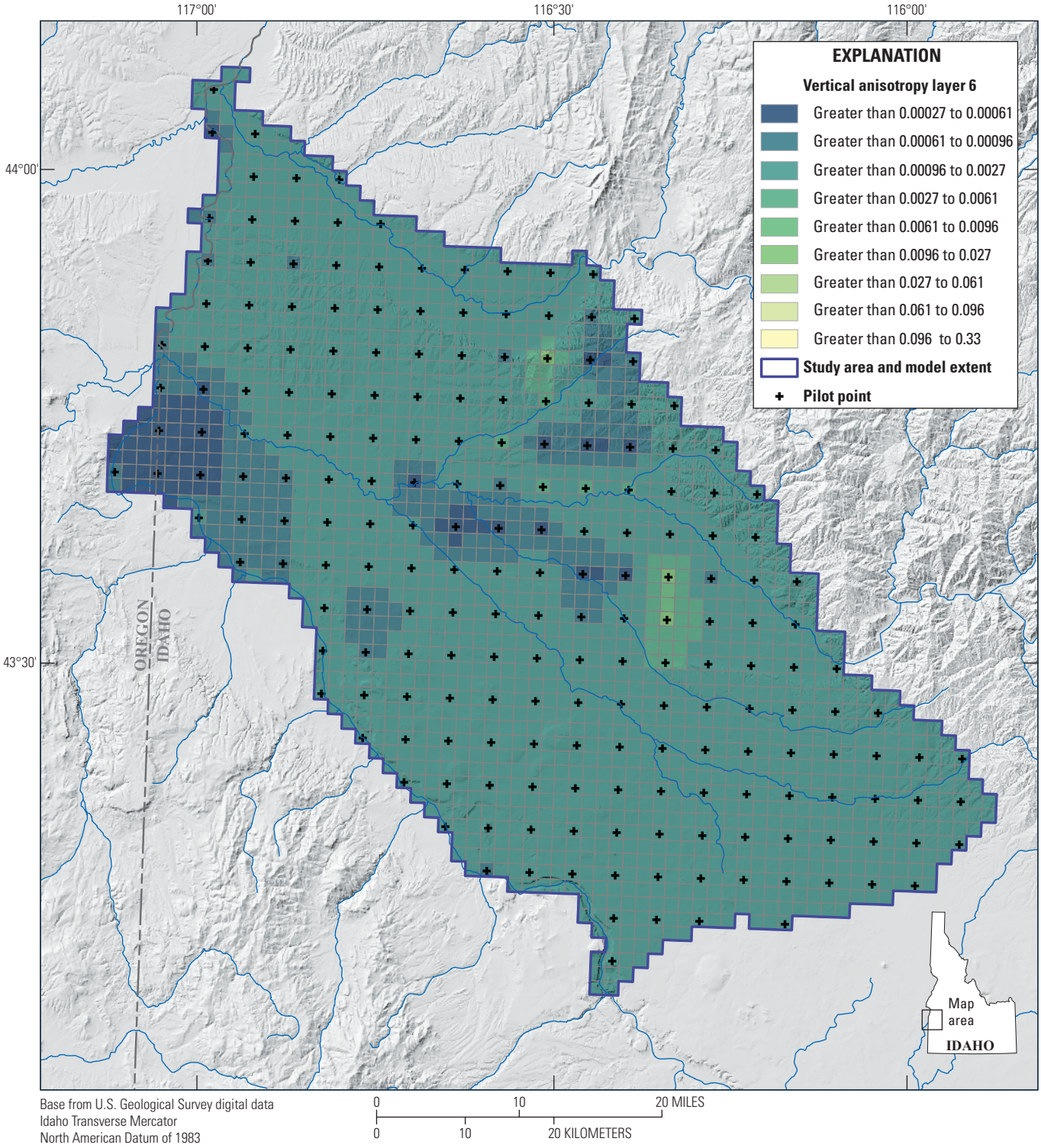

Figure 40. Vertical hydraulic conductivity anisotropy ratio in layer 6 of the Treasure Valley Groundwater Flow Model, southwestern Idaho and easternmost Oregon (Hundt, 2023).

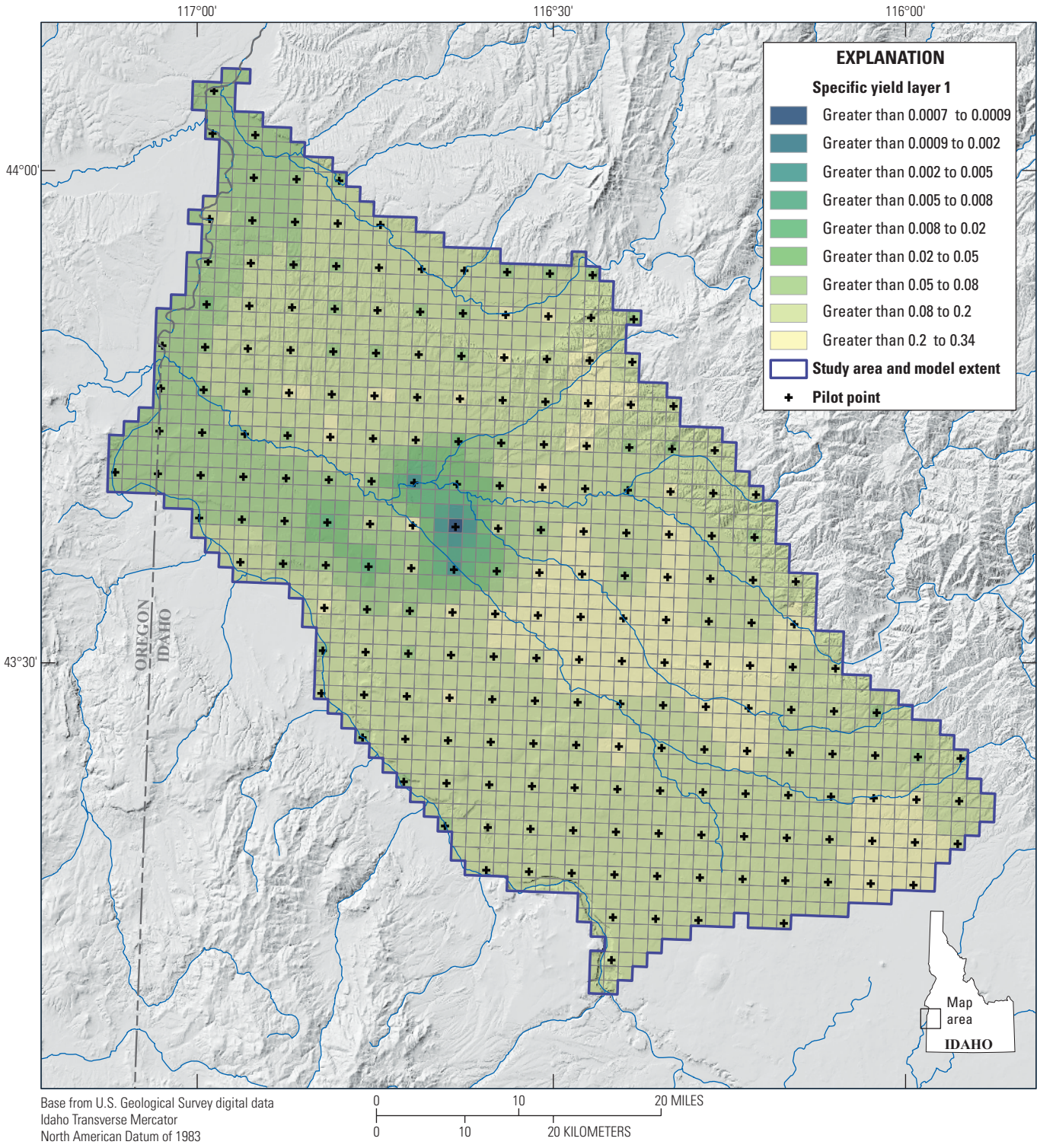

Figure 41. Specific yield in layer 1 of the Treasure Valley Groundwater Flow Model, southwestern Idaho and easternmost Oregon (Hundt, 2023).

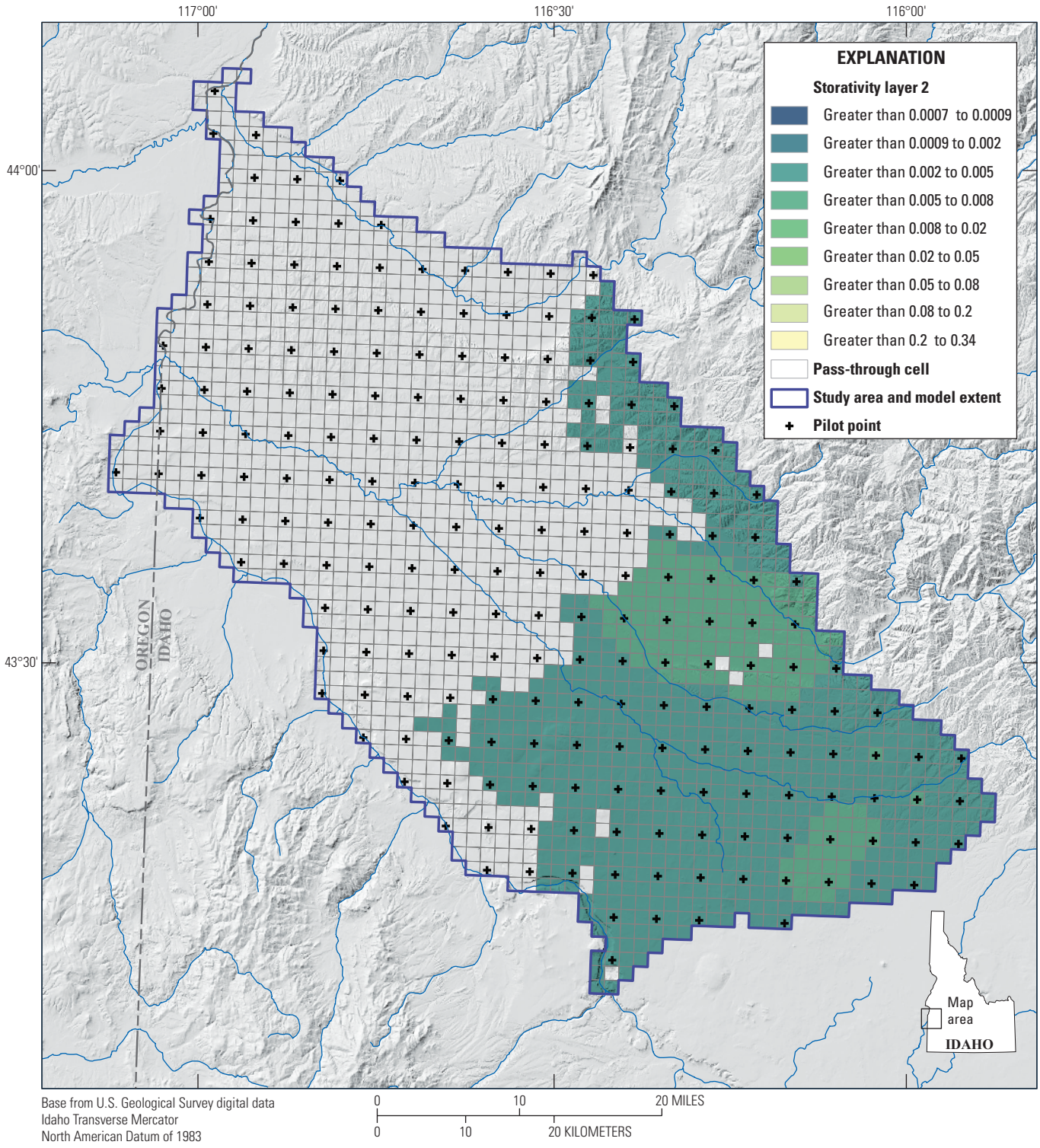

Figure 42. Storativity in layer 2 of the Treasure Valley Groundwater Flow Model, southwestern Idaho and easternmost Oregon (Hundt, 2023).

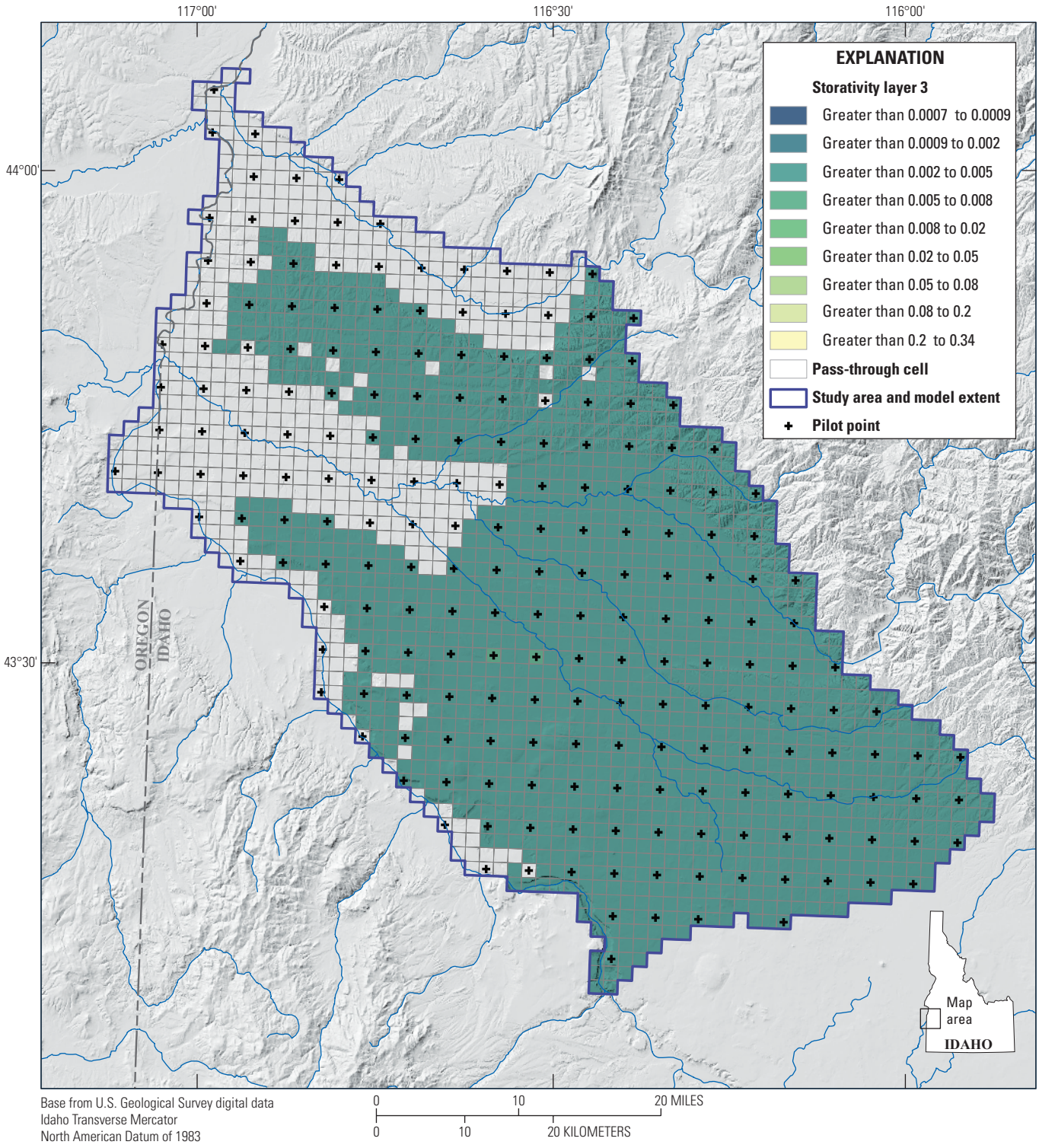

Figure 43. Storativity in layer 3 of the Treasure Valley Groundwater Flow Model, southwestern Idaho and easternmost Oregon (Hundt, 2023).

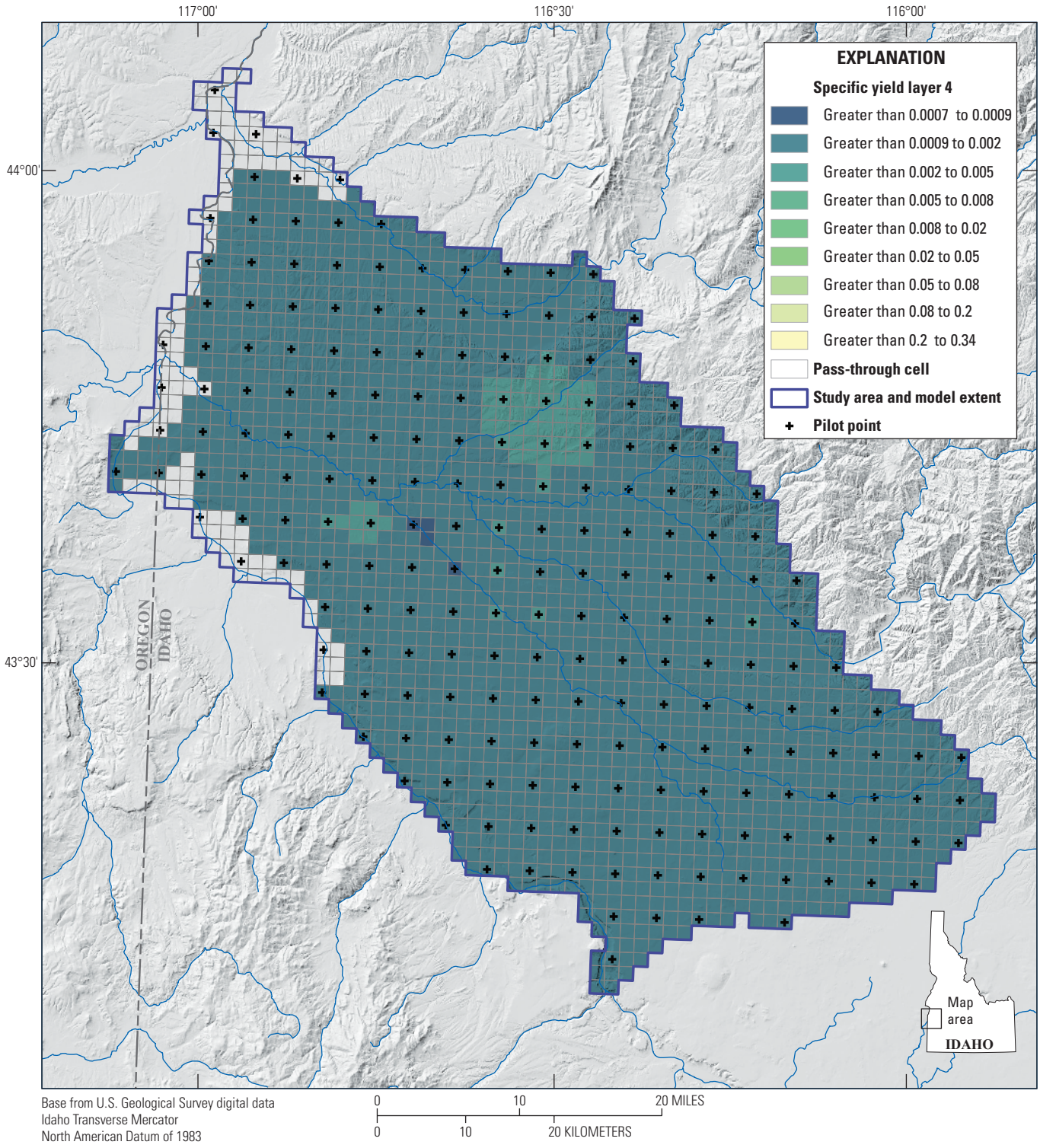

Figure 44. Storativity in layer 4 of the Treasure Valley Groundwater Flow Model, southwestern Idaho and easternmost Oregon (Hundt, 2023).

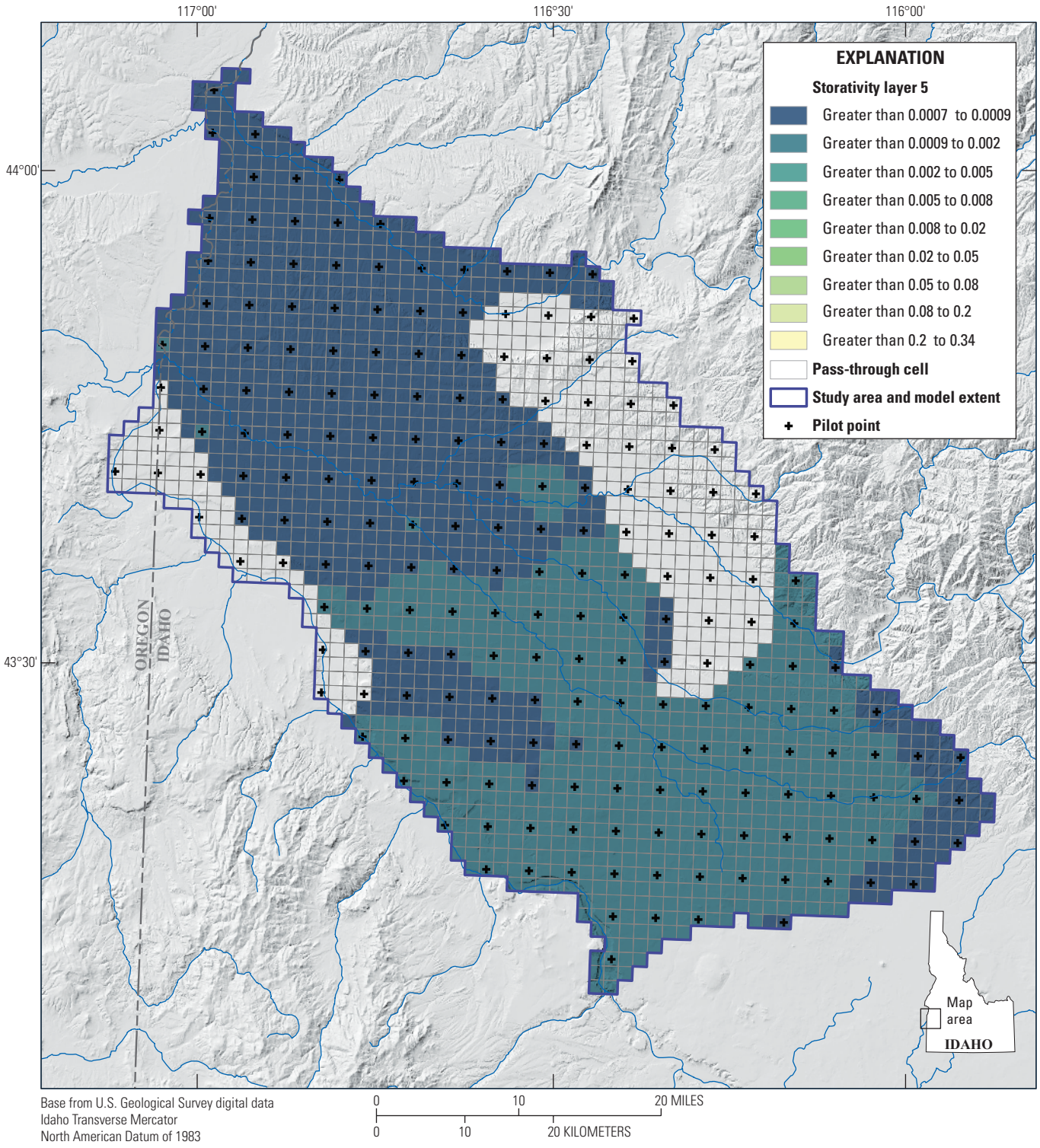

Figure 45. Storativity in layer 5 of the Treasure Valley Groundwater Flow Model, southwestern Idaho and easternmost Oregon (Hundt, 2023).

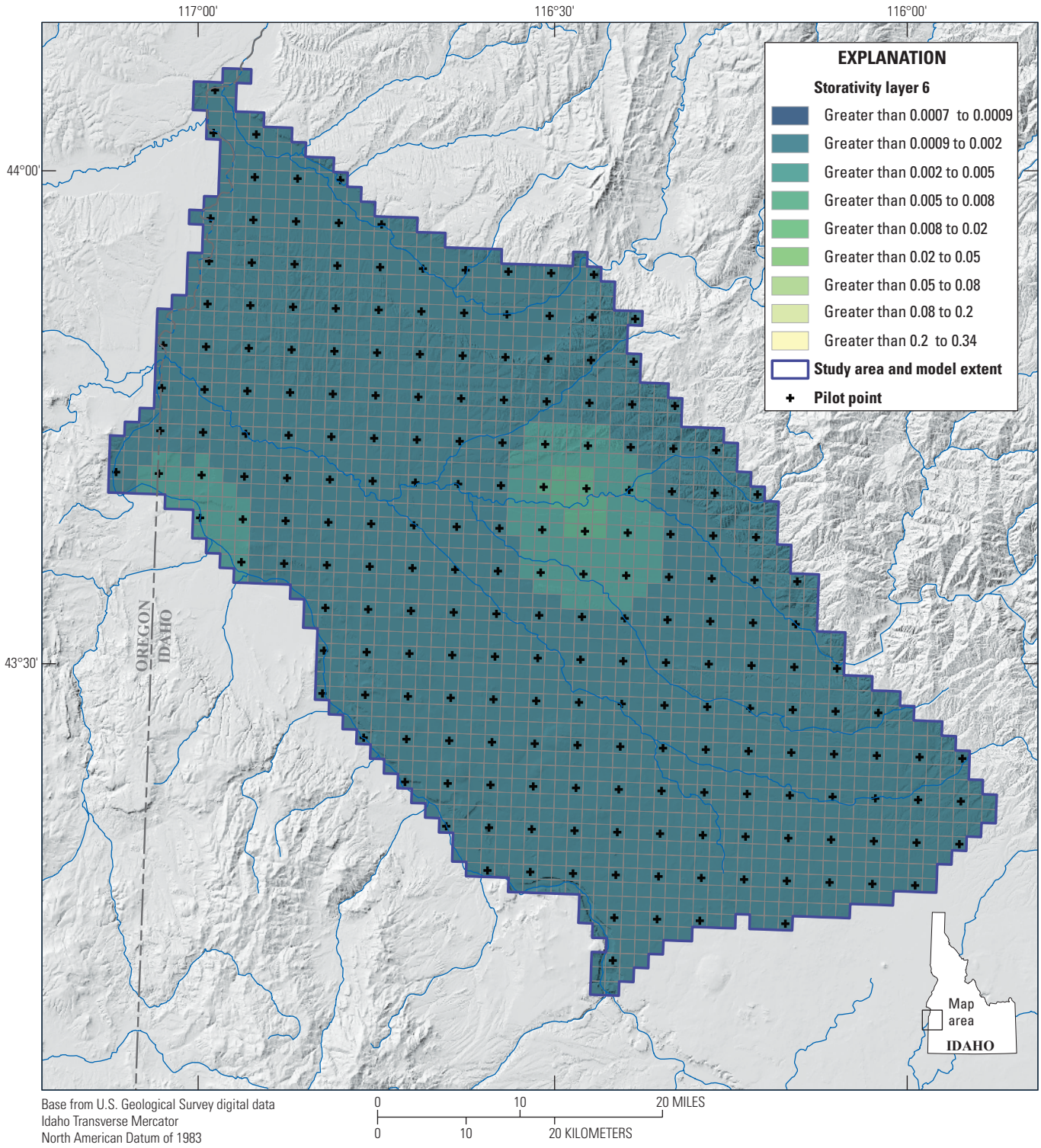

Figure 46. Storativity in layer 6 of the Treasure Valley Groundwater Flow Model, southwestern Idaho and easternmost Oregon (Hundt, 2023).

Assessment of Residuals

The full collection of observation residuals is contained in the data release (Hundt, 2023). Residuals are further summarized below with tables and figures that highlight various aspects of model performance.

The residuals of each observation group are summarized using several statistics (table 7). The number column is a count of all observation targets with non-zero weights. The minimum and maximum values of observation targets are included, with the difference between these shown as the range. The mean absolute residual is the mean of the absolute values of residuals, or the mean distance each residual lies from the ideal value of zero. For aquifer heads, dividing this by the range of observed values puts these values into context. Low values of this ratio (less than 5 percent) are considered good, but these values can be sensitive to outliers in the observation dataset, which tend to affect range more than mean residuals and lead to a lower value. A low mean error is achieved by either low residuals or a balance of positive and negative residuals. The root-mean-square error (RMSE) is calculated with squared residuals, giving large residuals a greater influence than in the other statistics. This statistic, while more difficult to interpret than mean error (ME) or mean absolute error (MAE), is similar in form to the objective function that drives the parameter estimation process. Residual percentiles demonstrate the spread of residuals, with the ideal being smaller and more symmetric values around a 50th percentile value of zero.

The best performance is seen in the absolute and temporal difference groups for both water levels and drain discharge. Each group has an MAE/range below 5 percent, a relatively low 50th percentile value, and symmetric spreads of residuals. The 33.4 ft MAE and 15.4 ft ME for the water levels observation group (consistent with the interquartile range of 35 ft) should be noted as it may preclude the model from some uses that require a greater level of accuracy. The vertical water level difference group has moderate performance, with an MAE/range below 10 percent and a relatively low 50th percentile value. The mean statistics and spread of percentiles all demonstrate a bias towards too little vertical difference in these modeled quantities. The river and unmeasured drain discharge group has an MAE/range value that is misleadingly low due to the very large range of values in the observation dataset. Other statistics show large but relatively unbiased residuals in this group. Finally, both Lake Lowell observation groups show poor performance.

The full set of residuals for each group, as well as a histogram, are displayed graphically in the plots of figures 47–54. The top plot of each figure shows observed and simulated values. Residuals of zero would place the point on the dashed 1-to-1 line, with over-simulated values falling in the upper left and under-simulated values the lower right. The bottom plot shows observed values against residuals, with an ideal fit having points fall upon the dashed horizontal line of zero. The presence of trend in these values indicates that the model is missing or not fully reproducing some phenomenon that is observed in the aquifer. A histogram of residuals is shown on the bottom right. Ideally, these would have a large peak around zero and away from which values would taper sharply and symmetrically.

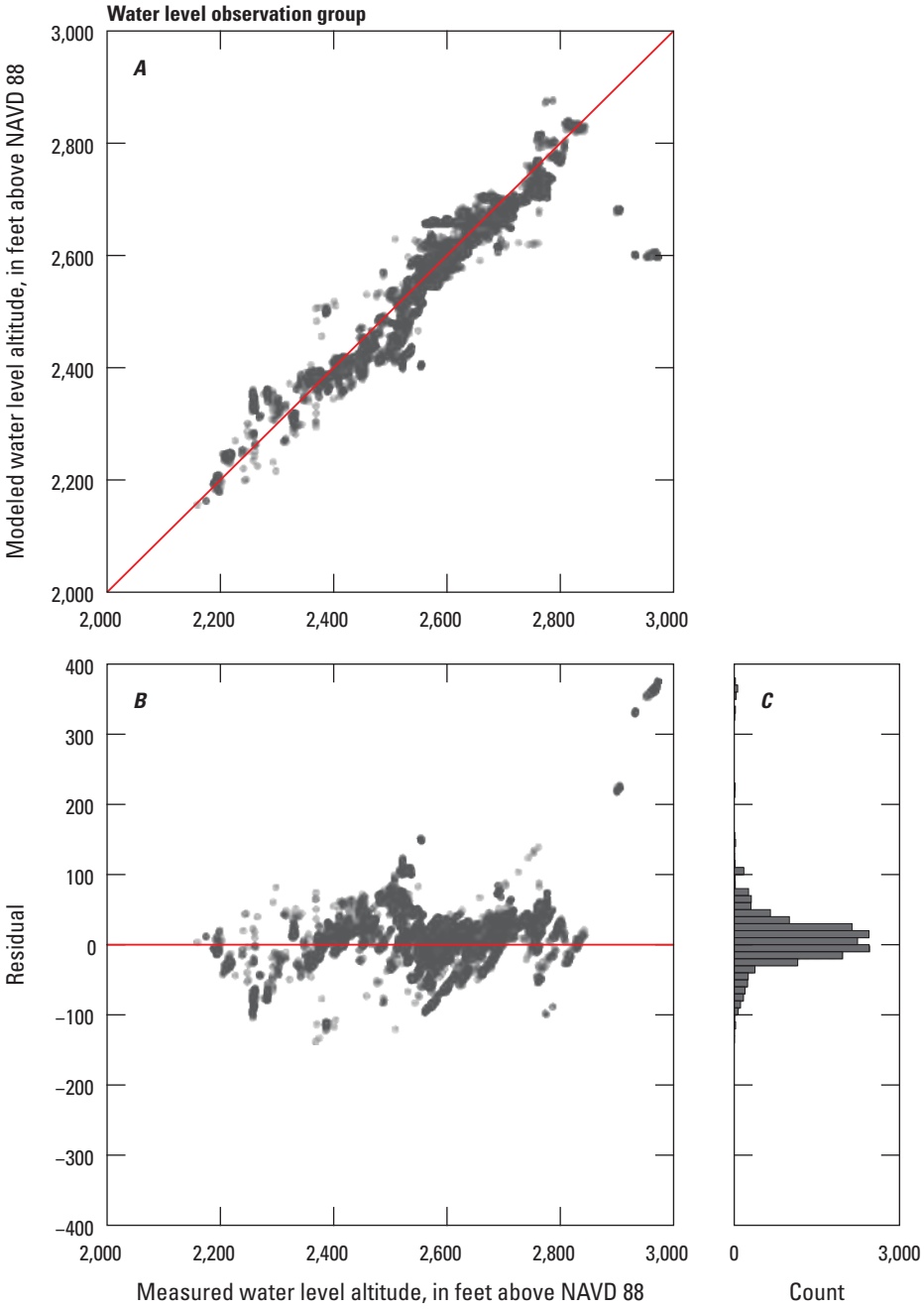

Figure 47. Residual plots for water level observation group of the Treasure Valley Groundwater Flow Model, southwestern Idaho and easternmost Oregon (Hundt, 2023). NAVD 88, North American Vertical Datum of 1988.

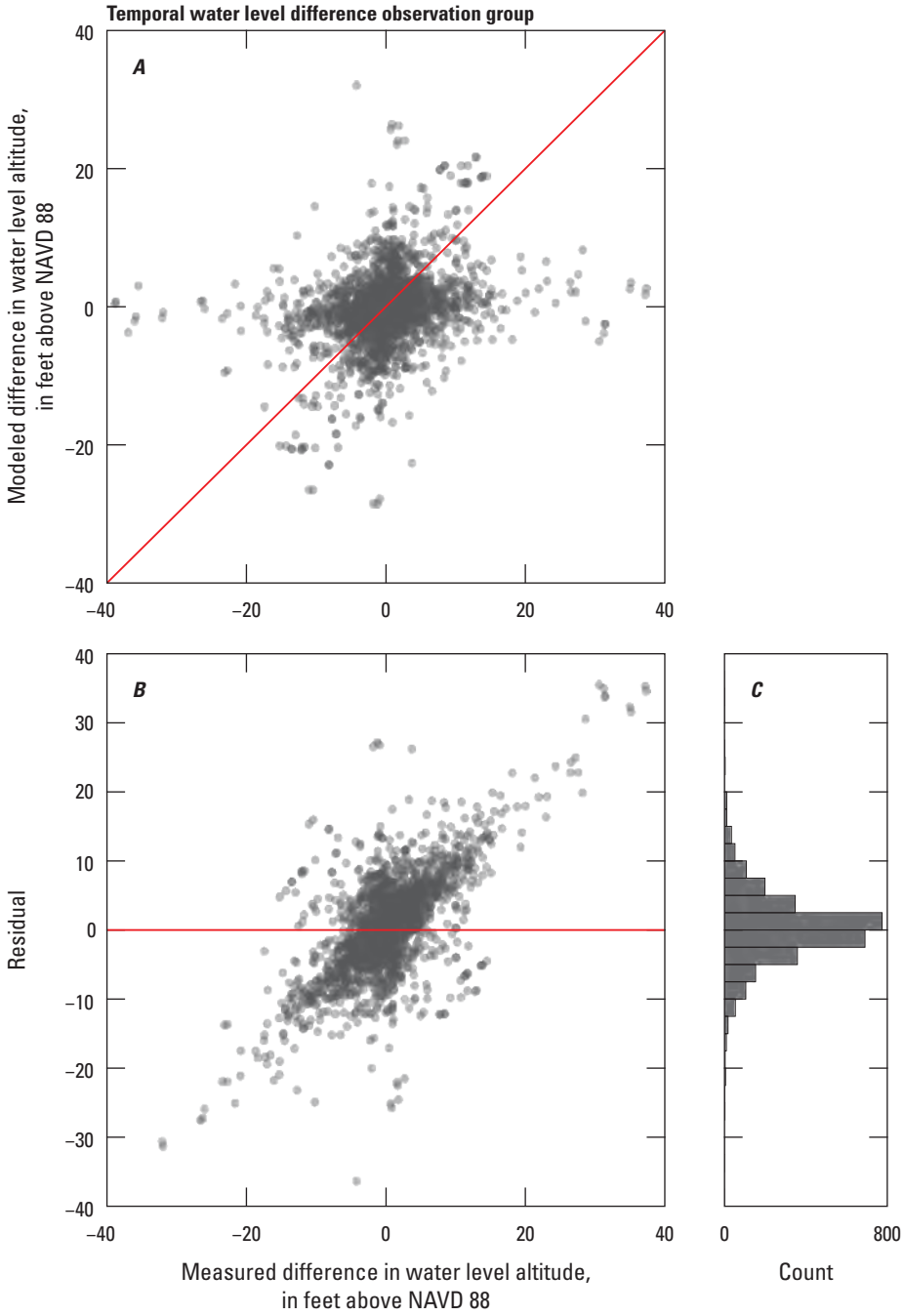

Figure 48. Residual plots for temporal water level differences observation group of the Treasure Valley Groundwater Flow Model, southwestern Idaho and easternmost Oregon (Hundt, 2023).

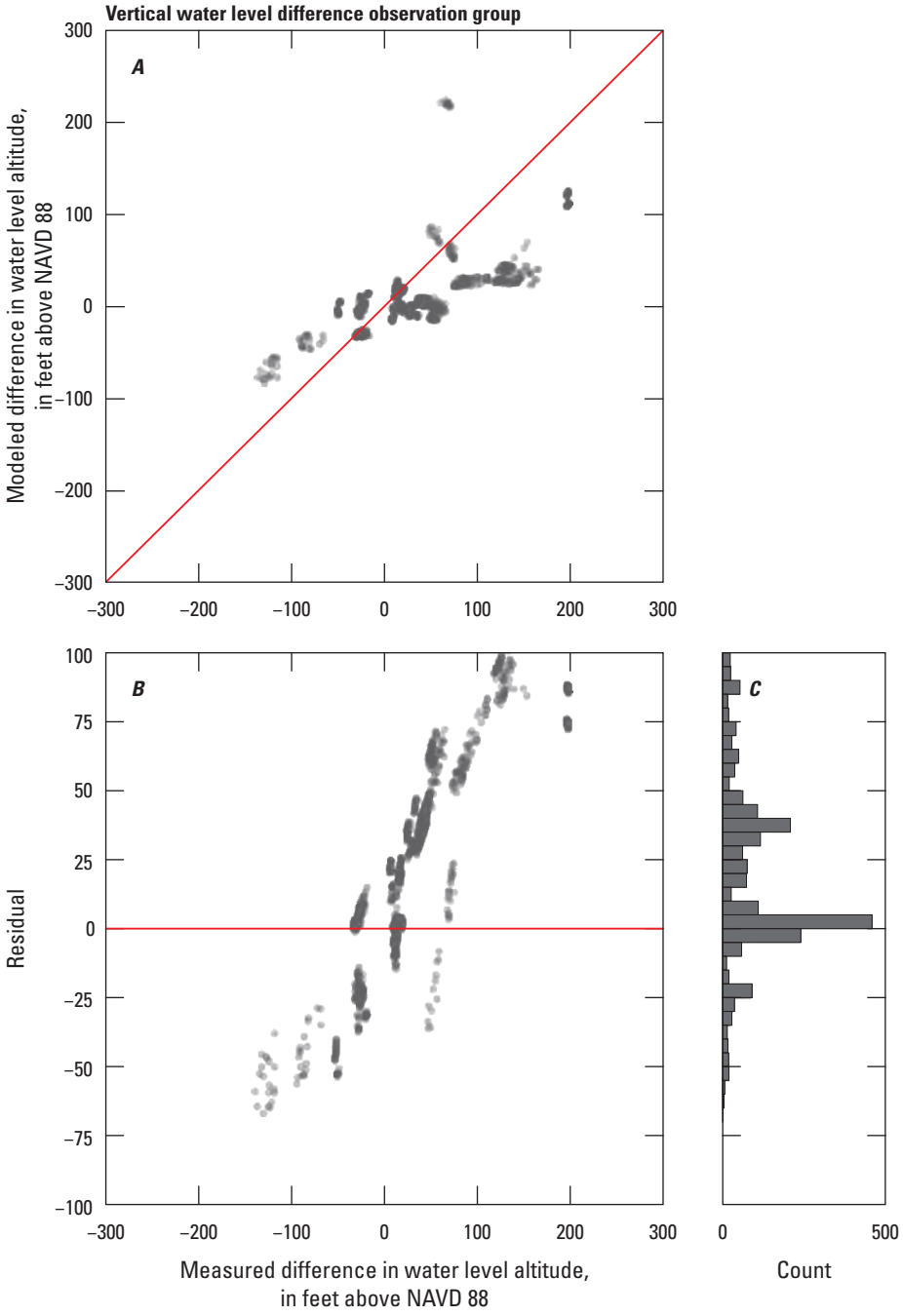

Figure 49. Residual plots for vertical water level differences observation group of the Treasure Valley Groundwater Flow Model, southwestern Idaho and easternmost Oregon (Hundt, 2023).

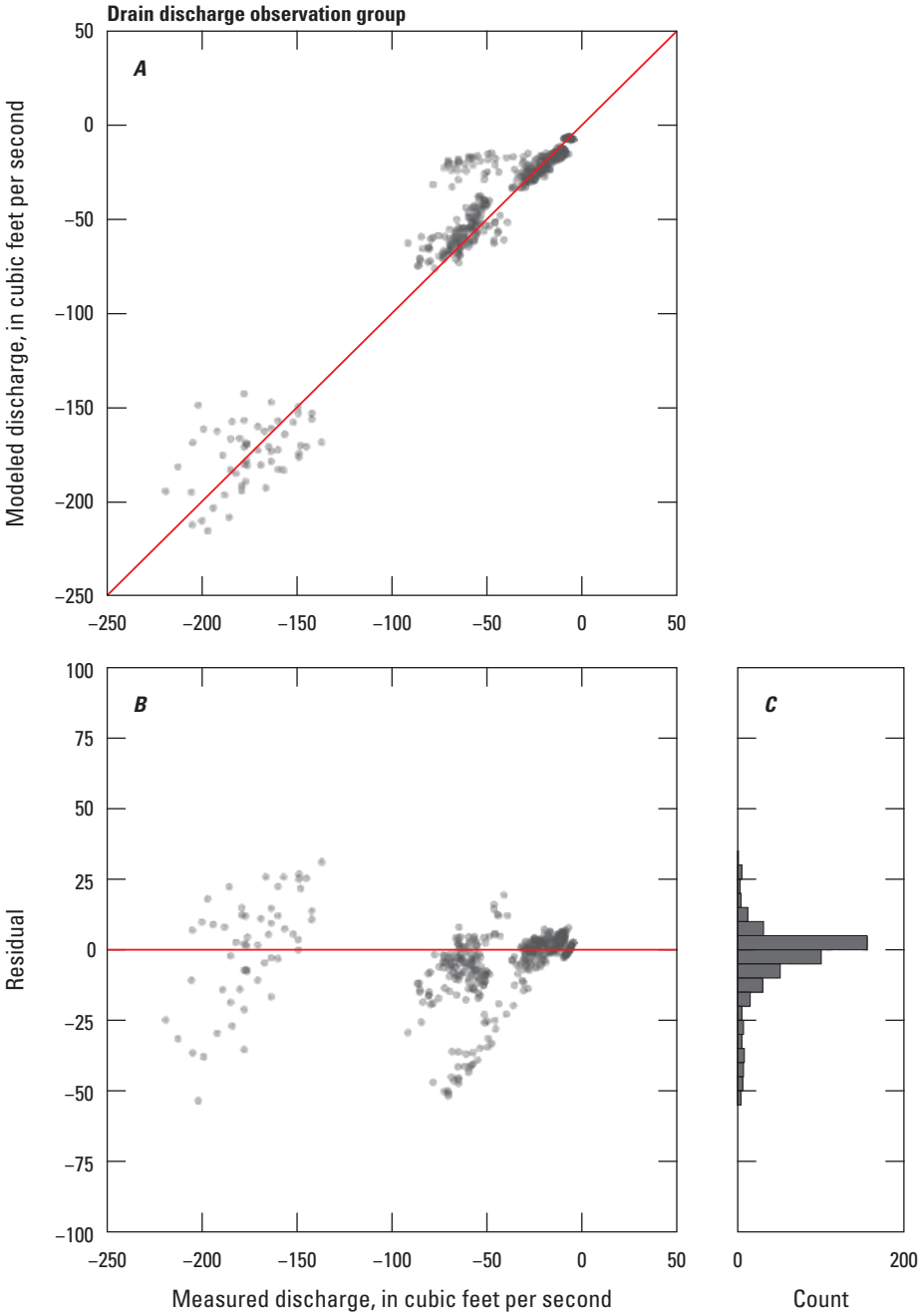

Figure 50. Residual plots for drain discharge observation group of the Treasure Valley Groundwater Flow Model, southwestern Idaho and easternmost Oregon (Hundt, 2023).

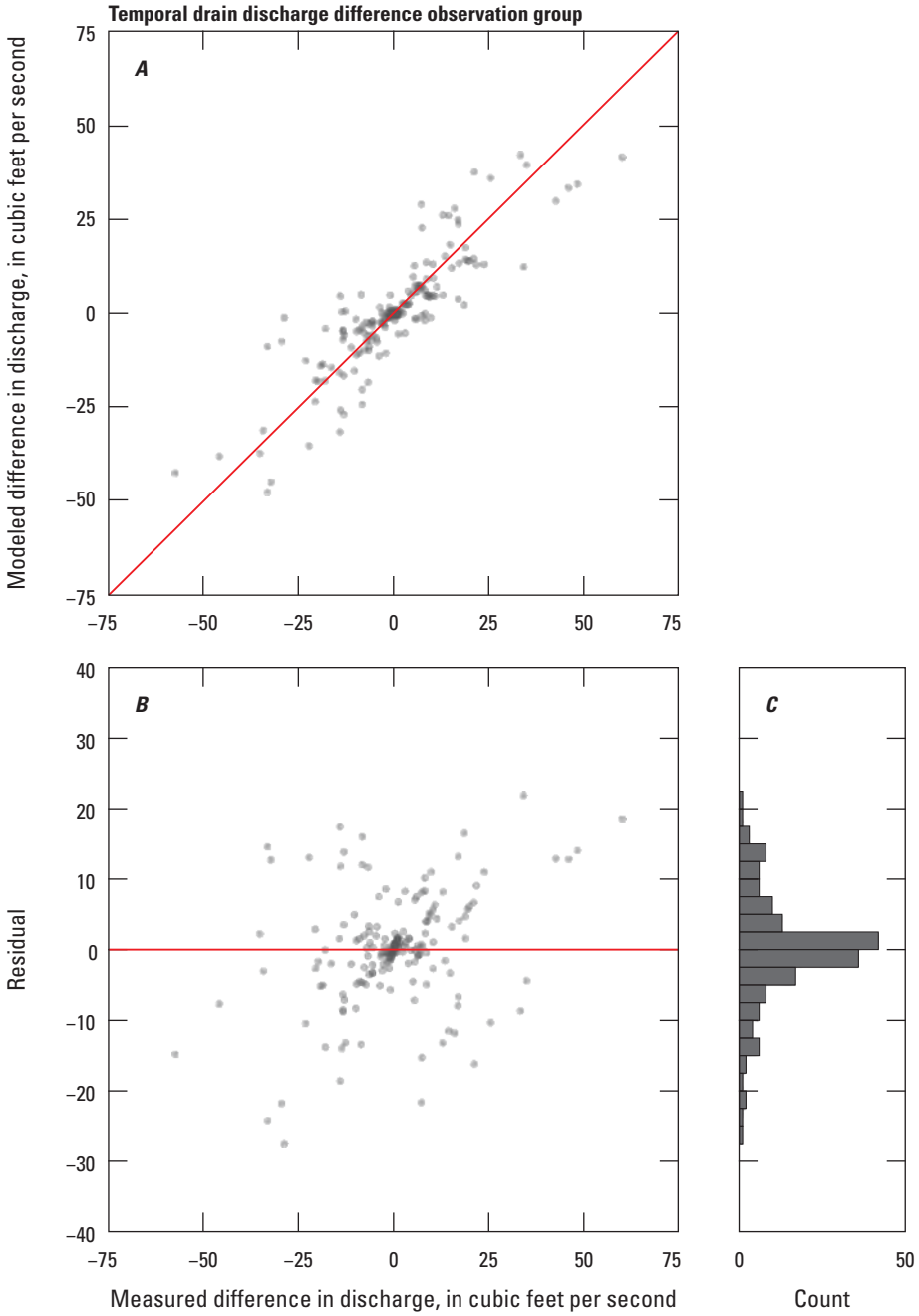

Figure 51. Residual plots for temporal drain discharge observation group of the Treasure Valley Groundwater Flow Model, southwestern Idaho and easternmost Oregon (Hundt, 2023).

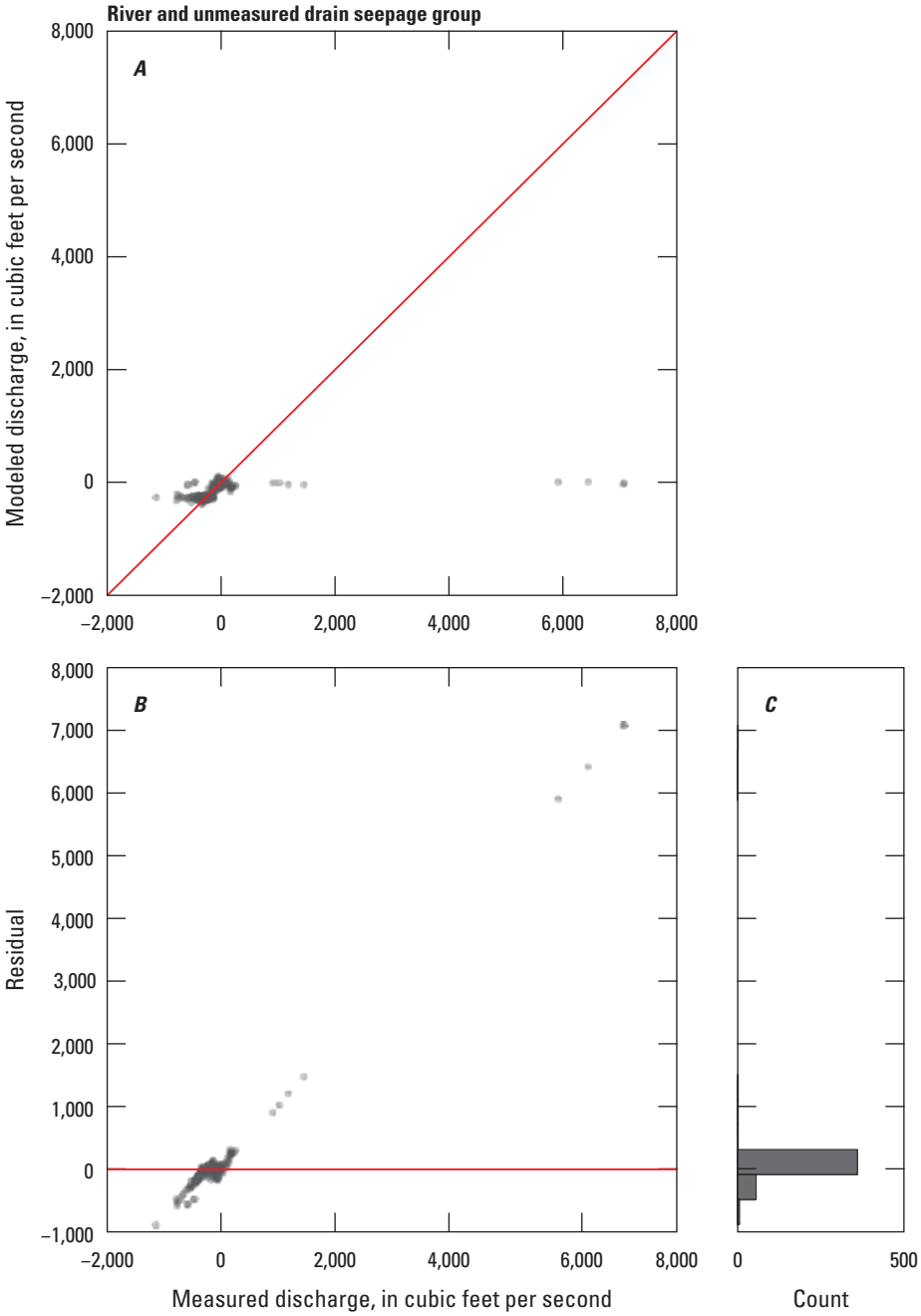

Figure 52. Residual plots for river and unmeasured drain seepage group of the Treasure Valley Groundwater Flow Model, southwestern Idaho and easternmost Oregon (Hundt, 2023).

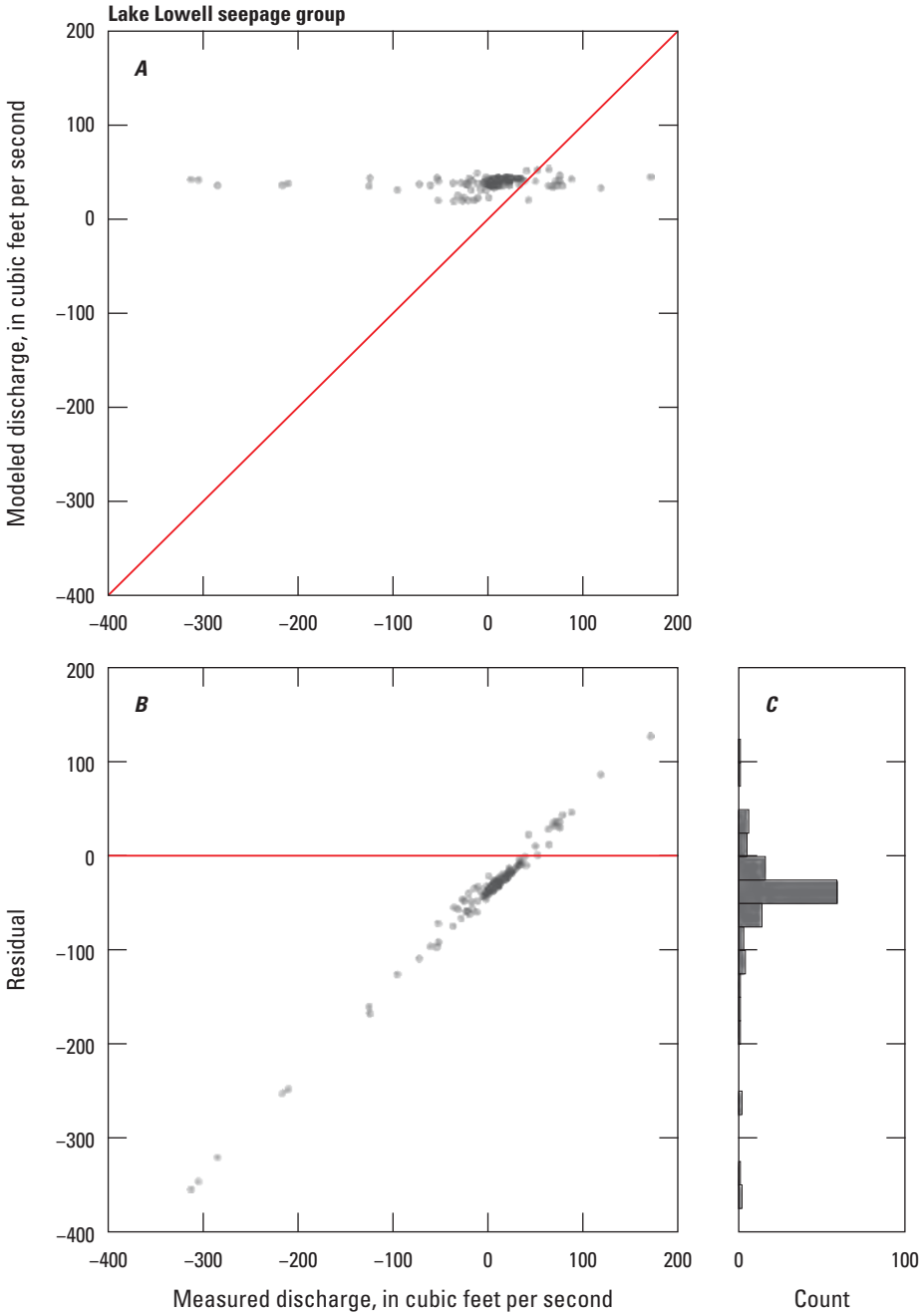

Figure 53. Residual plots for Lake Lowell seepage observation group of the Treasure Valley Groundwater Flow Model, southwestern Idaho and easternmost Oregon (Hundt, 2023).

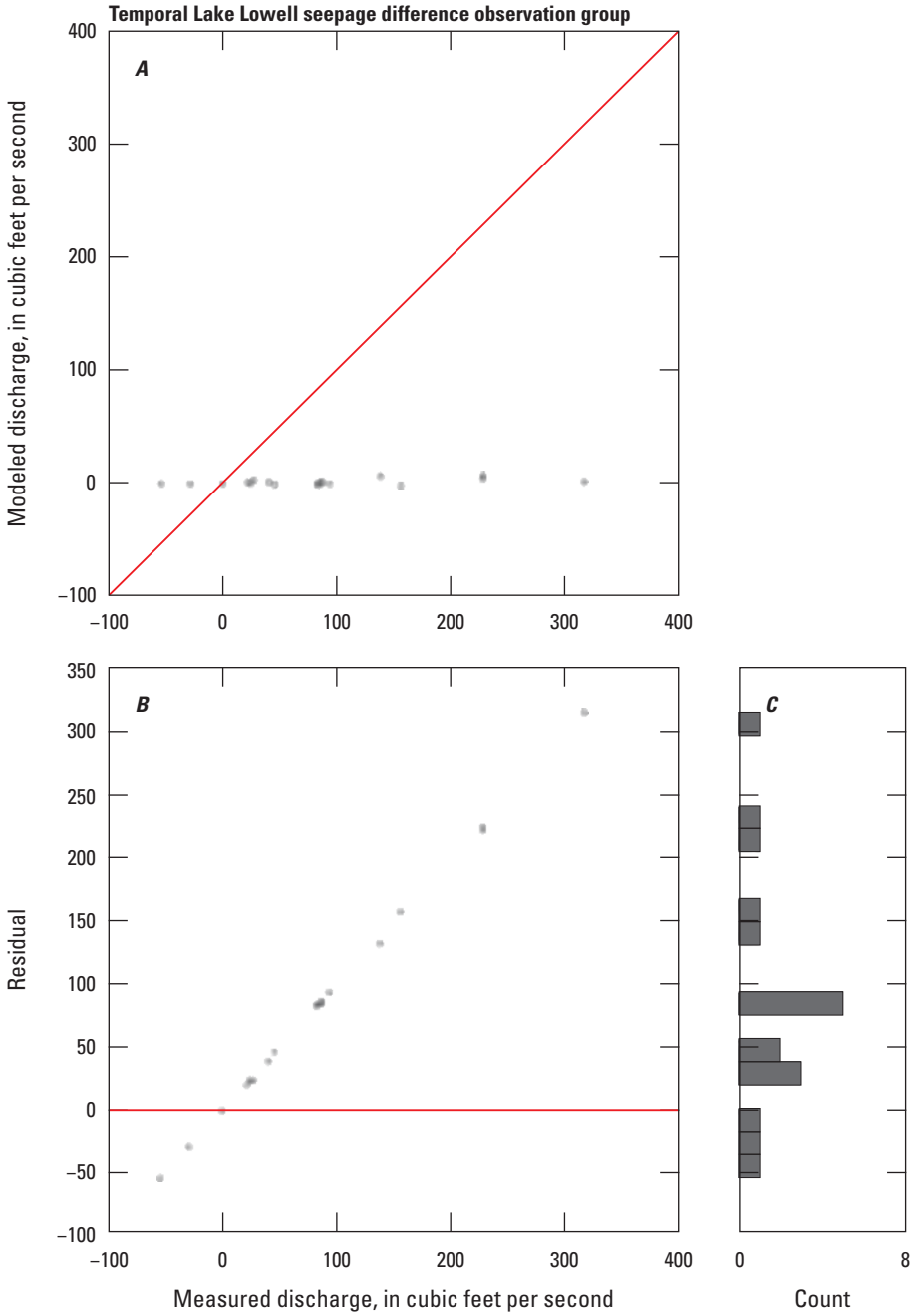

Figure 54. Residual plots for temporal Lake Lowell seepage difference observation group of the Treasure Valley Groundwater Flow Model, southwestern Idaho and easternmost Oregon (Hundt, 2023).

Maps of the mean water level residual across all stress periods for each observation point are shown on figures 55–60. Green triangles show where water levels are over-simulated and red triangles where they are under-simulated. One map is shown for each of the six layers, including all (non-zero weighted) wells open to that layer. Wells open across multiple layers will be shown on multiple figures. Notable regions of under-simulation can be seen in the foothills on the eastern edge of the study area, near Indian Creek in the southeast, and to the northwest of Lake Lowell. Notable regions of over-simulation can be seen southwest of Lake Lowell, near the New York Canal, and near the City of Eagle.

Figure 61 contains a map of the mean residual value for the vertical water level difference observation group. All points are shown on a single map, regardless of which layers the pairs of wells are open to. The color of the point represents the size of the residual between the observed vertical gradient and the simulated vertical gradient. The direction of the gradient, observed or simulated, is not represented on this figure.

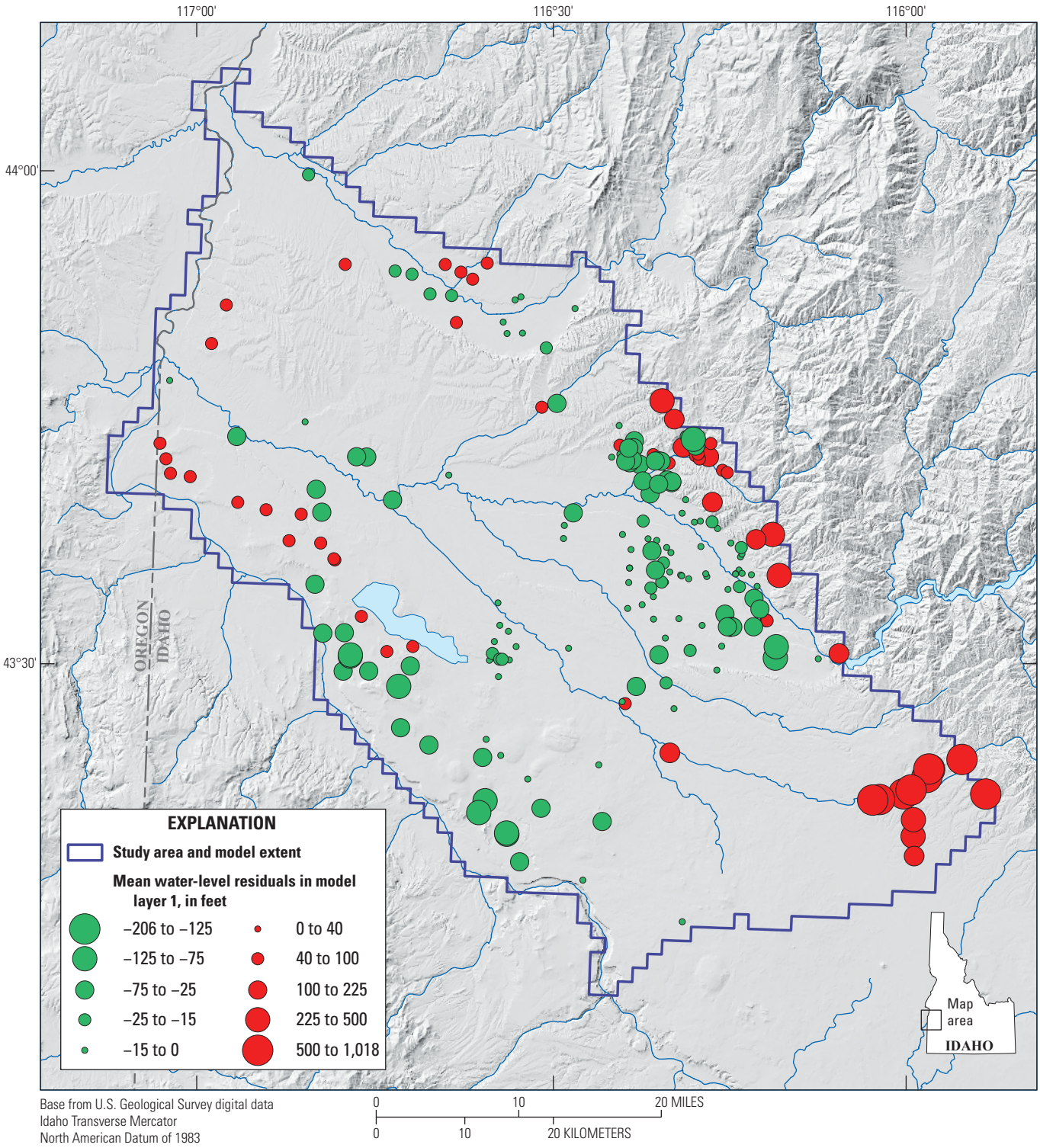

Figure 55. Mean water level residuals (measured minus modelled) in layer 1 of the Treasure Valley Groundwater Flow Model, southwestern Idaho and easternmost Oregon (Hundt, 2023).

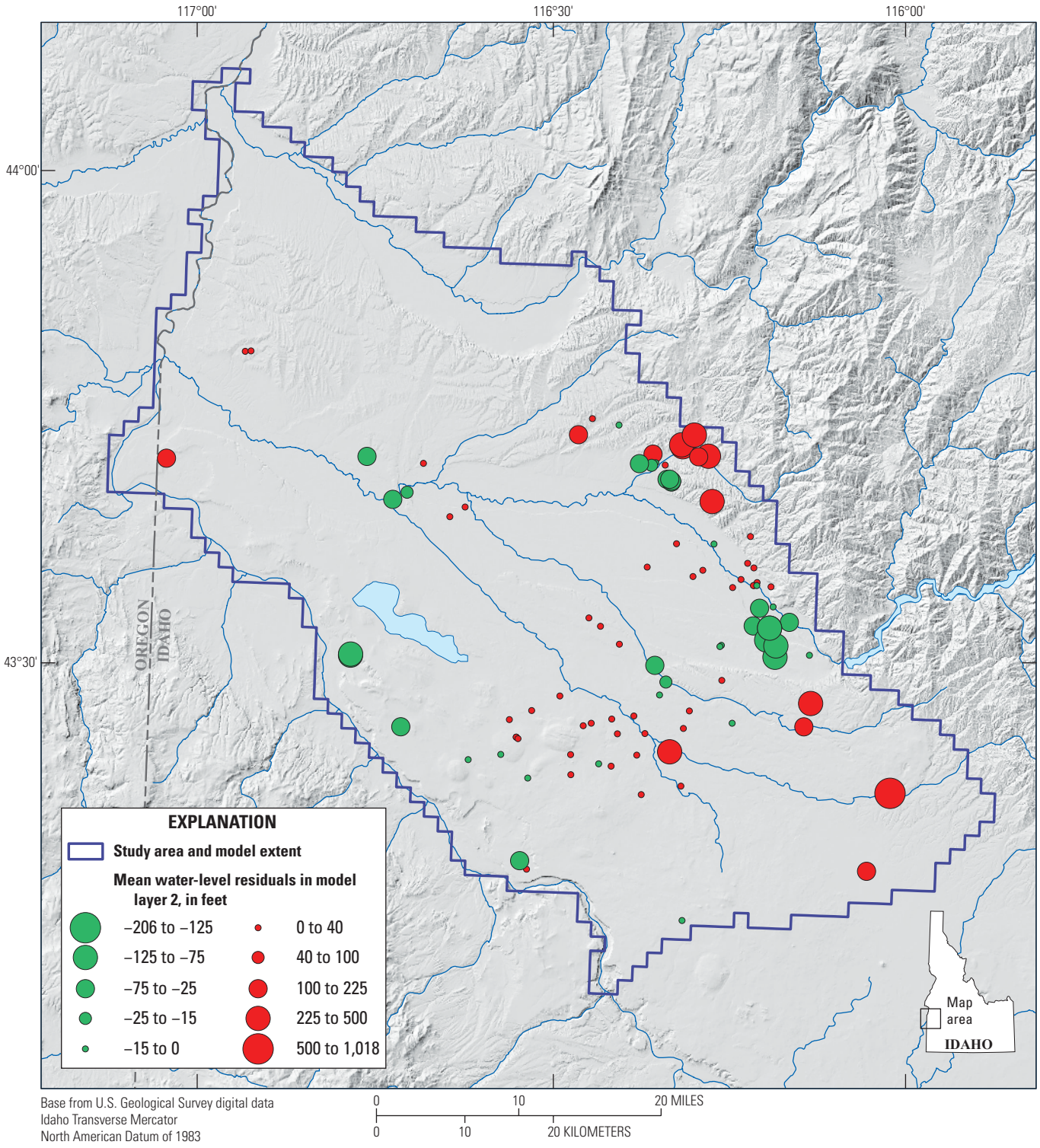

Figure 56. Mean water level residuals (measured minus modelled) in layer 2 of the Treasure Valley Groundwater Flow Model, southwestern Idaho and easternmost Oregon (Hundt, 2023).

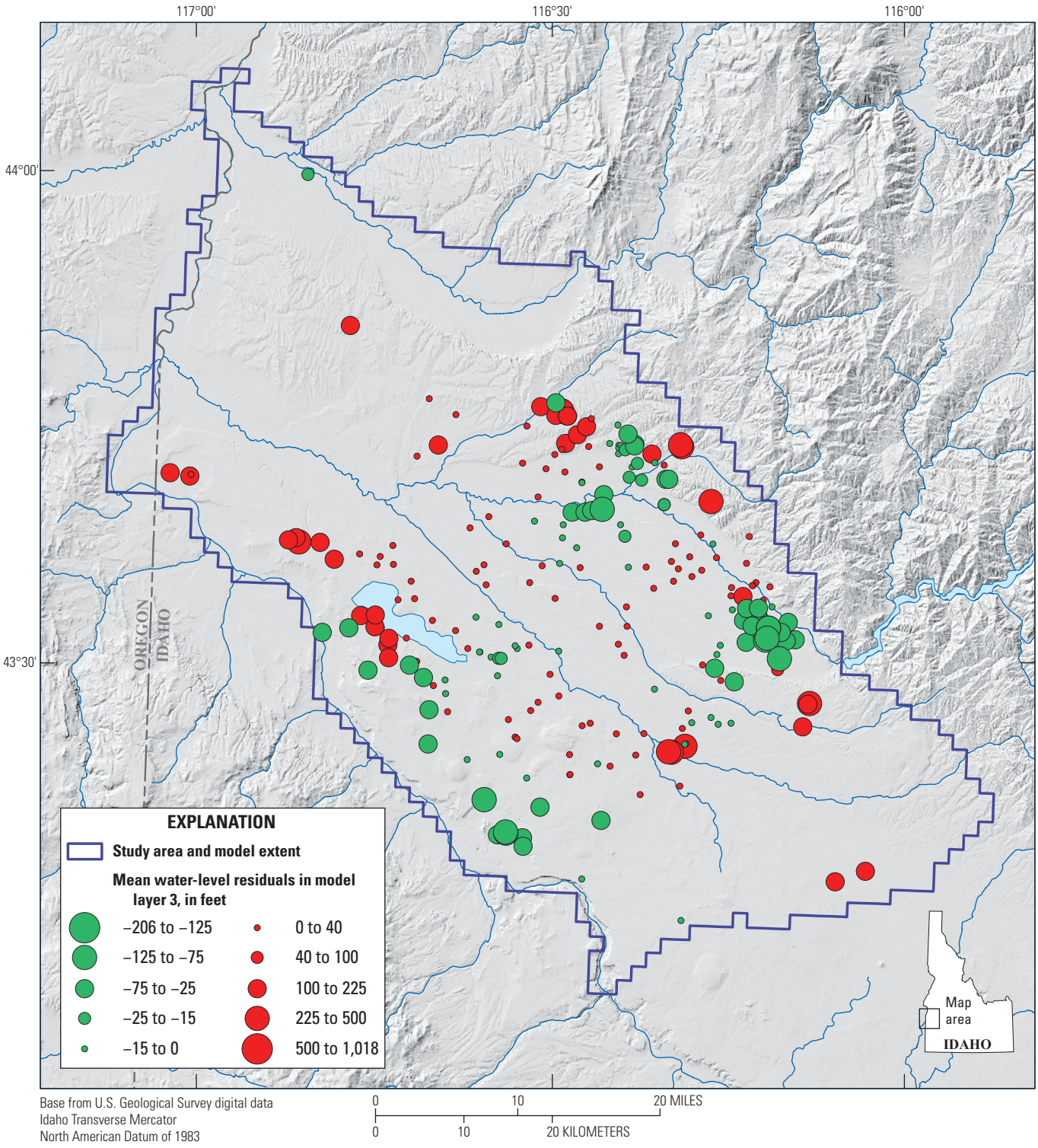

Figure 57. Mean water level residuals (measured minus modelled) in layer 3 of the Treasure Valley Groundwater Flow Model, southwestern Idaho and easternmost Oregon (Hundt, 2023).

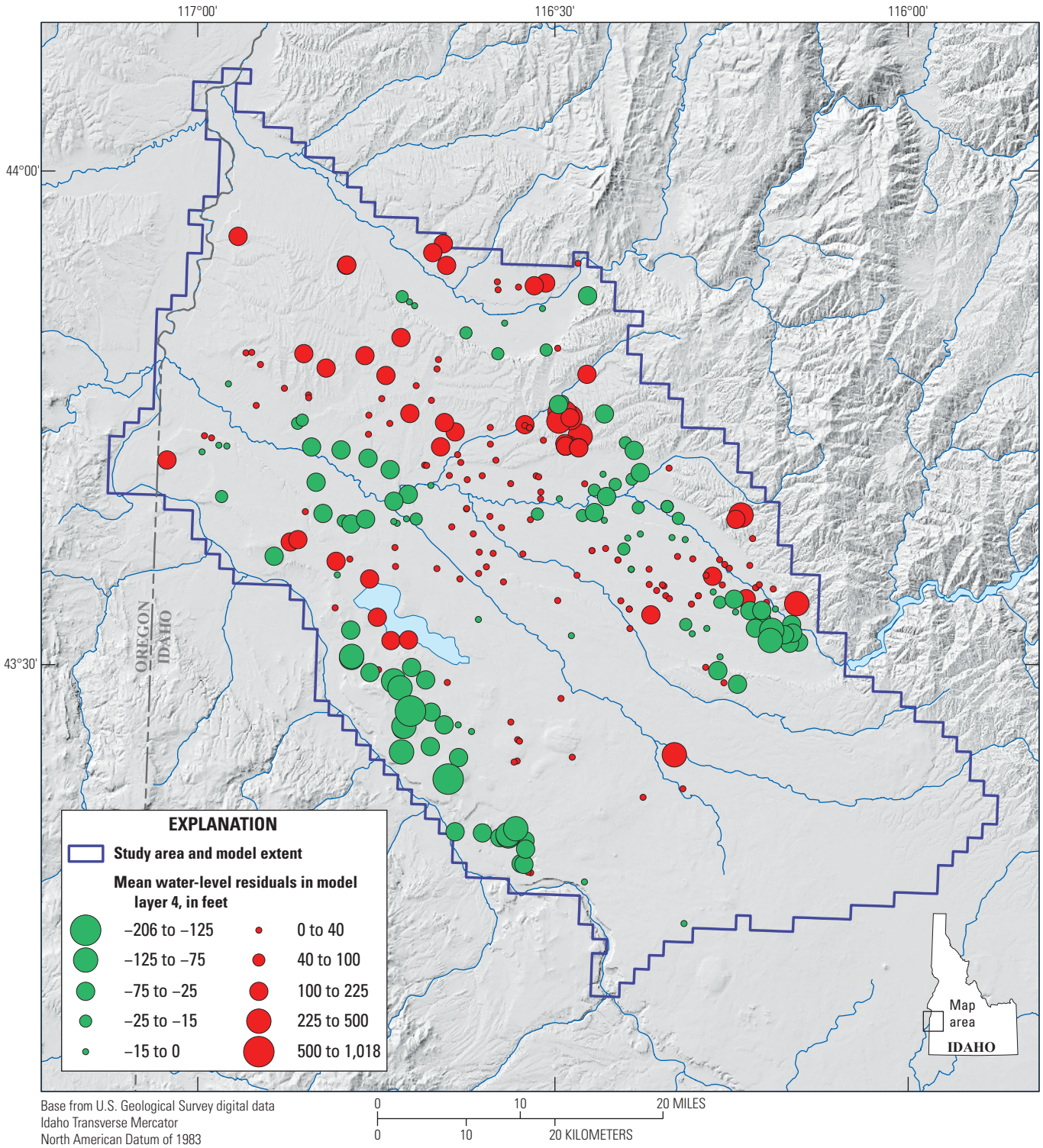

Figure 58. Mean water level residuals (measured minus modelled) in layer 4 of the Treasure Valley Groundwater Flow Model, southwestern Idaho and easternmost Oregon (Hundt, 2023).

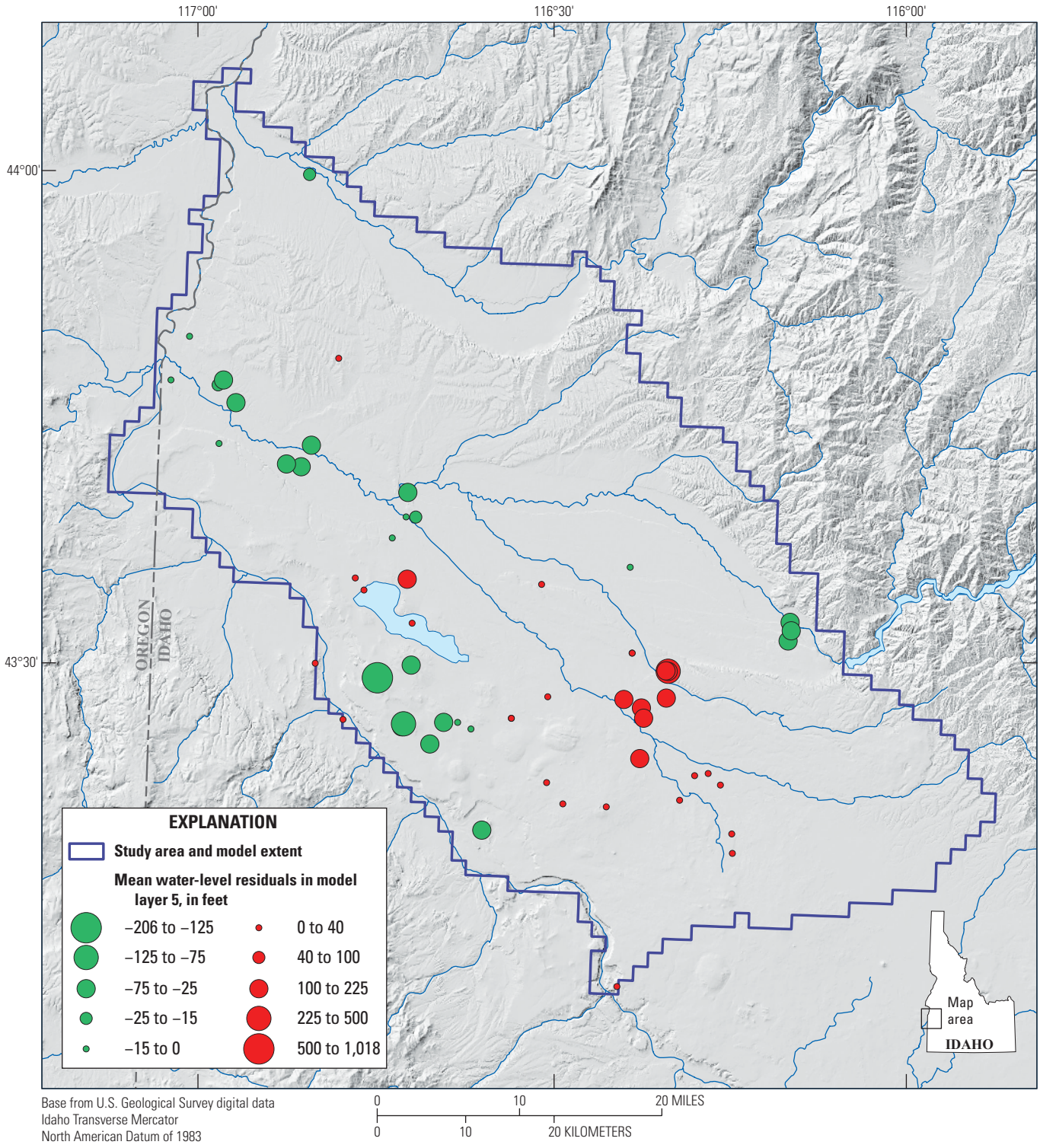

Figure 59. Mean water level residuals (measured minus modelled) in layer 5 of the Treasure Valley Groundwater Flow Model, southwestern Idaho and easternmost Oregon (Hundt, 2023).

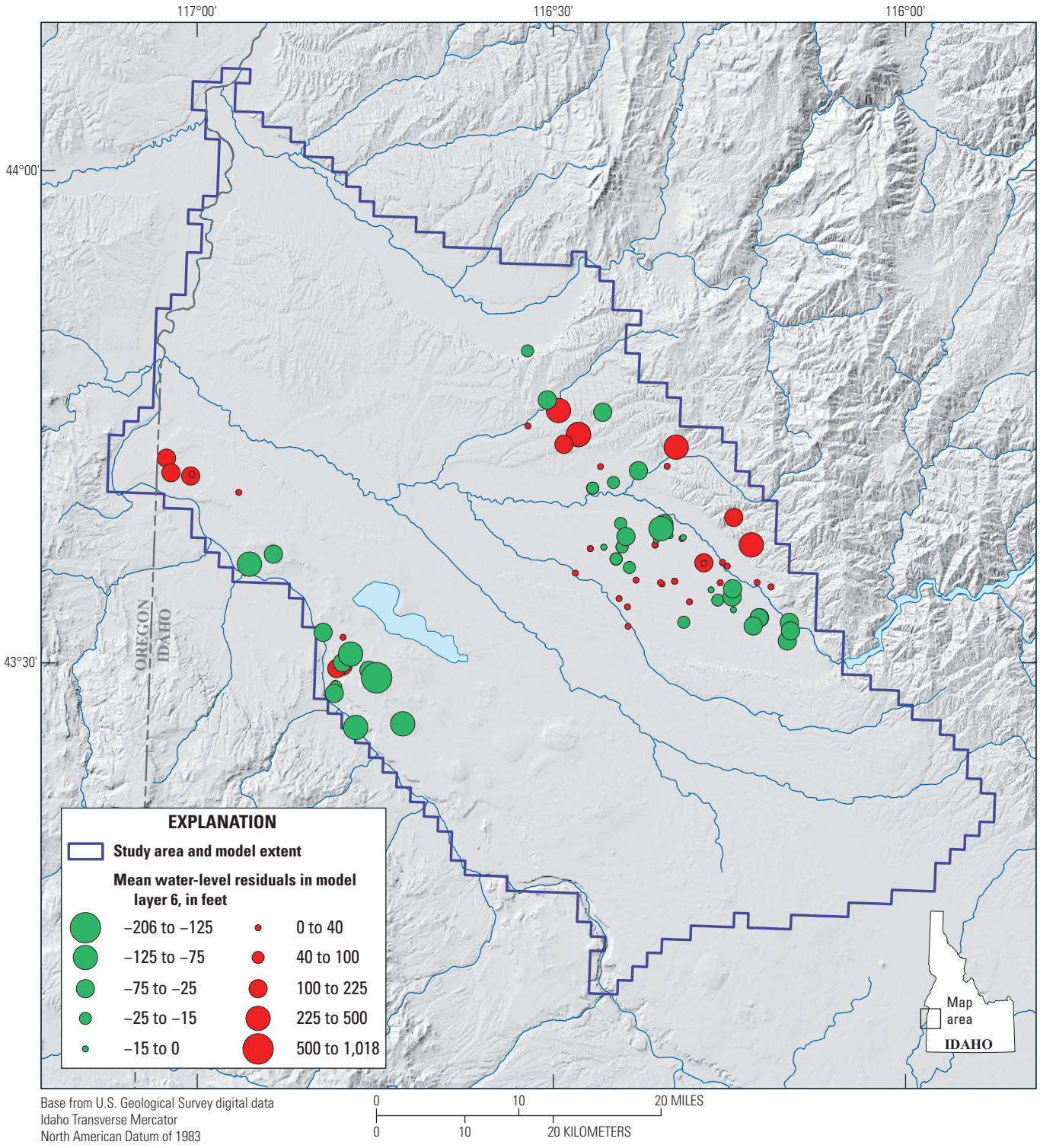

Figure 60. Mean water level residuals (measured minus modelled) in layer 6 of the Treasure Valley Groundwater Flow Model, southwestern Idaho and easternmost Oregon (Hundt, 2023).

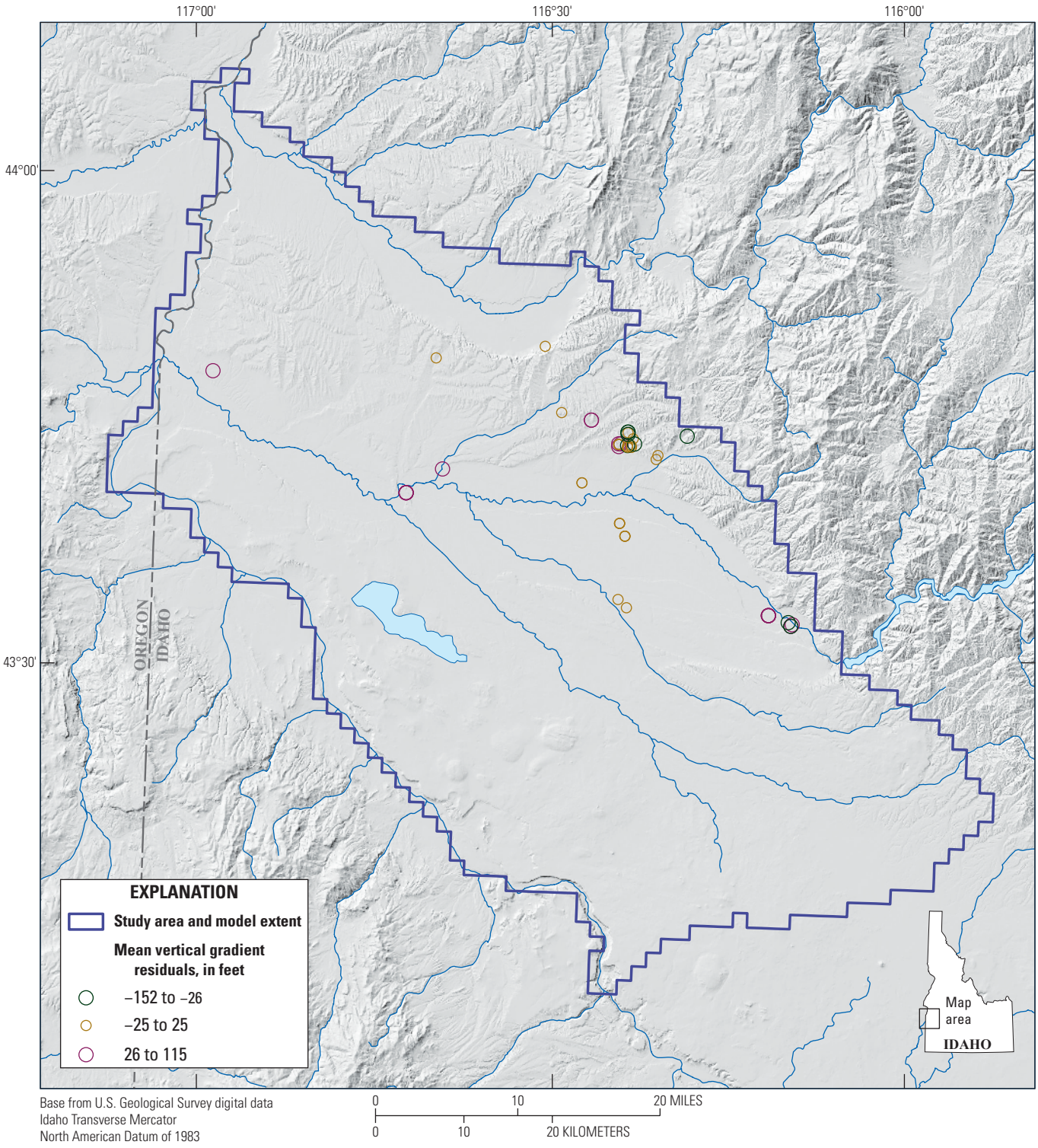

Figure 61. Mean vertical water level difference residuals for all layers of the Treasure Valley Groundwater Flow Model, southwestern Idaho and easternmost Oregon (Hundt, 2023).

Figures 62–67 show the contour maps of simulated water levels for all model layers for the stress period representing June 2015. Notable features of these maps include a local groundwater divide along the New York Canal, elevated water levels near Lake Lowell, and sharp water level gradients along the Snake River upstream of its confluence with the Boise River.

Budgets of simulated inflows to and outflows from the aquifer are summarized for three areas of the model area: the entire model area, a zone aligning with the TVHP model boundary (Petrich, 2004), and a zone covering the Payette Valley (fig. 68). Figures 69–71 show annual total budget components, and figures 72–74 show average monthly budget components. Average annual budget totals and proportions of total inflow and outflows are shown on table 10. Tables 11 and 12 show average annual totals for selected years for the TVHP and Payette budget zones and how they compare to previous water budget estimates from Urban (2004) and Sukow (2012).

A few noteworthy behaviors can be seen in the annual and seasonal variability in water budgets. First, because all inflows and outflows are accounted for (including change in storage), the overall size of the budget changes from year to year, with wet years showing a greater overall budget volume and dry years a lesser volume. Next, the magnitude of the water budget is much greater during the growing season, when irrigation water (and the associated recharge) is being delivered. During the irrigation season a large net increase in groundwater storage is induced, as the inflows of (mostly) irrigation water exceeds the outflows to (mostly) rivers and drains. During the non-irrigation season little recharge is observed and a net decrease in groundwater storage observed as groundwater continues to discharge to rivers and drains. Finally, the water budgets of the Boise and Payette valleys show broadly similar behavior, with the Boise seeing greater canal seepage and infiltration and pumping for semi-irrigated lands.

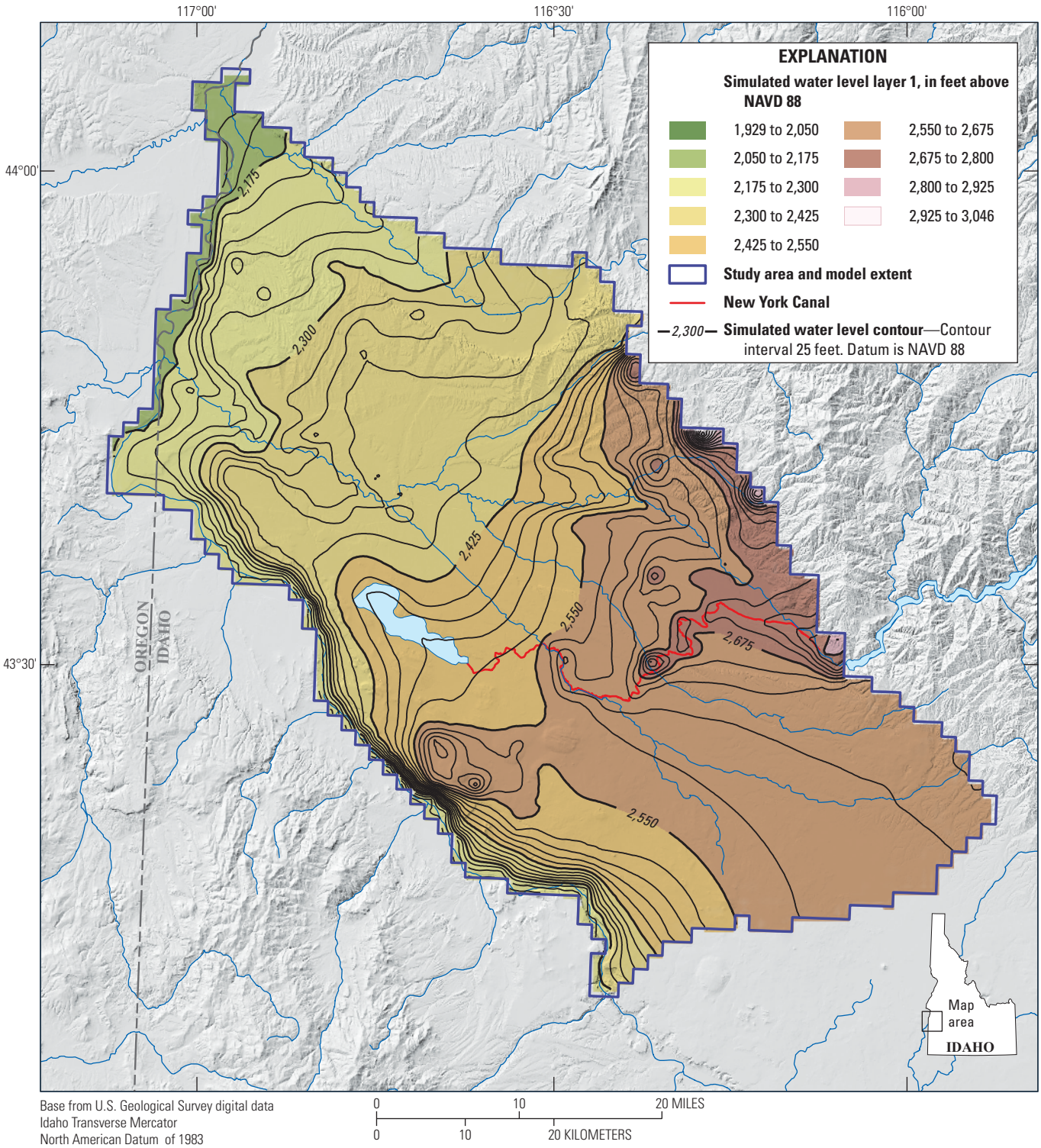

Figure 62. Simulated water level contours for June 2015 in layer 1 of the Treasure Valley Groundwater Flow Model, southwestern Idaho and easternmost Oregon (Hundt, 2023). NAVD 88, North American Vertifcal Datum of 1988.

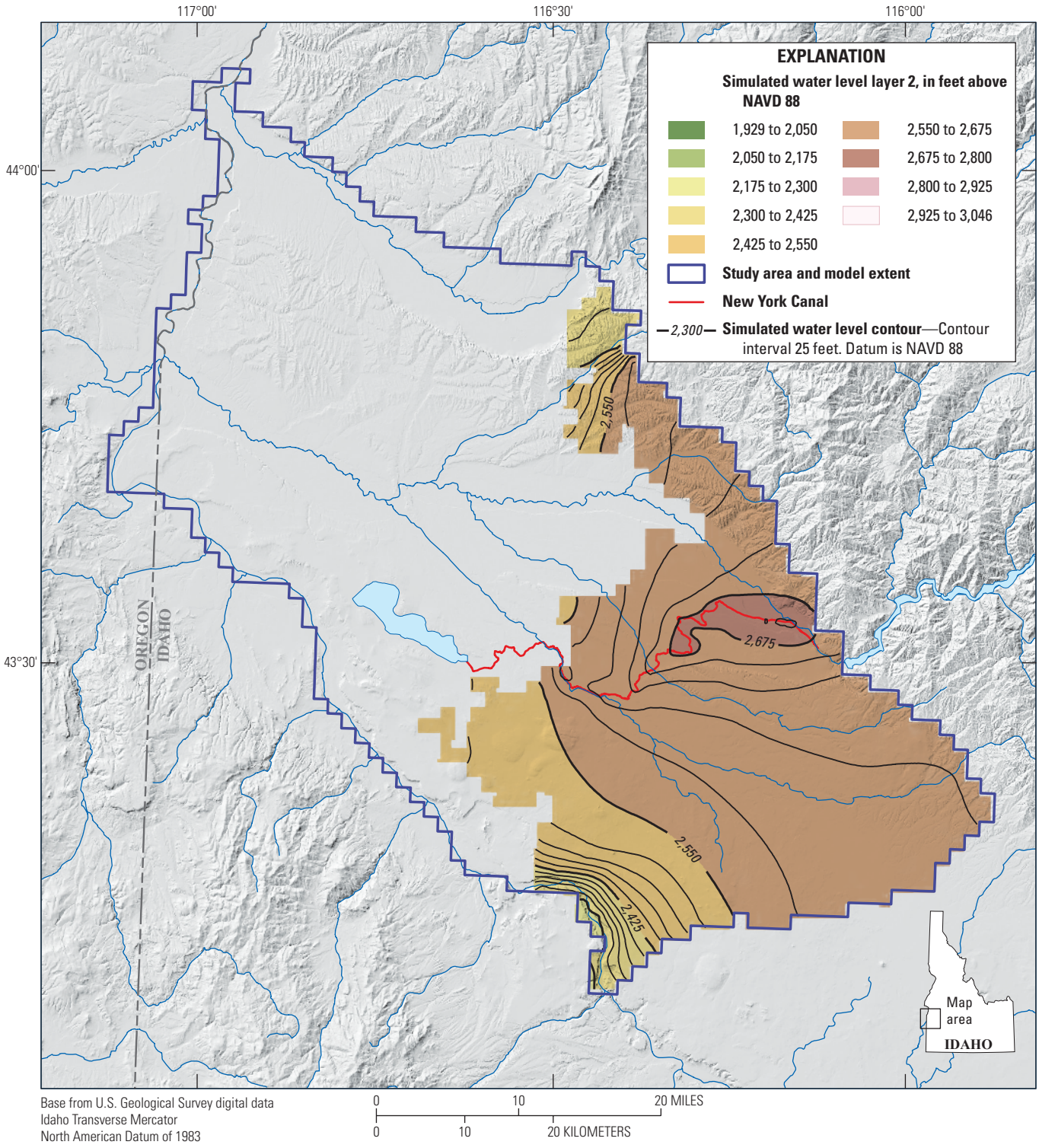

Figure 63. Simulated water level contours for June 2015 in layer 2 of the Treasure Valley Groundwater Flow Model, southwestern Idaho and easternmost Oregon (Hundt, 2023). NAVD 88, North American Vertifcal Datum of 1988.

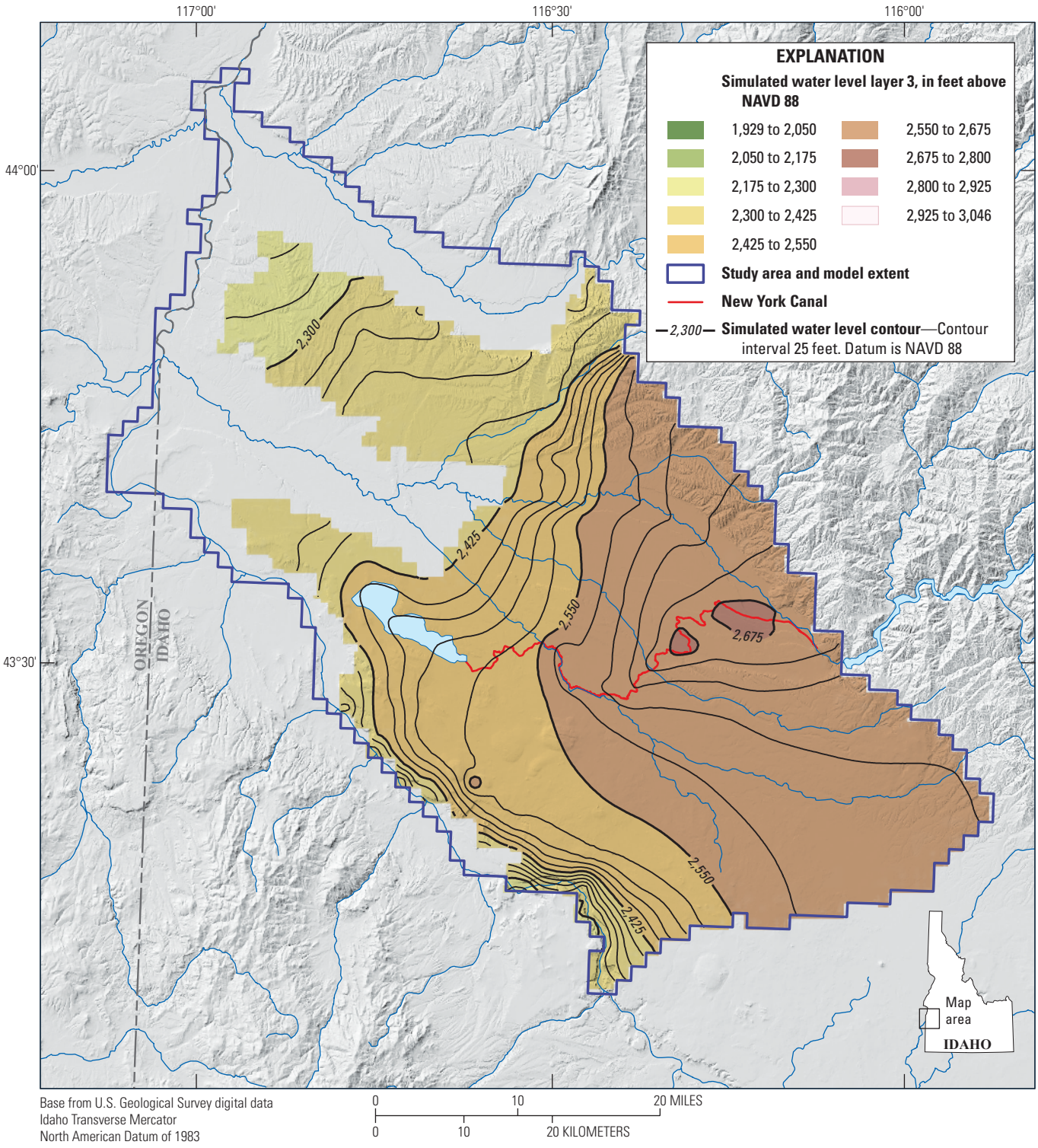

Figure 64. Simulated water level contours for June 2015 in layer 3 of the Treasure Valley Groundwater Flow Model, southwestern Idaho and easternmost Oregon (Hundt, 2023). NAVD 88, North American Vertifcal Datum of 1988.

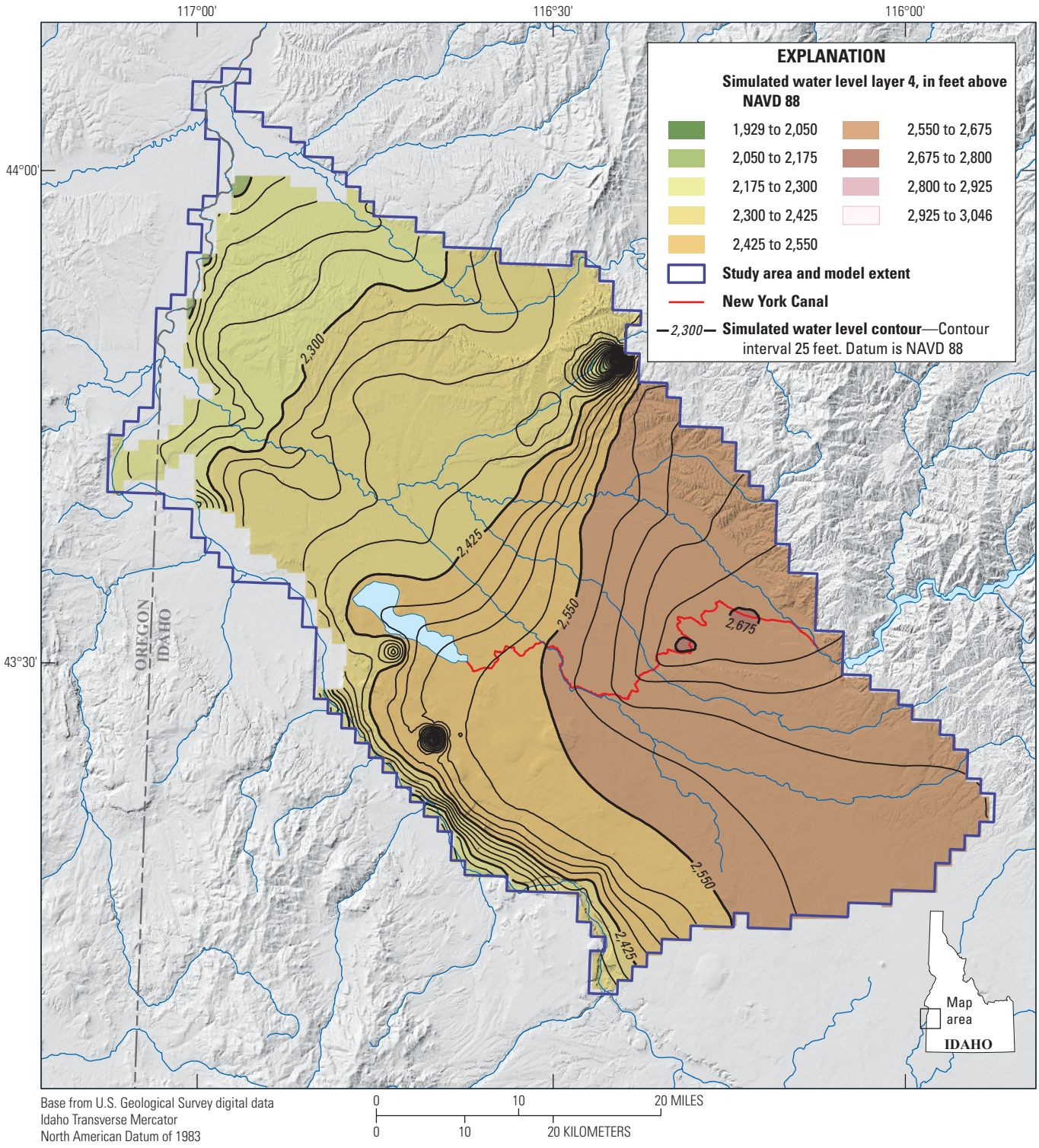

Figure 65. Simulated water level contours for June 2015 in layer 4 of the Treasure Valley Groundwater Flow Model, southwestern Idaho and easternmost Oregon (Hundt, 2023). NAVD 88, North American Vertifcal Datum of 1988.

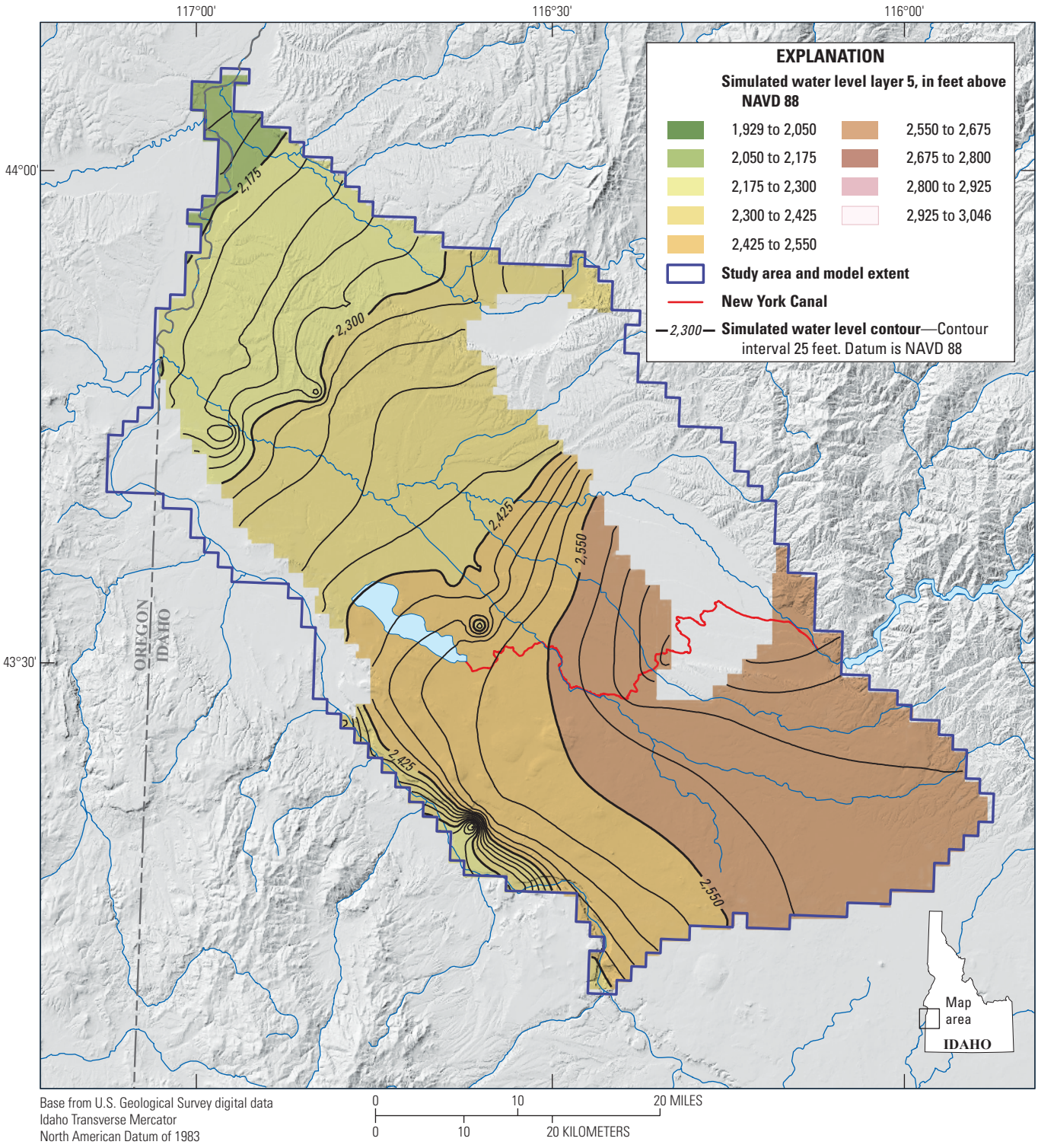

Figure 66. Simulated water level contours for June 2015 in layer 5 of the Treasure Valley Groundwater Flow Model, southwestern Idaho and easternmost Oregon (Hundt, 2023). NAVD 88, North American Vertifcal Datum of 1988.

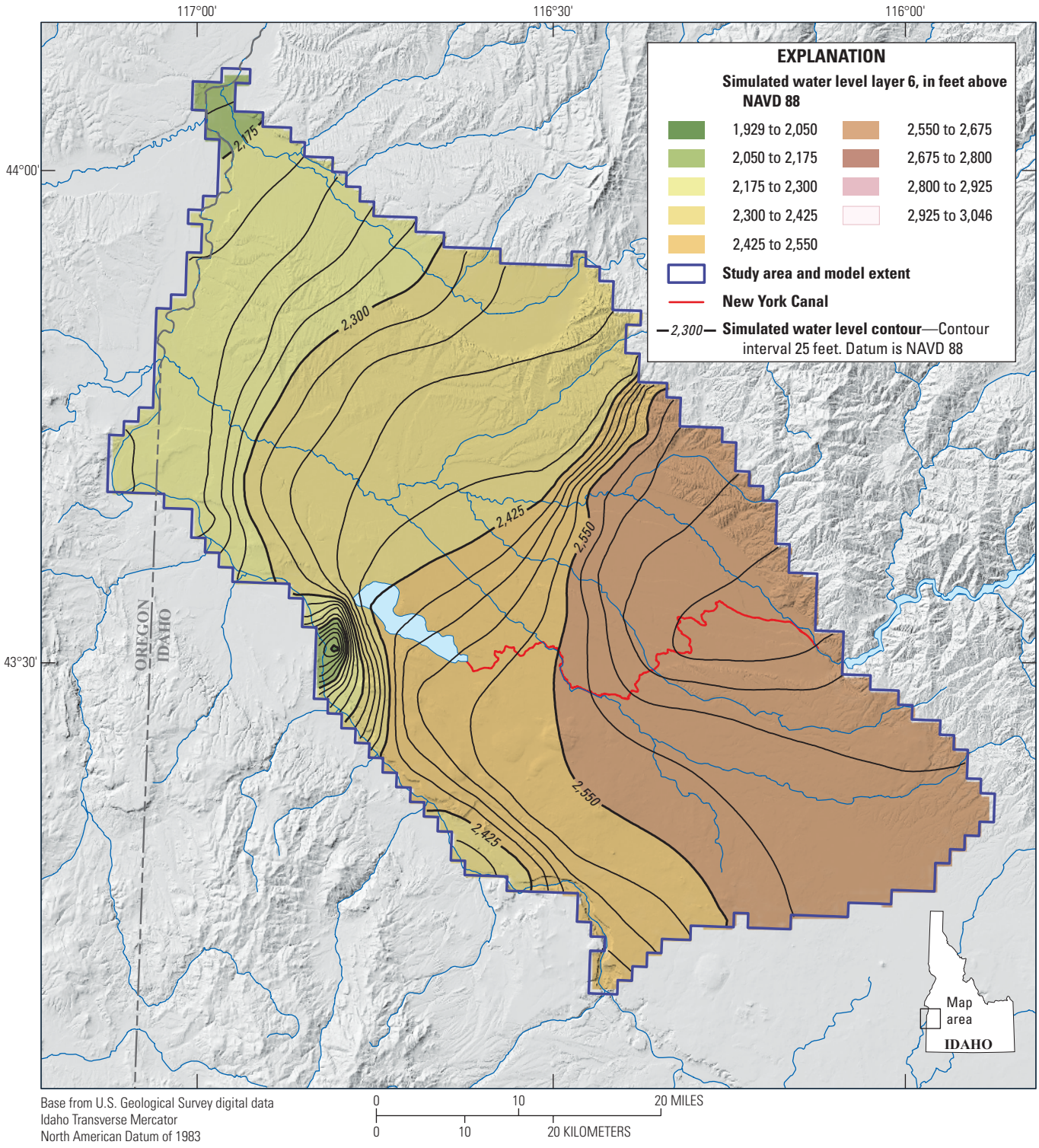

Figure 67. Simulated water level contours for June 2015 in layer 6 of the Treasure Valley Groundwater Flow Model, southwestern Idaho and easternmost Oregon.Water Budget (Hundt, 2023). NAVD 88, North American Vertifcal Datum of 1988.

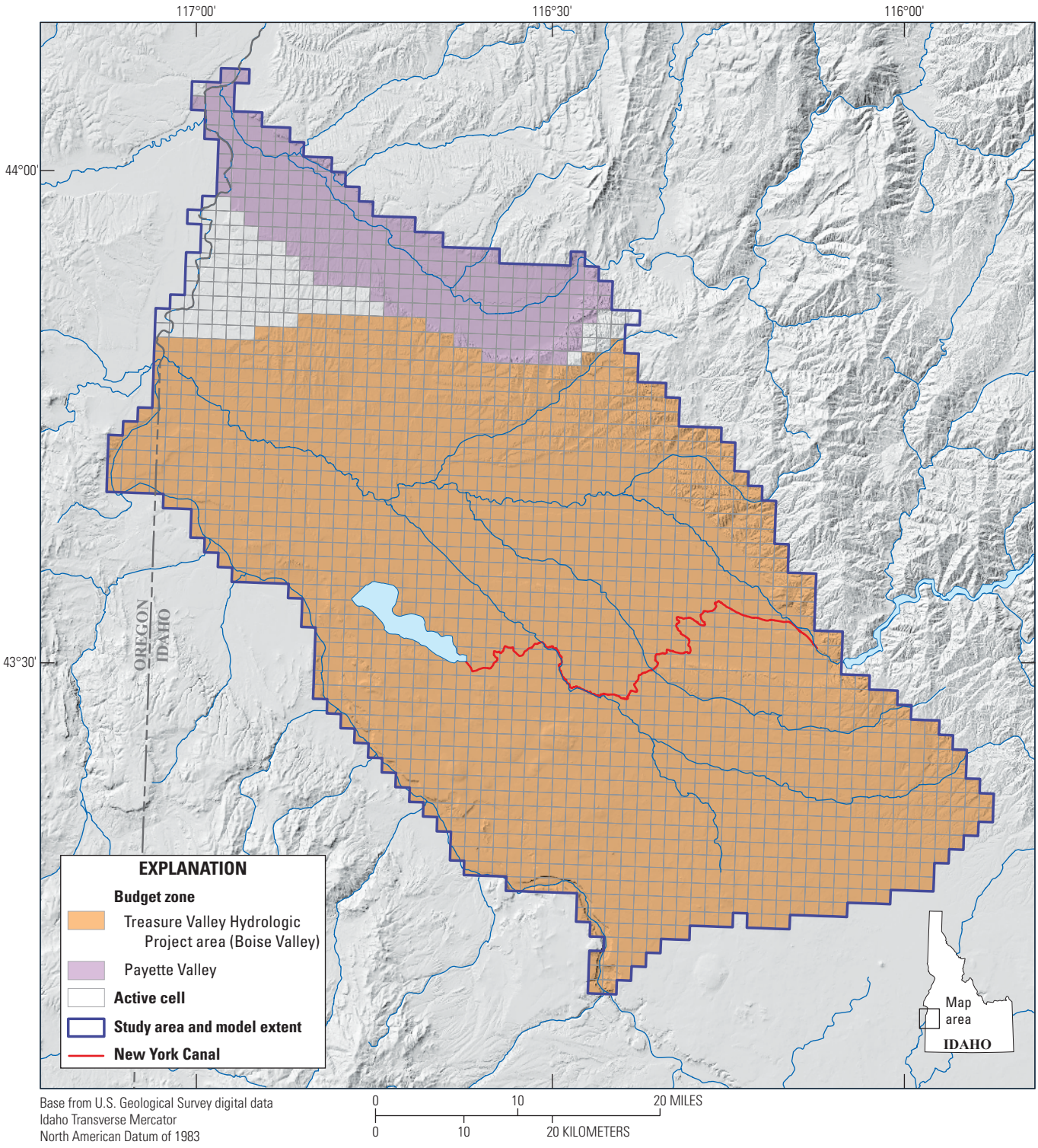

Figure 68. Water budget summary zones of the Treasure Valley Groundwater Flow Model, southwestern Idaho and easternmost Oregon (Hundt, 2023).

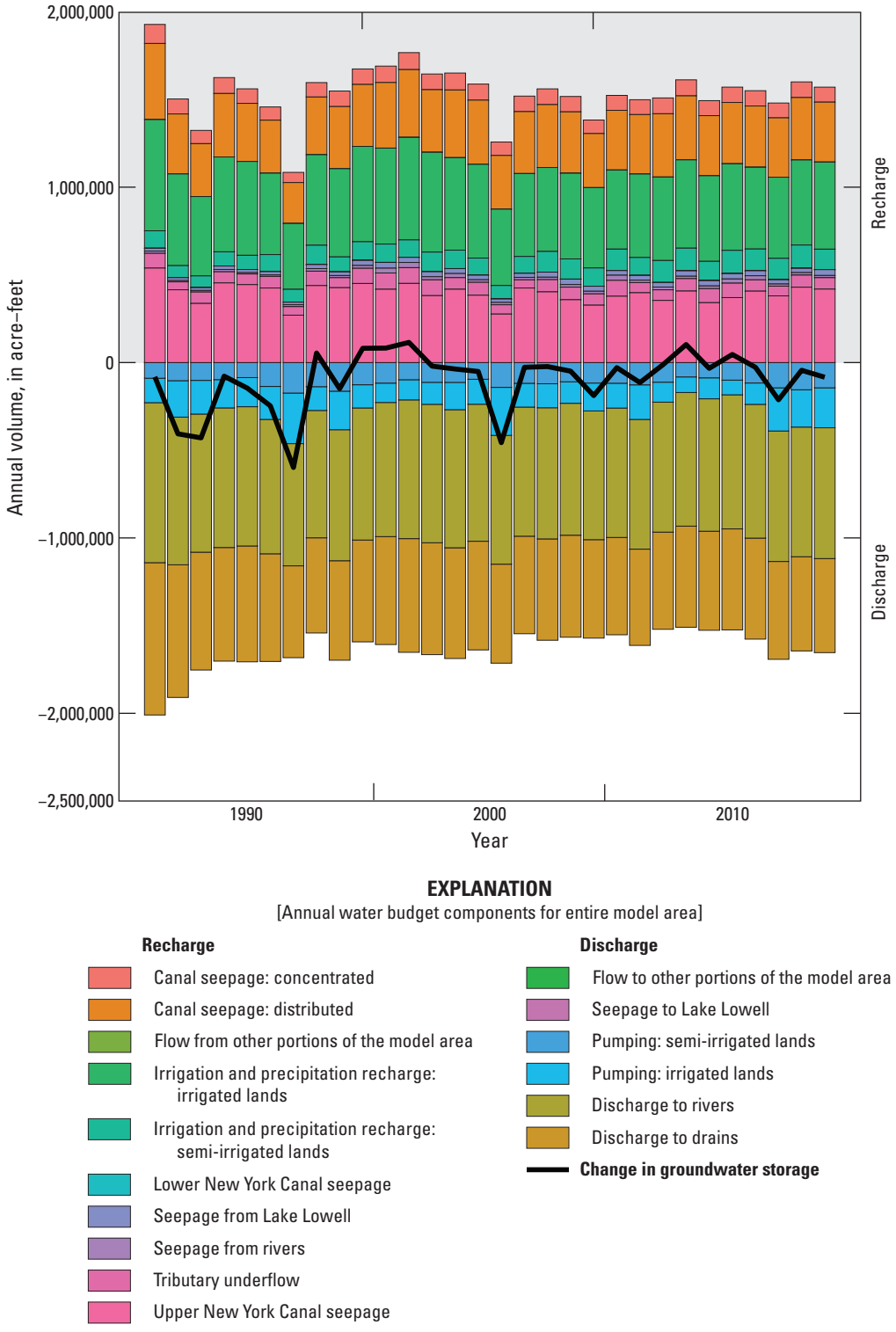

Figure 69. Annual water budget components for entire Treasure Valley Groundwater Flow Model area, southwestern Idaho and easternmost Oregon (Hundt, 2023).

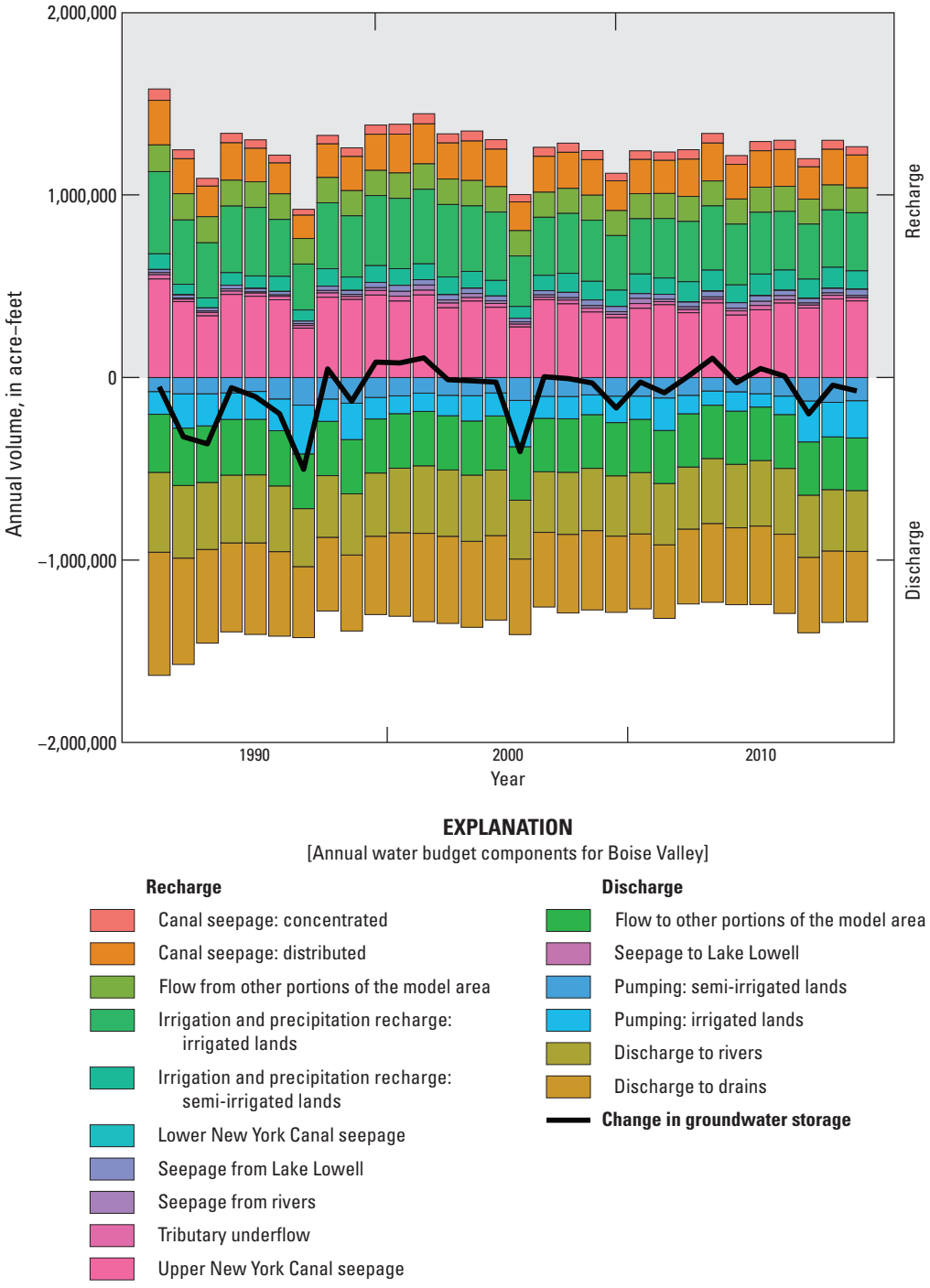

Figure 70. Annual Boise Valley water budget components for the Treasure Valley Groundwater Flow Model, southwestern Idaho and easternmost Oregon (Hundt, 2023).

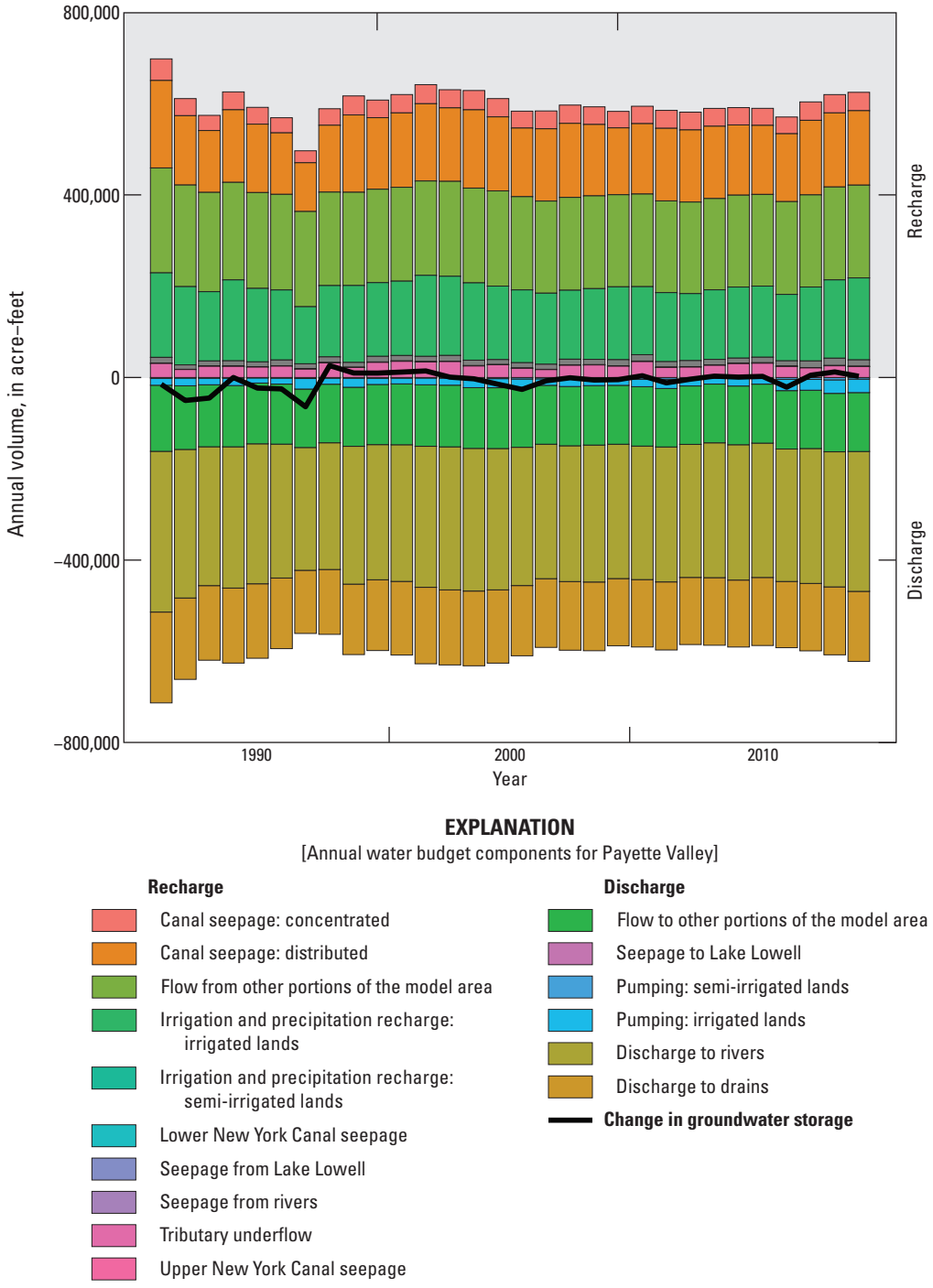

Figure 71. Annual Payette Valley water budget components the Treasure Valley Groundwater Flow Model, southwestern Idaho, and easternmost Oregon (Hundt, 2023).

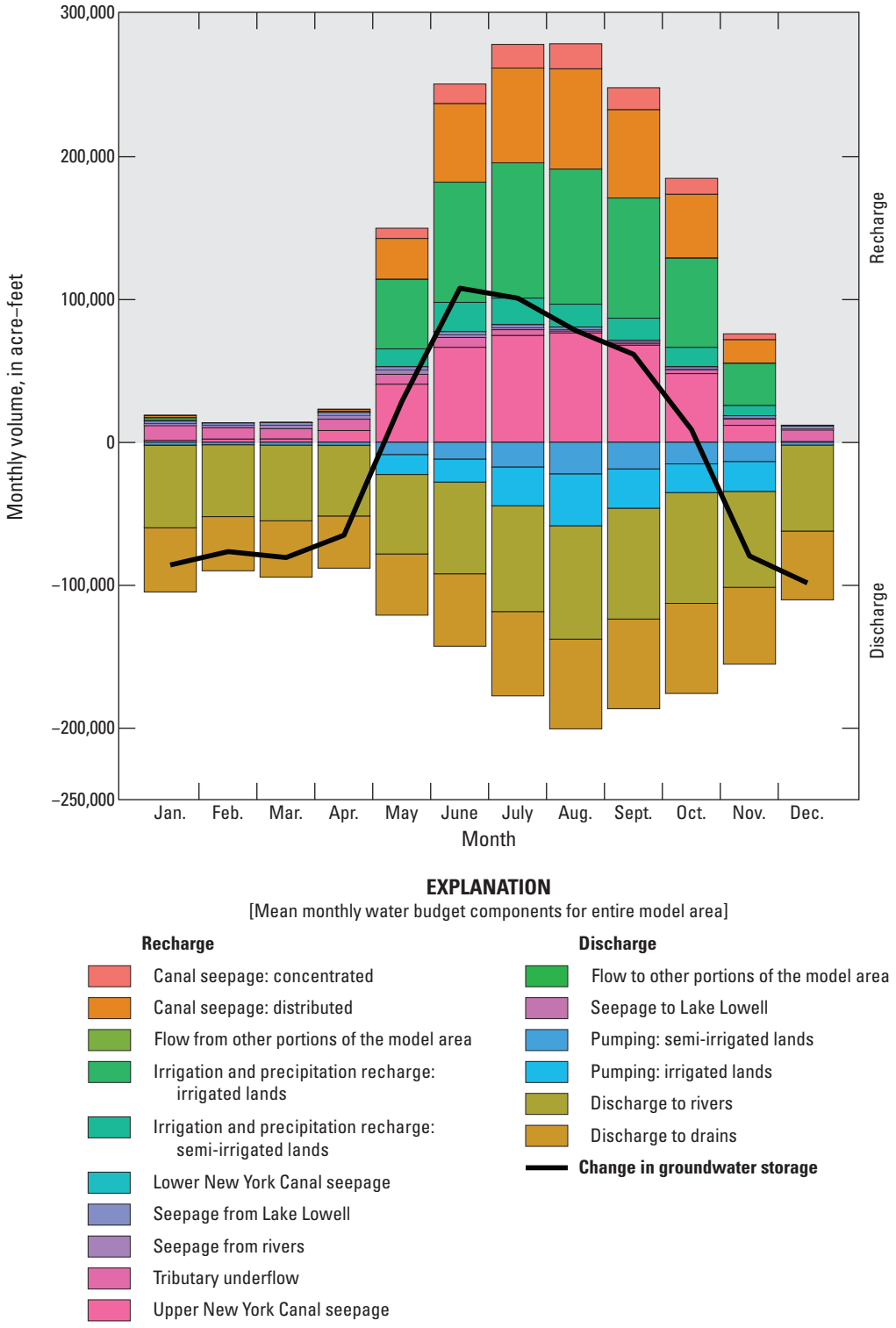

Figure 72. Mean monthly water budget components for the entire Treasure Valley Groundwater Flow Model area, southwestern Idaho, and easternmost Oregon (Hundt, 2023).

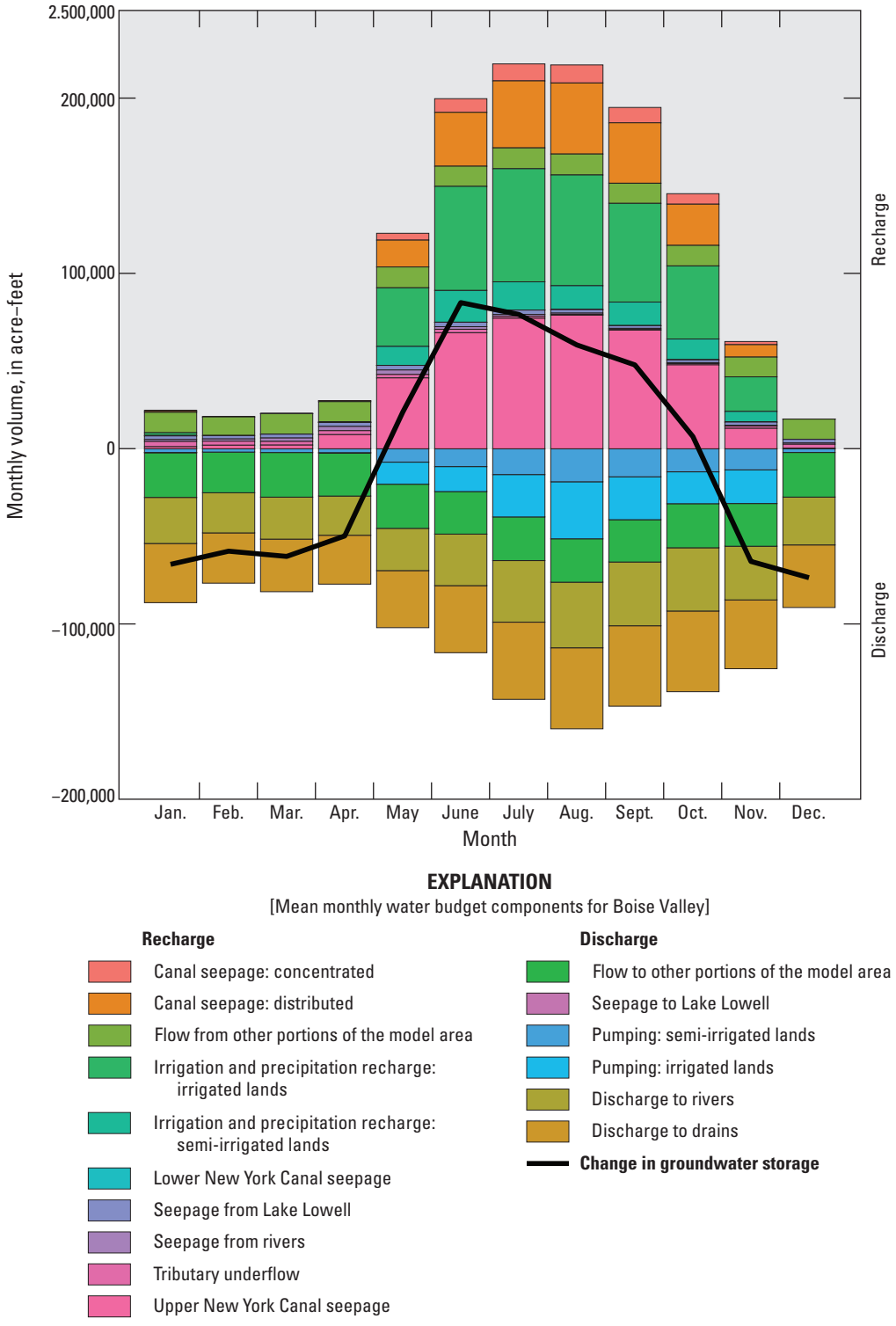

Figure 73. Mean monthly Boise Valley water budget components for the Treasure Valley Groundwater Flow Model, southwestern Idaho, and easternmost Oregon (Hundt, 2023).

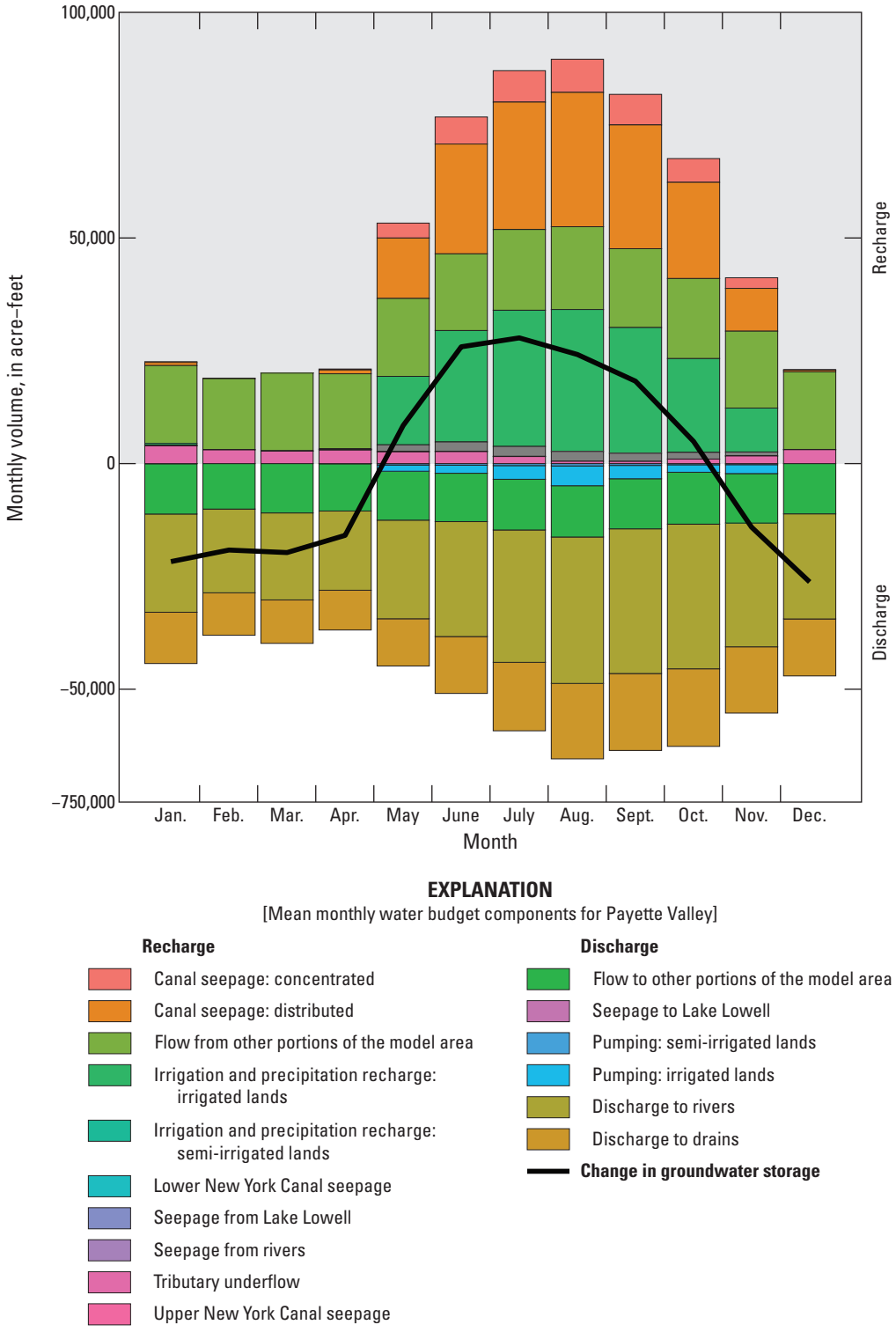

Figure 74. Mean monthly Payette Valley water budget components for the Treasure Valley Groundwater Flow Model, southwestern Idaho, and easternmost Oregon (Hundt, 2023).

Table 10. Average annual volume by water budget component for the Treasure Valley Groundwater Flow Model area and Boise and Payette Valleys, southwestern Idaho and easternmost Oregon (Hundt, 2023).

[**Abbreviation**: acre-ft, acre-feet; –, not applicable]

Component	Total model area	Boise Valley		Payette Valley	
	Average annual volume (acre-ft)	Average annual volume (acre-ft)	Percentage of total	Average annual volume (acre-ft)	Percentage of total
Recharge					
Drawdown (withdrawal of water from storage)	668,456	508,165	76.0	109,197	16.3
Irrigation and precipitation recharge: irrigated lands	499,325	339,666	68.0	122,407	24.5
Upper New York Canal seepage	397,654	397,654	100.0	–	–
Canal seepage: Distributed	345,758	191,012	55.2	129,972	37.6
Irrigation and precipitation recharge: semi-irrigated lands	103,751	90,316	87.1	10,027	9.7
Canal seepage: Concentrated	86,458	48,559	56.2	33,748	39.0
Tributary underflow	69,066	19,934	28.9	26,618	38.5
Seepage from Lake Lowell	24,984	24,984	100.0	–	–
Seepage from rivers	15,690	14,906	95.0	771	4.9
Lower New York canal seepage	84	84	100.0	–	–
Discharge					
Discharge to rivers	−764,339	−351,466	46.0	−263,427	34.5
Discharge to drains	−600,316	−447,633	74.6	−115,572	19.3
Recovery (deposit of water into storage)	−564,990	−428,472	75.8	−104,633	18.5
Pumping: irrigated lands	−162,050	−145,479	89.8	−4,034	2.5
Pumping: semi–irrigated lands	−118,106	−102,747	87.0	−1,415	1.2
Seepage to Lake Lowell	−4	−4	100.0	–	–

Discussion

The TVGWFM may be used for water resource planning, for understanding the interactions of groundwater and surface water, and for facilitating conjunctive management. The features of the model, as described in the numerical model section, allow for a variety of scenarios that can suit these purposes. Importantly, the TVGWFM builds upon the work of previous models in Petrich (2004) and Johnson (2013). For this reason, the discussion below highlights those aspects of TVGWFM that add capabilities not previously available in existing models of the Treasure Valley.

The TVGWFM is a transient model with monthly stress periods and a 30-year (1986–2015) historical simulation period. This transient model can simulate how groundwater levels and discharge change in response to new stresses–such as new pumping or reduced recharge. Because it is transient, the TVGWFM can simulate stresses that are temporary, irregular, or which vary from year to year and whose impacts persist over multiple years. For example, the TVGWFM could simulate the cumulative impact over time from recurring droughts with different lengths, magnitude, or frequency. Finally, the 30-year historical period that was constructed for parameter estimation can be used as a starting point for developing scenarios, serving as both a baseline for comparison and a template for developing other transient simulations.

The TVGWFM was developed with six layers that were based upon observations of vertical water level gradients. While these vertical water level gradients were often underestimated by the model, their information was incorporated into the estimates of hydraulic conductivity and vertical anisotropy. Furthermore, the model was seen to be capable of matching these observed vertical gradients with greater accuracy when greater weight was placed upon them in parameter estimation.

The observation datasets used to constrain parameter values include newly collected measurements of groundwater discharge to major agricultural drain networks (U.S. Geological Survey, 2021). Petrich (2004) identified agricultural drains as the largest category of discharge from the aquifer and a major source of uncertainty in his model. For the historical 1986–2015 period, the TVGWFM showed low residuals in the simulation of drain discharge. As a result, the

Table 11. Comparison of Treasure Valley Groundwater Flow Model and Treasure Valley Hydrologic Project water budgets for the Boise Valley, southwestern Idaho (Hundt, 2023).

[**Abbreviations**: TVHP, Treasure Valley Hydrologic Project; TVGWFM, Treasure Valley Groundwater Flow Model; –, not applicable]

Component	1996				2000			
	TVHP		TVGWFM		TVHP		TVGWFM	
	Acre-feet	Percentage of total	Acre-feet	Percentage of total	Acre-feet	Percentage of total	Acre-feet	Percentage of total
Recharge								
Canal seepage	626,000	61	684,575	55	521,500	47	640,998	51
Seepage from rivers and streams	16,000	2	26,311	2	77,000	7	14,146	1
Seepage from Lake Lowell	19,000	2	32,858	3	21,200	2	26,226	2
Underflow	4,300	0	27,098	2	4,300	0	21,236	2
Flood irrigation and precipitation (all agricultural incidental recharge)	302,000	30	384,689	31	404,400	37	373,974	30
Recharge by other land uses (all semi-irrigated incidental recharge)	53,000	5	91,046	7	70,300	6	85,406	7
Net decrease in storage	–	–	0	0	–	–	27,396	2
Total recharge	1,020,300	–	1,246,578	–	1,098,700	–	1,189,381	–
Discharge								
Pumping for municipal, industrial, rural, and other non-agricultural uses	127,000	13	100,196	8	122,000	12	84,137	7
Pumping for agricultural irrigation	72,000	7	97,203	8	53,000	5	125,831	10
Discharge to rivers and drains	800,000	80	809,798	65	881,600	83	820,341	66
Net flow to other parts of the model	–	–	160,948	13	–	–	159,072	13
Net increase in storage	–	–	78,434	6	–	–	0	0
Total discharge	1,020,300	–	1,246,578	–	1,098,700	–	1,189,381	–

Table 12. Comparison of expanded Bureau of Reclamation/Idaho Water Resources model and Treasure Valley Groundwater Flow Model water budgets for the Payette Valley, southwestern Idaho (Hundt, 2023).

[**Abbreviations**: BOR, Idaho Water Resources model; TVGWFM, Treasure Valley Groundwater Flow Model; %, percentage; –, no data]

Component	1967–97		1986–97	
	BOR		TVGWFM	
	acre-feet	% of total	acre-feet	% of total
Recharge				
Canal seepage	210,091	45	190,481	0
Seepage from rivers and streams	–	–	754	0
Underflow	59,389	13	26,638	0
Flood irrigation and precipitation (all agricultural incidental recharge)	173,000	37	162,638	0
Recharge by other land uses (all semi-irrigated incidental recharge)	1,793	0	11,428	0
Dry land infiltration	17,616	4	–	–
Net decrease in storage	–	–	12,527	0
Net flow from other parts of the model	–	–	77,731	0
Total recharge	461,889	–	482,197	–
Discharge				
Pumping for municipal, industrial, rural, and other non-agricultural uses	5,729	1	1,514	0
Pumping for agricultural irrigation	7,185	2	15,280	0
Discharge to rivers and drains	435,890	93	465,403	1
Wetlands and water bodies	18,189	4	–	–
Total discharge	466,993	–	482,197	–

TVGWFM provides an improved representation of discharge from the aquifer and is well suited to simulate how changes in stresses to the aquifer will impact these discharges.

The TVGWFM includes an agricultural and urban water supply and demand model to estimate the quantity and location of canal seepage, incidental recharge of irrigation water, and pumping from unmeasured wells. This model incorporates two important new datasets: (1) monthly ET maps that should improve the spatial and temporal estimates of how much water was delivered to meet ET; (2) land use maps that allow the model to differentiate the irrigation practices of agricultural and urban areas. These features allow the TVGWFM to simulate how urban development may impact the hydrologic system by accounting for the associated change in ET and irrigation practices.

The hydrogeologic framework of Bartolino (2019a) was used to inform the range of possible values and spatial variation of hydraulic conductivity, vertical anisotropy, and storage. This dataset provided additional stability and uniqueness to the parameter estimation routine in a way that honored the observed stratigraphy of the Treasure Valley Aquifer System. With this information, locations with inaccurately represented boundary conditions can be easier to identify. These instances may be found where major residuals occur, but parameters are reasonable, or where parameters were required to move to the edge of their realistic range to lower residuals.

In addition to the TVGWFM model itself, the associated data release (Hundt, 2023) includes parameter estimation files, data used to develop the model, and scripts that were used to process input files and construct model files. This data package serves multiple uses. The input data and scripts provide a complete document of all analysis decisions that were made in the creation of the model—something that is not possible in a narrative model report. The input data and scripts can also be adapted to develop updated or improved versions of the model or model scenarios. The parameter estimation files can be used to approach parameter estimation with different algorithm settings, parameter ranges, observations weights, or new observation data. Finally, the input data are a collection of hydrologic datasets that may have other applications.

Model Limitations and Suggestions for Additional Work

The Treasure Valley Groundwater Flow Model was developed as a tool for water resource planning, for understanding the interactions of groundwater and surface water, and for facilitating conjunctive management. As a regional and multi-purpose tool, it may lack the precision necessary for water rights administration at a local scale but may be refined to suit that need. It is important to understand the accuracy and limitations of the model while using it for

any purpose. The accuracy of the simulated aquifer system is affected by several factors: (1) the quality, resolution, and availability of information used to develop the model and constrain parameter estimates; (2) the decisions on how the hydrologic system will be represented numerically; (3) assumptions made to overcome data gaps. The factors are discussed at length in the preceding sections of this report, but their impact on simulation accuracy was not quantified. Rather, a selection of important limitations is described qualitatively below along with examples of additional work that could further the understanding of the Treasure Valley aquifer system and lead to future enhancements to the model.

Measurements of inflows and outflows to the Snake River are insufficient to estimate aquifer discharge. This is a limitation in the observation target dataset that may allow for unrealistic discharge through the western model boundary. While the major sources of recharge are constrained by existing data, this recharge can be altered in quantity and in space with parameters that were included as an acknowledgement of data uncertainty. With fewer constraints on the aquifer water balance, the estimation of these parameters, and thus aquifer recharge, has greater potential for error throughout the model area. This limitation of the model could be improved by measuring seepage along the Snake River and estimating the contribution of flow from the east versus the west side of the river.

The spatial distribution of canal seepage and infiltration of irrigation water recharge, the largest sources of recharge to the system, are unknown and approximated indirectly. While the combined quantity of these recharge sources is constrained by measurements of river diversions and estimates of ET, the spatial distribution is likely to have many errors. The spatial resolution of surface water deliveries is known only at the level of irrigation entities, which cover 10s to 100s of square miles. Within these areas, many factors contribute to the spatial distribution of recharge but are unaccounted for in the irrigation supply and demand model. An incomplete list of these factors includes soil properties, irrigation practices, the stage and continuity of flow in canals, banks storage in canals, the status and quality of canal lining, and others. Inaccurate placement of recharge may degrade the model's performance at a site scale, especially near canals where concentrated recharge may be a local driver of water levels and seasonal variations.

There is poor understanding of how canal seepage and incidental recharge change as land is converted from agricultural (irrigated) to suburban (semi-irrigated). The irrigation supply and demand model was designed to separate irrigated and semi-irrigated water use, but uncertainty remains in how their properties differ. Greater uncertainty lies in the behavior of canal seepage, due to the coarse spatial scale of delivery measurements and the lack of measurements in canals. As a result, canal seepage was assumed to be insensitive to land-use. If this assumption is untrue, the model may underestimate the hydrologic impact of the conversion from agricultural to suburban land use.

The model limitations stemming from the poor understanding of recharge from the irrigation system may be improved in a few ways. One is to measure flows within the surface water conveyance system at a higher spatial resolution. These could improve estimates of canal seepage and incidental recharge, their spatial distribution, and how these differ between irrigated and semi-irrigated land uses. Developing a better understand of seepage along the New York Canal could also improve the model. An understanding of seepage volumes, seasonal variation, spatial distribution, and the impact of lining could all improve model performance. This major source of recharge is being altered without a full understanding of impacts to groundwater. Additional data collection could allow this model to be adapted to perform these analyses.

The model has relatively high residuals in simulating seepage at Lake Lowell. It is unknown whether this is caused by error in the calculation of seepage or from a numerical misrepresentation of the boundary. As a result, simulations of fluxes, heads, and seasonal variations thereof may have elevated uncertainty near this boundary and model results in this area should be used with caution. This limitation of the model could be improved by collecting additional data to refine the water budget for Lake Lowell and the Lower New York Canal during multiple seasons.

Regions of poor performance are evident in maps of water level residuals (figs. 55–60). Scenarios that require the simulation of absolute water levels, rather than difference in water levels, will have performance that varies based upon the locations of interest. This also applies to any scenario that relies upon accurate estimates of the thickness of the unsaturated zone. For example, scenarios of managed aquifer recharge and recovery may be affected by errors in estimates of the total volume of pore space of unsaturated sediments. This limitation of the model could be improved by further adjusting parameter estimates to improve areas of model underperformance, including allowing more dramatic hydraulic parameter variations in those areas.

The model was built with multiple, broadly expressed objectives:

1. to improve the understanding of groundwater and surface water interactions;
2. to facilitate conjunctive water management;
3. to provide a tool for water resources planning; and
4. to provide a tool for water allocation.

As a result, model design decisions did not optimize performance for specific uses. This could be improved if specific uses emerge in the future. Options include refining the model, collecting additional measurements, applying more complex boundary representation, or re-estimating parameters to emphasize model performance for those specific uses. As it is now, this is a general-purpose model.

Summary

The Treasure Valley Groundwater Flow Model (TVGWFM) described in this report is a transient, three-dimensional, finite-difference groundwater flow model with a historical period of 360 monthly stress periods from 1986 to 2015. The TVGWFM was developed as a tool for water resource planning, for understanding the interactions of groundwater and surface water, and for facilitating conjunctive management. The TVGWFM may lack the resolution needed for water rights administration at a local scale.

The TVGWFM builds upon the models of Petrich (2004) and Johnson (2013) by incorporating new data and features. New data include a 3D hydrogeologic framework, maps of monthly ET, maps of historical irrigation status, measurements of discharge from major agricultural drains, and water levels from multi-layer well clusters. Notable capabilities include fully transient simulations, the representation of localized vertical gradients, improved estimates of aquifer discharge, hydraulic parameter estimates that roughly follow the observation of the 3D hydrogeologic model, a demand and supply model that simulates recharge and pumping as a functions of ET, land-use, canal locations, and surface water deliveries, and a data release (Hundt, 2023) that packages the model, parameter estimation files, input data, and pre-processing tools.

The model domain is bounded by the Snake River to the south and west, the Payette River to the north, the foothills of the Boise Front to the northeast and a groundwater divide near the Ada-Elmore County to the southeast. The model area is divided into a regular grid of 64 by 65 1-mile square cells and six layers of varying depth and lateral extent. The historical 1986–2015 period is divided into 360 month-long stress periods. The historical period is initiated with a steady-state period that represents average conditions for 1998–2006, a period over which water levels begin and end at a similar state.

The TVGWFM includes six model layers. The hydrogeologic framework study (Bartolino, 2019a) did not find well-defined and continuous hydrogeologic units, with the exception of a previously mapped mudstone facies (Wood, 1997). However, vertical heterogeneity in aquifer properties and water levels are known to occur at a local scale. To capture these, the aquifer above the mudstone facies was divided into layers using observation of vertical water level gradients.

TVGWFM boundary conditions are represented within 15 MODFLOW (Langevin and others, 2017) stress package modules:

1. agricultural drains with the drain (DRN) package;
2. the Boise, Payette, and Snake Rivers with the river (RIV) package;
3. canal seepage with two well (WEL) packages for concentrated and distributed seepage;
4. incidental recharge in irrigated and semi-irrigated lands with two well (WEL) packages;
5. Lake Lowell with a general-head boundary (GHB) package;
6. the New York Canal with a well (WEL) package in the upper reach and river in the lower reach;
7. groundwater pumping with four well (WEL) packages–one each for irrigated lands, semi-irrigated lands, measured municipal, and other pumping; and
8. tributary underflow with two well (WEL) packages for shallow and deep zones.

The TVGWFM includes an irrigation supply and demand model to estimate incidental recharge, canal seepage, and unmeasured pumping. The model area is divided into supply and demand areas over which total ET demand summed from UI actual ET estimates and canal seepage and incidental recharge are then estimated. These totals are compared to surface water diversions to calculate supplemental pumping. Within these areas, incidental recharge is distributed in proportion to ET, canal seepage in proportion to ET and canal locations, and pumping in proportion to ET and water rights. The supply and demand model differentiates between irrigated and semi-irrigated land to account for difference in irrigation practice and to facilitate model scenarios that simulated the impacts of urban growth.

TVGWFM model parameters were estimated with the PEST (Doherty, 2005) software and manual adjustments. Model parameters from 17 groups were estimated: 3 groups for distributed hydraulic properties of conductivity, vertical anisotropy, and storge; 4 groups of boundary conductance; and 10 groups of factors for the irrigation supply and demand model. These parameters were adjusted in PEST to minimize an objective function made up of eight groups of observation targets: water levels, temporal differences of water levels, vertical differences of water levels, drain discharge, temporal difference of drain discharge, river and unmeasured drain discharge, Lake Lowell seepage, and temporal difference of Lake Lowell seepage.

The quality of the fit between simulated results and observations varied by group. The best performance is seen in the absolute and temporal difference groups for both water levels and drain discharge. The mean error (ME), mean-absolute error (MAE), and MAE/range were 15.4 feet (ft), 33.4 ft, and 2.6 percent for the water level observations and −3.9 cubic feet per second (ft^3/s), 8.4 ft^3/s, and 3.9 percent for the drain discharge observations. The vertical water level difference group has moderate performance, with an MAE/range below 10 percent and a relatively low 50th percentile value. The river and unmeasured drain seepage group has moderate performance with an MAE/range of 1.6 percent that is misleadingly low due to the very large range of values in the observation dataset. Finally, both Lake Lowell observation groups show poor performance with ME and MAE of −40 ft^3/s and 49 ft^3/s for seepage and 86 ft^3/s and 95 ft^3/s for temporal difference of seepage.

The TVGWFM can be used as a tool for water resource planning, for understanding the interactions of groundwater and surface water, and for facilitating conjunctive management, but may lack the precision needed for water rights administration at a local scale. Additional sources of uncertainty or limitation of the model are noted. Measurements of inflows and outflows to the Snake River are insufficient to accurately estimate aquifer discharge, adding additional uncertainty to estimates of discharge and estimates of the water budget components estimated in the irrigation supply and demand model. The spatial distribution of canal seepage and infiltration of irrigation water recharge, the largest sources of recharge to the system, are unknown and approximated indirectly. There is poor understanding of how canal seepage and incidental recharge change as land is converted from agricultural (irrigated) to suburban (semi-irrigated). These uncertainties will affect any scenarios that investigate changes to land use or irrigation practices. Finally, the model has poor performance around and to the southwest of Lake Lowell, limiting the precision of scenarios that address water level impacts in that region.

The model was built with multiple, broadly expressed objectives, and did not optimize performance for specific uses. However, the model and the tools included in the data release (Hundt, 2023) provide ample flexibility to improve the model for specific uses. Adjustments and improvements could be made by refining the model, collecting additional measurements, applying more complex boundary representation, or re-estimating parameters to emphasize model performance for specific uses.

References Cited

Aishlin, P.S., 2006, Groundwater recharge estimation using chloride mass balance Dry Creek Experimental Watershed: Boise, Boise State University, M.S. Thesis 622, 102 p. [Also available at https://scholarworks.boisestate.edu/td/622/.]

Aishlin, P.S., and McNamara, J.P., 2011, Bedrock infiltration and mountain block recharge accounting using chloride mass balance: Hydrological Processes, v. 25, no. 12, p. 1934–1948.

Allen, R.G., and Robison, C.W., 2017, Evapotranspiration and consumptive irrigation water requirements for Idaho: Moscow, University of Idaho Research and Extension Center at Kimberly, 17 p. + summary.

Allen, R.G., Tasumi, M., Morse, A., Trezza, R., Wright, J.L., Bastiaanssen, W., Kramber, W., Lorite, I., and Robison, C.W., 2007, Satellite-based energy balance for mapping evapotranspiration with internalized calibration (METRIC)—Applications: Journal of Irrigation and Drainage Engineering, v. 133, no. 4, p. 395–406.

Anderson, M.P., Woessner, W.W., and Hunt, R.J., eds., 2015, Applied groundwater modeling (2nd ed.): San Diego, Academic Press, 630 p.

Bartolino, J.R., 2019a, Hydrogeologic framework of the Treasure Valley and surrounding area, Idaho and Oregon: U.S. Geological Survey Scientific Investigations Report 2019–5138, 31 p. [Also available at https://doi.org/10.3133/sir20195138.]

Bartolino, J.R., 2019b, Hydrogeologic framework of the Treasure Valley and surrounding area, Idaho and Oregon—Model, well data, and model animation: U.S. Geological Survey data release, accessed June 25, 2023, at https://doi.org/10.5066/P9CAC0F6.

Bartolino, J.R., and Vincent, S., 2017, A groundwater-flow model for the Treasure Valley and surrounding area, southwestern Idaho: U.S. Geological Survey Fact Sheet 2017–3027, 4 p.

Beranek, L.P., Link, P.K., and Fanning, C.M., 2006, Miocene to Holocene landscape evolution of the western Snake River Plain region, Idaho—Using the SHRIMP detrital zircon provenance record to track eastward migration of the Yellowstone hotspot: Geological Society of America Bulletin, v. 118, no. 9–10, p. 1027–1050.

Bureau of Reclamation, 2009, Modeling spatial water allocation and hydrologic externalities in the Boise Valley: Boise, Idaho, Bureau of Reclamation, Pacific Northwest Region.

Bureau of Reclamation, 2019, AgriMet weather data: Bureau of Reclamation database, accessed July 23, 2019, at https://www.usbr.gov/pn/agrimet/wxdata.html.

Bureau of Reclamation, 2020a, AgriMet, Evapotranspiration summaries: Bureau of Reclamation, accessed April 27, 2020, at https://www.usbr.gov/pn/agrimet/etsummary.html.

Bureau of Reclamation, 2020a, AgriMet, Evapotranspiration summaries: Bureau of Reclamation, accessed April 27, 2020, at https://www.usbr.gov/pn/agrimet/etsummary.html.

Bureau of Reclamation, 2020b, HydroMet, Evapotranspiration summaries: Bureau of Reclamation, accessed April 23, 2020, at https://www.usbr.gov/pn/hydromet/arcread.html.

Cosgrove, D.M., 2010, Evaluation of ground water models in the Treasure Valley, Idaho Area: Idaho Falls, Western Water Consulting, Inc., 134 p. [Also available at https://idwr.idaho.gov/wp-content/uploads/sites/2/projects/east-ada-county/20100601-Evaluation-of-Groundwater-Models-in-the-Treasure-Valley-Idaho-Area-Cosgrove.pdf.]

Community Planning Association of Southwest Idaho, 2020, Demographics, current and historical population estimates: Community Planning Association of Southwest Idaho, accessed July 27, 2020, at https://www.compassidaho.org/prodserv/demo-current.htm.

Doherty, J.E., 2005, PEST, Model-independent parameter estimation—User manual (5th ed.): Brisbane, Australia, Watermark Numerical Computing. [Also available at https://pesthomepage.org/documentation.]

Doherty, J.E., Fienen, M.N., and Hunt, R.J., 2010, Approaches to highly parameterized inversion—Pilot-point theory, guidelines, and research directions: U.S. Geological Survey Scientific Investigations Report 2010–5168, 36 p. [Also available at https://pubs.usgs.gov/sir/2010/5168/.]

Douglas, S.L., 2007, Development of a numerical ground water flow model for the M3 Eagle development area near Eagle, Idaho: Boise, Idaho, Boise State University, Master's thesis, 345 p. [Also available at https://idwr.idaho.gov/wp-content/uploads/sites/2/projects/north-ada-county/200712-Dev-of-Numerical-GW-Flow-Model-near-Eagle-Idaho.pdf.]

Ferrari, R.L., 1995, Lake Lowell Reservoir—1994 Reservoir Survey: Bureau of Reclamation, 11 p.

Freeze, R.A., and Cherry, J.A., 1979, Groundwater: Englewood Cliffs, Prentice-Hall, Inc., 604 p.

Gesch, D.B., Evans, G.A., Oimoen, M.J., and Arundel, S., 2018, The National Elevation Dataset: American Society for Photogrammetry and Remote Sensing, p. 83–110.

Hundt, S.A., 2023, Data and archive for a Groundwater Flow Model of the Treasure Valley aquifer system, southwestern Idaho: U.S. Geological Survey data release, accessed June 25, 2023, at https://doi.org/10.5066/P9U6OOPH.

Idaho Department of Water Resources, 2011, Irrigation organizations: Idaho Department of Water Resources, accessed September 10, 2019, at https://data-idwr.opendata.arcgis.com/pages/gis-data/.

Idaho Department of Water Resources, 2018a, Groundwater levels: Idaho Department of Water Resources, accessed June 27, 2018, at https://idwr.idaho.gov/water-data/groundwater-levels/.

Idaho Department of Water Resources, 2018b,Water Measurement Research and Maps: Idaho Department of Water Resources, accessed June 27, 2018, at https://idwr.idaho.gov/water-data/water-measurement/research/.

Idaho Department of Water Resources, 2019, Water right and adjudication search: Idaho Department of Water Resources database, accessed June 3, 2019, at https://research.idwr.idaho.gov/apps/waterrights/wrajsearch/SearchPage.aspx.

Idaho Department of Water Resources, 2020a, Well construction search: Idaho Department of Water Resources database, accessed August 20, 2020, at https://idwr.idaho.gov/Apps/appsWell/WCInfoSearchExternal/.

Idaho Department of Water Resources, 2020b, Irrigated lands and the Treasure Valley: Idaho Department of Water Resources, accessed June 25, 2023, at https://data-idwr.hub.arcgis.com/search?q=Irrigated%20Lands%20for%20the%20Treasure%20Valley.

Idaho Department of Water Resources, 2020c, Digital ET images for water rights, hydrologic models, regional planning: Idaho Department of Water Resources, accessed June 25, 2023, at https://data-idwr.hub.arcgis.com/search?tags=evapotranspiration.

Idaho Senate Resources and Environment Committee, 2016, Senate Concurrent Resolution 137: Legislature of the State of Idaho, 63rd, 2nd session, 2 p. [Also available at https://legislature.idaho.gov/legislation/2016/SCR137Bookmark.htm.]

Johnson, J., 2013, Development of a transient groundwater model of the Treasure Valley aquifer: Idaho, Bureau of Reclamation, 43 p.

Langevin, C.D., Hughes, J.D., Banta, E.R., and Niswonger, R.G., Panday, Sorab, and Provost, A.M., 2017, Documentation for the MODFLOW 6 Groundwater Flow Model: U.S. Geological Survey Techniques and Methods, book 6, chap. A55, 197 p., accessed September 12, 2023, at https://doi.org/10.3133/tm6A55.

Lewis, R.S., Link, P.K., Stanford, L.R., and Long, S.P., 2012, Geologic map of Idaho: Moscow, Idaho Geological Survey M-9, scale 1:750,000, 1 sheet, 18 p. booklet. [Also available at https://www.idahogeology.org/Products/reverselook.asp?switch=title&value=GeologicMapofIdaho.]

Lindgren, J.E., 1982, Application of a ground water model to the Boise Valley aquifer in Idaho: Moscow, University of Idaho, M.S. thesis.

Moore, R.B., McKay, L.D., Rea, A.H., Bondelid, T.R., Price, C.V., Dewald, T.G., and Johnston, C.M., 2019, User's guide for the National Hydrography Dataset Plus (NHDPlus) high resolution: US Geological Survey Open-File Report 2019–1096, 66 p. [Also available at https://pubs.usgs.gov/publication/ofr20191096.]

National Oceanic and Atmospheric Administration, 2019, Climate data online: National Oceanic and Atmospheric Administration database, accessed May 29, 2019, at https://www.ncdc.noaa.gov/cdo-web/.

Newton, G.D., 1991, Geohydrology of the regional aquifer system, western Snake River plain, southwestern Idaho: U.S. Geological Survey Professional Paper 1408-G, 52 p., 1 pl. in pocket. [Also available at https://doi.org/10.3133/pp1408G.]

O'Connor, J.E., 1990, Hydrology, hydraulics, and sediment transport of Pleistocene Lake Bonneville flooding on the Snake River, Idaho: Tucson, University of Arizona, Ph.D. dissertation, 192 p., accessed October 31, 2018, at http://hdl.handle.net/10150/191159.

Pacific Groundwater Group, 2008a, M3 Eagle Groundwater Flow model and analysis of pumping impacts—First year progress report: Seattle, Washington, Pacific Groundwater Group.

Pacific Groundwater Group, 2008b, Model refinement and recalibration—Re-simulation of 50-year drawdown and assessment of effects of reduced canal leakage (M3 Eagle Groundwater flow model): Seattle, Washington, Pacific Groundwater Group, Memorandum to Hydro Logic, Inc.

Petrich, C.R., 2004, Simulation of ground water flow in the lower Boise River basin: Moscow, University of Idaho Water Resources Research Institute, Research Report IWRRI-2004-02, 131 p. [Also available at https://idwr.idaho.gov/wp-content/uploads/sites/2/projects/treasure-valley/TVHP-Model.pdf.]

PRISM Climate Group, 2020, Oregon State University: PRISM Climate Group, accessed August 20, 2020 at https://prism.oregonstate.edu.

Water Engineering, S.P.F., 2016, Treasure Valley DCMI water-demand projections (2015–2065): Boise, SPF Water Engineering, 131 p., 3 apps. [Also available at https://idwr.idaho.gov/wp-content/uploads/sites/2/publications/20160808-OFR-Treasure-Valley-Water-Demand-2015-2065.pdf.]

Schmidt, R.D., 2008, Modeling drain interactions with shallow groundwater in the Boise Valley using analytic elements: Boise, Idaho, RD Schmidt and Associates, prepared for the Bureau of Reclamation.

Schmidt, R.D., Cook, Z., Dyke, D., Goyal, S., McGown, M., and Tarbet, K., 2008, A distributed parameter water budget data base for the lower Boise Valley: Bureau of Reclamation, Pacific Northwest Region, 109 p. [Also available at https://idwr.idaho.gov/wp-content/uploads/sites/2/projects/north-ada-county/200801-Distributed-Parameter-Water-Budget-Data-Base-for-Lower-Boise-Valley.pdf.]

Sukow, J., 2012, Expansion of Treasure Valley Hydrologic Project groundwater model: Boise, Idaho Department of Water Resources, 34 p. [Also available at https://idwr.idaho.gov/wp-content/uploads/sites/2/projects/treasure-valley/Treasure-Valley-Model-Grid-Expansion-Report.pdf.]

Sukow, J., 2016, Evaluation of transient groundwater model of the Treasure Valley Aquifer and recommendations for future work: Boise, Idaho Department of Water Resources, draft memorandum, 19 p.

U.S. Board on Geographic Names, 2019, U.S. Board on Geographic Names: U.S. Geological Survey website, accessed May 20, 2019, at https://www.usgs.gov/core-science-systems/ngp/board-on-geographic-names.

U.S. Census Bureau, 1983, 1980 census of population: U.S. Department of Commerce, 269 p. + 4 apps. [Also available at https://www2.census.gov/prod2/decennial/documents/1980/1980censusofpopu8011uns_bw.pdf.]

U.S. Census Bureau, 2005, Population estimates for states, counties, places and minor divisions—Annual time series, April 1, 1990 Census to July 1, 2000 estimate: U.S. Census Bureau, accessed September 16, 2020, at https://www2.census.gov/programs-surveys/popest/tables/1990-2000/2000-subcounties-evaluation-estimates/sc2000f_id.txt.

U.S. Census Bureau, 2019, Annual estimates of the resident population for incorporated places in Idaho—April 1, 2010 to July 1, 2019: U.S. Census Bureau, accessed September 16, 2020, at https://www2.census.gov/programs-surveys/popest/tables/2010-2019/cities/totals/SUB-IP-EST2019-ANNRES-16.xlsx.

Urban, S.M., 2004, Water budget for the Treasure Valley aquifer system for the years 1996 and 2000: Moscow, University of Idaho Water Resources Research Institute, Treasure Valley Hydrologic Research Report, variously paged. [Also available at https://idwr.idaho.gov/wp-content/uploads/sites/2/projects/treasure-valley/TVHP-Water-Budget-1996-2000.pdf.]

U.S. Geological Survey, 2020, 3D Elevation Program: U.S. Geological Survey, web, accessed August 22, 2020, at https://www.usgs.gov/core-science-systems/ngp/3dep.

U.S. Geological Survey, 2021, National Water Information System: U.S. Geological Survey, web, accessed January 03, 2021, at https://waterdata.usgs.gov/nwis/.

Waag, C.J., and Wood, S.H., 1987, Geothermal investigations in Idaho, part 16-1, Evaluation of the Boise geothermal system: Boise, Idaho Department of Water Resources, Water Information Bulletin 30, part 16-1, variously paged. [Also available at https://idwr.idaho.gov/wp-content/uploads/sites/2/publications/wib30p16p1-geothermal-boise-system.pdf.]

Western Regional Climate Center, 2019, Idaho Climate Summaries: Western Regional Climate Center Web site, accessed May 29, 2019, at https://wrcc.dri.edu/summary/climsmid.html.

Wood, S., 1997, Structure contour map of the top of the mudstone facies, Western Snake River Plain: Idaho, Geosciences Department, Boise State University.

For more information concerning the research in this report, contact the

Director, Idaho Water Science Center
U.S. Geological Survey
230 Collins Road
Boise, Idaho 83702-4520
https://www.usgs.gov/centers/id-water

Manuscript approved on August 9, 2023

Publishing support provided by the U.S. Geological Survey
Science Publishing Network, Tacoma Publishing Service Center
Edited by Jeff Suwak
Layout and design by Yanis Xavier Castillo and Luis Menoyo
Illustration support by Teresa A. Lewis and JoJo Mangano

ISSN 2328-0328 (online)
https://doi.org/10.3133/2sir20235096